LIQUEFACTION-INDUCED GROUND DISPLACEMENT HAZARAD MAPS FOR A M7.0 SCENARIO EVENT ON THE SALT LAKE CITY SEGMENT OF THE WASATCH FAULT ZONE, SALT LAKE COUNTY, UTAH

Steven F. Bartlett

Associate Professor

Department of Civil and Environmental Engineering, University of Utah

Daniel W. Hinckley

Graduate Research Assistant

Department of Civil and Environmental Engineering, University of Utah

Travis M. Gerber

Assistant Professor

Department of Civil and Environmental Engineering, Brigham Young University

November 30th, 2016

ABSTRACT

This report describes liquefaction-induced lateral spread displacement and vertical ground settlement displacement failure maps developed for a magnitude M7.0 scenario earthquake occurring on the Salt Lake City segment of the Wasatch fault zone in Salt Lake County, Utah. The hazard maps were developed to aid engineers, developers, and city planners in identifying areas that may require additional geotechnical evaluations and potential liquefaction mitigation.

These maps were developed for Utah using an extensive geotechnical subsurface database correlated to surficial geological mapping. The **M**7.0 scenario event was based on estimates of strong motion obtained from deterministic mapping. Liquefaction-induced ground deformation hazard calculations were performed using state-of-practice methodologies: estimates of lateral spread horizontal ground displacement were calculated from multiple liner regression models; and estimates of vertical ground settlement were calculated from procedures developed by U.S. and Japanese researchers. The horizontal and vertical displacement estimates from these methods were plotted within the corresponding surficial geologic units, and the units were in turn assigned horizontal and vertical displacement values based on statistical analyses of the displacement distribution within each unit. In order to assign a conservative displacement value for hazard ordinance purposes, the mapped units for the **M**7.0 event were assigned an overall displacement value that has an 85 percent probability, or greater, of non-exceedance. In general, the ground failure maps show relatively high lateral spread and ground settlement values are possible along and near the margins of the Jordan River and tributary creeks, and in recent alluvial, river, stream, and lake deposits generally found in the northern part of the Salt Lake Valley.

ACKNOWLEDGMENTS

TABLE OF CONTENTS

LIST OF FIGURES

1   INTRODUCTION

Liquefaction and its associated ground deformation effects occur when high excess pore pressures are generated in relatively loose, saturated, granular soil deposits subjected to cyclic loading caused by moderate to large earthquakes. In the liquefied state, the shear resistance of the soil is significantly reduced and severe loss of strength may lead to ground failure effects (e.g., flow failure, lateral spread and ground oscillation). In addition to these primarily horizontal ground movement effects, vertical and differential ground settlement may also occur as excess pore pressure dissipates and the soil reconsolidates to a denser configuration. Infrastructure, embankments and retaining walls atop liquefied ground may additionally suffer from bearing capacity failure and other types of damage resulting from the liquefied condition of the foundation soils.

Lateral spread is generally the most damaging and pervasive type of liquefaction induced ground failure. During lateral spread, blocks of relatively intact surficial soil located atop a liquefied soil at depth displace down slope or towards a free face (e.g., river channel or bluff). Such displacement can cause considerable damage. For example, lateral spreads generated by the 1906 San Francisco earthquake damaged or destroyed numerous buildings, bridges, roads and pipelines (Lawson, 1908; Youd and Hoose, 1978). Most notably, lateral spread along Valencia Street between 17th and 18th Streets severed water lines to downtown San Francisco. The resulting interruption of water greatly hampered fire fighting during the ensuing fire and significantly added to the earthquake losses. Additionally, lateral spreads caused by the 1964 Alaska earthquake disrupted many bridges, buildings, pipelines and other lifelines in cities such as Anchorage, Homer, Kodiak, Valdez, Seward, Portage and Whittier, Alaska. Approximately $80 million of liquefaction damage (1964 dollars) to 266 bridges and numerous sections of embankment along the Alaska Railroad and Highway (McCulloch and Bonilla, 1970; Kachadoorian, 1968). In that same year, liquefaction caused widespread damage to buildings, roads and bridges in Niigata, Japan (Hamada et al., 1986). More recently, ground settlement associated with liquefaction caused extensive

damage in Japan, Turkey and New Zealand (Kaneko et al., 1995; Yoshida et al., 2001; McSaveney, 2013). In the case of New Zealand, wide spread liquefaction-induced ground settlement and lateral spread caused extensive damage in the city of coastal Christchurch during the 22 February 2011, M_w 6.2, Canterbury earthquake. This event caused 185 fatalities with most of the loss of life and damage occurring in the Central Business District of Christchurch. Early estimates placed the cost of this earthquake at $4 billion (Nz) (McSaveney, 2013). Damage occurred to medium and low rise reinforced concrete and steel buildings, masonry buildings, industrial facilities, and timber-frame residential structures, as well as lifelines, including water supply, wastewater, drainage, natural gas, power, telecommunications and transportation networks. Ground deformation varied from strong shaking in the absence of permanent soil displacement to large levels of liquefaction-induced lateral spread and settlement (Bray et al., 2013.)

The Wasatch Front in Utah has a relatively high liquefaction hazard due to the presence of several nearby, active faults. The Salt Lake City segment of the Wasatch fault zone is capable of producing a **M**7.0 or greater event (Machette et al., 1992) which would likely trigger liquefaction in many areas along the Wasatch Front. Additionally, the Working Group on Utah Earthquake Probabilities has estimated that there is a 43 percent probability of one or more **M**6.75, or greater, earthquakes, and a 57 percent probability of one or more **M**6.0, or greater, earthquakes in the Wasatch Front region in the next 50 years (WGUEP, 2016). Because the Salt Lake and other valleys along the Wasatch Front are relatively deep, sedimentary basins with shallow groundwater containing loose, saturated, potentially liquefiable soil deposits, liquefaction damage resulting from major earthquakes is expected to be widespread. Further, when coupled with the relatively rapid rate of growth of infrastructure in earthquake and liquefaction prone areas, this urbanization requires continual assessment of geological hazards, urban planning and earthquake-resistant design to reduce Utah's seismic risk.

This report describes the development of liquefaction-induced lateral spread and ground settlement failure maps for the Salt Lake Valley, Utah, based on a characteristic

M7.0 event on the Wasatch fault zone. Additionally, recommendations on the implementation and use of these maps in hazard ordinances are presented.

2 GEOLOGIC SETTING OF THE SALT LAKE VALLEY

Quaternary unconsolidated sediments in the Salt Lake Valley are generally between 40 and 200 m thick (130 and 660 ft), except for the northeastern part of the valley, where they may be as thick as 700 m (2310 ft) (Arnow et al., 1970; Wong et al., 2002). Localized tilting caused by faulting and deepening of the sedimentary basin has produced the thicker section of unconsolidated sediments found in this part of the Salt Lake Valley. Holocene and Pleistocene deposits dominate the surficial geology of this intermountain basin (Figure 2-1, Table 2-1). Sediments in the northern part of the Salt Lake Valley predominately consist of Holocene lacustrine, marsh, fluvial and alluvial sediments that were deposited after the last major regression of Lake Bonneville, some 10,000 years before present (Lund, 1990). The northward flowing Jordan River and its tributary streams that generally flow northwesterly across the Salt Lake Valley overlay the Lake Bonneville deposits. These recent fluvial deposits are the primary source of the loose, saturated granular deposits, which are highly susceptible to liquefaction (Olsen et al., 2007). The groundwater table in this area is relatively shallow (generally less than 10 to 15 feet below the surface) and is also shallow near the Jordan River and its tributaries (Bartlett et al., 2005). In other parts of the valley, Holocene and late-Quaternary alluvium, alluvial fan, colluvial and glacial sediments have been deposited atop Lake Bonneville lacustrine, delta and terrace deposits. In the southern part of the valley and along its eastern margins, surficial deltaic deposits from Lake Bonneville and pre-Bonneville alluvial-fan deposits, late Tertiary/early Pleistocene fanglomerates are morphologically distinctive and generally thick in some areas (Lund, 1990).

The white areas shown in Figure 2-1 were not included in this study because they mainly consist of bedrock or very dense soils; hence are not susceptible to liquefaction. In addition, contemporaneous to or subsequent to this study, revised

surficial geologic mapping at the 1:24,000-scale has been undertaken in the western

part of the valley by the UGS (Solomon et al., 2007, McKean, A. P. and Hylland, 2013).
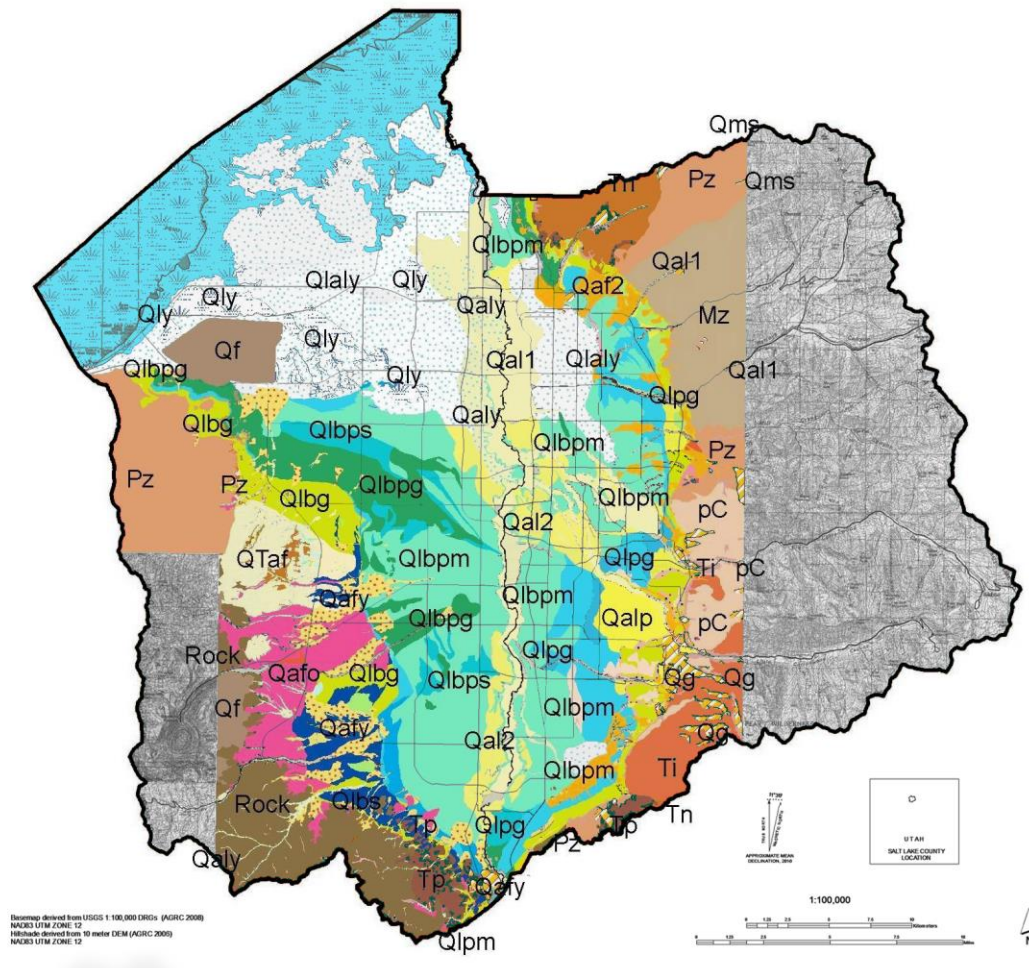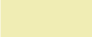
Figure 2-1. Surficial geology of the Salt Lake Valley, Utah (from Hinckley, 2010; modified from Personius and Scott, 1992; Biek et al., 2004; and Miller, 1980).

Table 2-1. Name, description and age of major surficial geologic units in the Salt Lake Valley (Personius and Scott, 1992; Biek et al., 2004; and Miller, 1980).

Map Symbol	Name	Description	Age
	Qal_1	Modern stream alluvium 1	Upper Holocene
	Qal_2	Stream alluvium 2	Middle Holocene to Upper Pleistocene
	Qaly	Younger stream alluvial deposits, undivided	Holocene to Upper Pleistocene
	Qalp	Stream alluvium related to the Provo (regressive) phase of the Bonneville lake cycle	Upper Pleistocene
	Qalb	Alluvial deposits related to the Bonneville (transgressive) phase of the Bonneville lake cycle	Upper Pleistocene
	Qaf_1	Modern alluvial-fan deposits 1	Upper Holocene
	Qaf_2	Alluvial-fan deposits 2	Middle Holocene to Upper Pleistocene
	Qafy	Younger alluvial-fan deposits, undivided	Holocene to Upper Pleistocene
	Qafp	Alluvial-fan deposits related to the Provo (regressive) phase of the Bonneville lake cycle	Upper Pleistocene
	Qafb	Alluvial-fan deposits related to the Bonneville (transgressive) phase of the Bonneville lake cycle	Upper Pleistocene
	Qaf_4	Alluvial-fan deposits 4	Upper to Middle Pleistocene
	Qaf_5	Alluvial-fan deposits 5	Middle Pleistocene
	Qafo	Older alluvial-fan deposits, undivided	Upper to Middle Pleistocene
	Qly	Young lacustrine and marsh deposits	Holocene
	Qlaly	Young lacustrine, marsh, and alluvial deposits	Holocene to Upper Pleistocene
	Qlpg	Lacustrine gravel and sand related to the Provo (regressive) phase of the Bonneville lake cycle	Upper Pleistocene
	Qlpm	Lacustrine clay and silt related to the Provo (regressive) phase of the Bonneville Lake Cycle	Upper Pleistocene

6

Map Symbol	Name	Description	Age
	Qlbg	Lacustrine gravel and sand related to the Bonneville (transgressive) phase of the Bonneville lake cycle	Upper Pleistocene
	Qlbs	Lacustrine sand and silt related to the Bonneville (transgressive) phase of the Bonneville lake cycle	Upper Pleistocene
	Qlbm	Laucstrine clay and silt related to the Bonneville (transgressive) phase of the Bonneville lake cycle	Upper Pleistocene
	Qlbpg	Lacustrine gravel and sand of the Provo and Bonneville lake cycles, undivided	Upper Pleistocene
	Qlbps	Lacustrine sand and silt of the Provo and Bonneville lake cycles, undivided	Upper Pleistocene
	Qlbpm	Lacustrine silt and clay of the Provo and Bonneville lake cycles, undivided	Upper Pleistocene
	Qmsy	Younger landslide deposits	Historical to Upper Pleistocene
	Qmls	Lateral-spread deposits	Holocene to Upper Pleistocene
	Qmt	Talus deposits	Holocene to Upper Pleistocene
	Qchs	Hillslope colluvium	Holocene to Upper Pleistocene
	Qca	Colluvium and alluvium, undivided	Holocene to Middle Pleistocene
	Qes	Eolian sand	Holocene to upper Pleistocene
	Qf	Artificial fill	Historical
	Tn	Tertiary sedimentary and volcanic rocks	Neogene
	Tp	Tertiary sedimentary and volcanic rocks	Paleogene
	Mz	Mesozoic sedimentary rocks	Cretaceous to Triassic
	Pz	Paleozoic sedimentary rocks	Permian to Cambrian
	pC	Precambrian metamorphic rocks	Proerozoic and Archean

3 FAULTING AND SEISMICITY

The Salt Lake Valley is located in the central Wasatch Front area of the Intermountain Seismic Belt which is a series of active, Quaternary normal faults extending from southern Montana to northern Arizona (Smith and Arabasz, 1991). The Salt Lake segment of the Wasatch fault zone poses the primary seismic hazard to the Salt Lake Valley (Scott and Shroba, 1985; Machette et al., 1992; Personius and Scott, 1992; WGEUP, 2016). This segment extends approximately 46 km (29 miles) from the Traverse Mountains salient (on the south) to the Salt Lake salient (on the north) (Personius and Scott, 1992). The Salt Lake City segment of the Wasatch fault zone is a complex normal fault system consisting of several parts that include (from north to south): (1) the Warm Springs fault along the Salt Lake salient, (2) the East Bench fault, located just east of downtown Salt Lake City, (3) the Cottonwood fault in southern Salt Lake Valley and (4) the western part of the Fort Canyon fault near the Traverse Mountains salient. Other faults in the north central-part of the valley form the West Valley fault zone, which appears to be antithetic to the Salt Lake segment; hence co-rupture is possible of the West Valley fault zone in combination with the Salt Lake City segment (e.g., Youngs et al., 1987; Keaton et al., 1993; DuRoss et al., 2014).

The mean recurrence interval for faulting of the Salt Lake segment is approximately 1,200 to 1,400 years (WGEUP, 2016). The weighted mean characteristic magnitude is 7.12 with a 5th percentile value of 6.91 and a 95th percentile value of 7.28 (WGEUP). No historical events have occurred on this segment, but well-documented evidence of prehistoric faulting has been observed in numerous paleoseismic, geologic and geotechnical investigations (Paleoseismology of Utah Series; Utah Geological Survey GeoData Archive System). Expected peak ground acceleration (pga) values for surficial soil conditions vary from about 0.1 to 1.1 g according to soil conditions and distance from the fault (Wong et al., 2002), which is the basis for the triggering analysis performed in Appendix B. Ground acceleration of this amplitude may cause liquefaction-induced ground failure in many parts of the central and northern valley, especially in the Holocene fluvial and alluvial deposits found in these areas.

4 PREVIOUSLY MAPPED LATERAL SPREAD DEPOSITS

Numerous paleoseismologic, geologic and geotechnical investigations conducted in the Salt Lake Valley have documented the presence of prehistoric ground failures, which in part, have been attributed to liquefaction-induced lateral spread (e.g., Osmond et al., 1965; Keaton and Anderson, 1995; Simon and Bymaster, 1999; Kleinfelder Inc., 1999; Cotton, Shires and Associates, 1999; Korbay and McCormick, 1999; Black el al., 2003).

Geologic mapping and investigations in downtown Salt Lake City have identified three areas of prehistoric ground failure: (1) lateral spread deposits (mapped as clsp unit of Holocene to middle Pleistocene age by Personius and Scott, 1992) located between 300 East and 600 East and extending from South Temple Street to about 300 South (Personius and Scott, 1992), (2) clsp unit located between 200 East and 400 East and extending between 400 and 500 South, where the Old Metropolitan Hall of Justice was located and the current location of the Salt Lake City Library is found (Osmond et al., 1965) (Personius and Scott, 1992) and (3) ground displacement located at the Salt Palace Convention Center (SPCC) Expansion Project (Simon-Bymaster, 1999; Kleinfelder, 1999; Cotton, Shires and Associates, 1999; Black et al., 2003; Leeflang 2008). The ground displacement features discovered at the SPCC during foundation excavations have been extensively studied and their causal mechanism(s) are somewhat controversial and uncertain (Simon and Bymaster, 1999; Kleinfelder, 1999; Cotton, Shires and Associates, 1999; Black et al., 2003; Korbay and McCormick, 1999). However, all of these SPCC investigations indicate that liquefaction occurred in this area due to the presence of liquefaction dikes observed in some of the trench walls, however it is likely that tectonic faulting may also be associated with the prehistoric ground failure mapped in this area.

5 REGIONAL LIQUEFACTION MAPPING

On a larger scale, subsurface and groundwater data in combination with surficial geologic maps can be used to create liquefaction hazard maps in areas where prehistoric liquefaction has not been discovered. Liquefaction hazard maps can be

classified into three general types: (1) liquefaction susceptibility maps, (2) liquefaction potential maps and (3) liquefaction ground failure maps (Youd and Perkins, 1978; Power and Holzer, 1996). Liquefaction susceptibility maps describe the relative vulnerability or susceptibility of the soil to liquefaction and are based on geological mapping of depositional environments and/or descriptions of the soil's texture and age. These maps do not consider the level or frequency of the earthquake shaking. In contrast, liquefaction potential maps combine soil susceptibility information with the seismicity of the area to describe the likelihood or potential of liquefaction for deterministic or probabilistic scenario events. Lastly, liquefaction ground failure maps show estimates of the expected amount of permanent ground displacement associated with an event or hazard level. These latter maps are considered the most useful type of map for assessment and mitigation of liquefaction-induced damage (Youd and Perkins, 1987).

Liquefaction potential maps have been compiled and interpreted to create liquefaction county hazard maps for development, planning and natural disaster preparation. The first liquefaction potential map for the Salt Lake Valley was developed by Anderson et al. (1987) and later revised by Anderson et al. (1994) and digitized by Jarva (1994). The Anderson et al. (1994) map is currently adopted by most municipalities in Salt Lake County for liquefaction hazard identification. This map was developed from geologic mapping, Standard Penetration Test (SPT) penetration resistance (blow count) N values and borehole soil descriptions using a relatively limited geotechnical database. From these data, estimates of the liquefaction potential were calculated and generalized to the mapped area. More recently, Solomon et al. (2004) developed a liquefaction ground failure map that presents the Liquefaction Severity Index (LSI) (Youd and Perkins, 1987) for the Salt Lake Valley. However, this approach did not implement subsurface geotechnical data, but was based solely on surficial geologic mapping. Recently, Erickson (2007) completed a probabilistic liquefaction potential map for the Salt Lake Valley using subsurface geotechnical data and surficial mapping that combines the input from the USGS probabilistic seismic hazard maps (Frankel et al., 2002) with the probability of triggering liquefaction using probabilistic curves developed

by Seed et al. (2003). Bartlett et al. (2005) and Olsen et al. (2007) have produced a lateral spread displacement hazard map for a **M**7.0 Wasatch fault scenario earthquake for northern Salt Lake Valley. This report extends the work of Bartlett et al. (2005) and Olsen et al. (2007) by developing liquefaction-induced lateral spread displacement and ground settlement failure maps for the entire Salt Lake Valley based on a **M**7.0 Wasatch fault event (Wong et al., 2002).

6 GEOTECHNICAL DATABASE DEVELOPMENT

6.1   Data Collection

The liquefaction failure mapping was based on an extensive geotechnical database compiled in ArcGIS® and was used to evaluate the lateral spread and ground settlement potential in the Salt Lake Valley (Bartlett et al., 2005; Olsen et al. 2007, Erickson, 2007). Efforts were made to gather subsurface information for nearly all major geologic units (Figure 2-1). The compiled database (U of U Utah Liquefaction Website) contains subsurface information from 963 boreholes drilled in the valley since 1959 (Figure 6-1).

Most of the borehole logs were obtained from recent Utah Department of Transportation highway projects, most notably: I-15 / I-80 Reconstruction (1997-2001); SR-154 Bangerter Highway (1988-1998); I-215 (1976-1989), I-80 Reconstruction (west-side (1986-1991). These subsurface explorations generally extends to depths of 15 m (50 ft), and were significant deeper near bridge structures 30 – 40 m (100 – 130 feet). In other areas of the valley, the major contributors of subsurface data were Salt Lake County, city municipalities and various geotechnical consultants.

The information compiled in the geotechnical database includes borehole logs, soil descriptions, groundwater levels, SPT blow counts, measurements of fines content, mean grain size and soil unit weight for the various subsurface layers. Bartlett et al., (2005) compiled a statistical description of the geologic units found in the northern part of the mapped area (mapped units located north of 3500 South Street, Figure 6-1) (Appendix A). This is included to describe the predominate soil-type, corrected N values

11

(i.e., $N1_{60}$) for granular soils, and plastic index fine-grained soils for the major geologic units found in the northern part of the mapped area (Appendix A).

Additionally, shear wave velocity (V_s) data for the Salt Lake Valley (Ashland and McDonald, 2003) for approximately 160 locations were added to the database: (http://www.civil.utah.edu/~bartlett/ULAG/vs_30_2004b_ed.xls). V_s estimates were required to complete probabilistic liquefaction evaluations performed by Erickson (2007). This V_s dataset and developed map (Figure 6-2) was used to assign the surficial mapping (Figure 2-1) to representative site-response unit groups based on similar subsurface profile characteristics (e.g., near-surface soil type, origin, deposition, age and average Vs values). V_s values were averaged over 12 and 30 m depths (i.e., Vs_{12} and Vs_{30}, respectively) (Erickson, 2007). Subsequently, each surficial geologic unit (Figure 2-1) was assigned to its corresponding site-response unit using the Vs_{30} soil map (Figure 6-2) where the site class definitions in this figure are from ASCE 7 (ASCE/SEI 7-10) as adopted by the 2015 International Building Code (IBC, 2015). In this system, site class A consists of hard rock with Vs_{30} values greater than 1500 m/s. Site class B consists of rock with Vs_{30} values between 760 and 1500 m/s. Site class C consists of very dense soil to soft rock with Vs_{30} values between 360 and 760 m/s. Site class D consists of stiff soil with Vs_{30} values between 180 and 360 m/s. Soil class E consists of soft soil with Vs_{30} values less than 180 m/s. Soil class F consists of soils vulnerable to failure or collapse under seismic loading (i.e. liquefaction), peats, highly organic clays, very high plasticity clays, and very thick soft to medium stiff clays problematic soils (not mapped) which require site response analysis and site-specific geotechnical investigations and evaluations (ASCE/SEI 7-10).
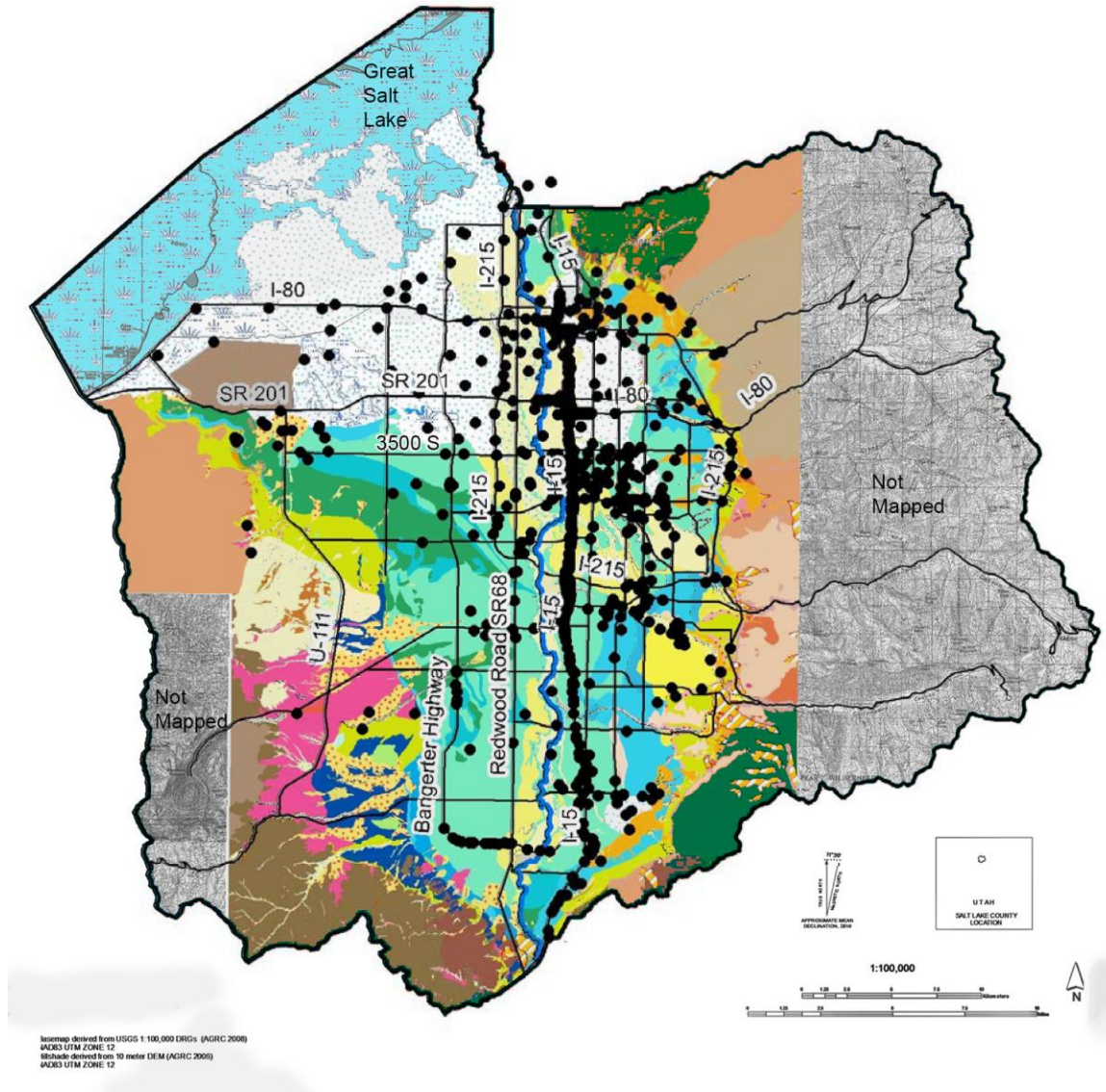
Figure 6-1. Locations of geotechnical boreholes contained in ArcGIS® geotechnical database, Salt Lake County, Utah.
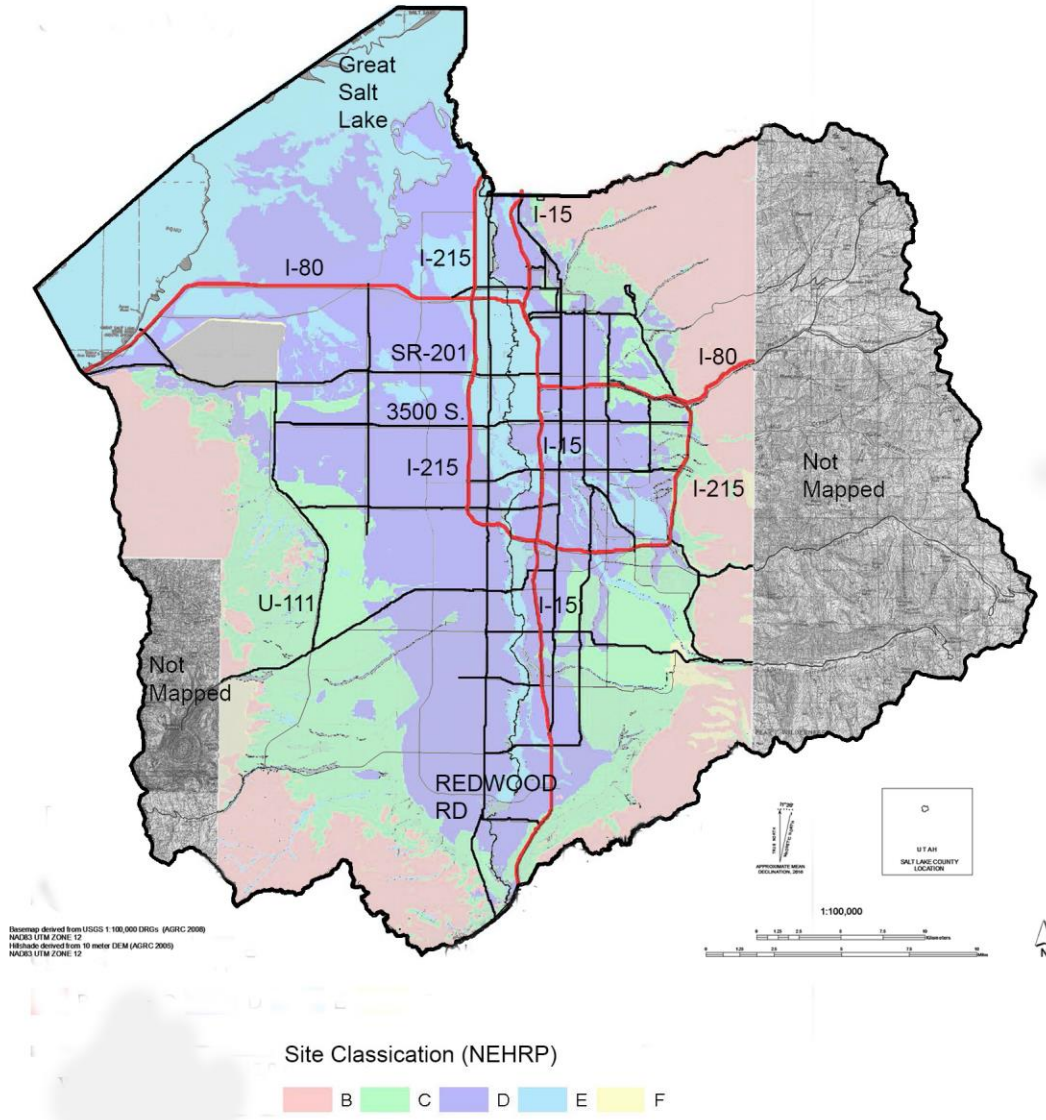
Figure 6-2. Site or soil classification map for Salt Lake County based on Vs$_{30}$ measurements according to National Earthquake Hazard Reduction Program (NEHRP) classification system as used in the International Building Code (2015).

6.2   Sample Size Assessment

Table 6-1 summarizes the number of geotechnical boreholes obtained in each of the mapped units found in Figure 2-1. It also shows the granularity of the soil (i.e., coarse-grained vs. fine-grained), age, relative liquefaction susceptibility, as defined by Youd and Perkins (1978), and the relative areal extent of the mapped unit.

Units with a moderate, or higher liquefaction susceptibility have been shaded in Table 6-1. This was done to evaluate these units in terms of their data support (i.e., number of boreholes obtained in each unit). In general, units that are widespread and have a moderate, or higher, liquefaction susceptibility have sample sizes greater than 100 boreholes (Table 6-1). However, a notable exception is the Qly unit (Holocene lacustrine and marsh deposits) located in the northeastern part of the mapped area (Figure 2-1). This unit contains only 5 boreholes and has been assigned a high liquefaction susceptibility by Castleton et al. (2011); hence it requires more investigation. In addition to this, alluvial and lacustrine units found in the southeast quadrant of the mapped area are under-sampled (Figure 6-1). However, these units (QTaf, Qafy, Qafo, Qlbg, Qlbs) were classified as having very low to low liquefaction susceptibility using the Youd and Perkins (1978) classification (Table 6-1). Their relatively low susceptibility is due to their older age (late Pleistocene, or older, in general) and type of depositional environment (lacustrine or alluvial fan deposits). Nonetheless, it would be beneficial to obtain more subsurface data in this under-sampled area to confirm this preliminary assessment and to evaluate the depth of groundwater in this area.

Lastly, the Qclsp unit (Lateral spread deposits) was investigated by Leeflang (2008) and found not to be susceptible to lateral spread ground failure. Also, the Qca unit has a very limited extent in the mapped area (Figures 2-1 and C-1); hence is not of great concern. In addition, it should be noted that the database does not contain boreholes within the Qf unit (Artificial fill). Fill material, depending on type of soil used, degree of construction compaction and groundwater conditions, can be susceptible to

liquefaction, if improperly compacted (Youd and Perkins, 1978). It is recommended that

fill material, due to its highly variable nature, be evaluated on a case-by-case basis.

Table 6-1. Number of database boreholes in major surficial geologic units.

Name	Description	No. of Boreholes	Granularity	Age	Liquefaction Susceptibility (Youd and Perkins, 1978)	Areal Extent in mapped area
Stream Alluvium						
Qal1	Modern stream alluvium 1	288	Coarse-grained	Upper Holocene	High	Wide-spread
Qal2	Modern stream alluvium 2	111	Coarse-grained	Upper Holocene	High	Wide-spread
Qalp	Stream alluvium related to the Provo (regressive) phase of Lake Bonneville	10	Coarse-grained	Upper Pleistocene	Low	Localized
Qaly	Stream alluvial deposits, undivided	15	Coarse-grained	Holocene-Upper Pleistocene	Low	Wide-spread
Alluvial Fan Deposits						
Qaf2	Alluvial fan deposits 2	28	Mixed	Holocene	Low	Localized
Qafy	Alluvial fan deposits, undivided	6	Mixed	Holocene-Upper Pleistocene	Low	Localized
Qafb	Alluvial fan deposits of the Bonneville (transgressive) phase	3	Mixed	Upper Pleistocene	Low	Very Localized
Qafo	Older alluvial fan deposits, undivided	1	Mixed	Upper to Middle Pleistocene	Low	Wide-spread
QTaf	Oldest alluvial fan deposits	1	Mixed	Middle Pleistocene to Upper Miocene	Low	Wide-spread
Young Lacustrine and Mixed-Environment Deposits						
Qly	Lacustrine and marsh deposits	5	Fine-Grained	Holocene	Moderate	Wide-spread
Qlaly	Lacustrine, marsh and alluvial deposits	136	Fine-Grained	Holocene-Upper Pleistocene	Moderate to Low	Wide-spread
Lake Bonneville Lacustrine Deposits						
Qlpd	Deltaic gravel of the Provo (regressive) phase	5	Coarse-grained	Upper Pleistocene	Low	Localized
Qlpg	Lacustrine gravel and sand of the Provo (regressive) phase	40	Coarse-grained	Upper Pleistocene	Low	Wide-spread

Name	Description	No. of Bore-holes	Granu-larity	Age	Lique-faction Suscepti-bility (Youd and Perkins, 1978)	Areal Extent in mapped area
Qlps	Lacustrine sand and silt of the Provo (regressive) phase	0	Fine-Grained	Upper Pleistocene	Low	Very Localized
Qlpm	Lacustrine clay and silt of the Provo (regressive) phase	0	Fine-Grained	Upper Pleistocene	Low	Wide-spread
Qlbg	Lacustrine gravel and sand of the Bonneville (transgressive) phase	14	Coarse-grained	Upper Pleistocene	Low	Wide-spread
Qlbs	Lacustrine sand and silt of the Bonneville (transgressive) phase	1	Mixed	Upper Pleistocene	Low	Very Localized
Qlbm	Lacustrine clay and silt of the Bonneville (transgressive) phase	5	Fine-Grained	Upper Pleistocene	Low	Very Localized
Qlbpg	Lacustrine gravel and sand of the Bonneville Lake cycle, undivided	12	Coarse-grained	Upper Pleistocene	Low	Wide-spread
Qlbps	Lacustrine sand and silt of the Bonneville Lake cycle, undivided	5	Mixed	Upper Pleistocene	Low	Wide-spread
Qlbpm	Lacustrine silt and clay of the Bonneville Lake cycle, undivided	269	Fine-grained	Upper Pleistocene	Low	Wide-spread

Colluvial Deposits

Name	Description	No. of Bore-holes	Granu-larity	Age	Lique-faction Suscepti-bility	Areal Extent in mapped area
Qclsp (Qmls)	Lateral spread deposits	2	Coarse-grained	Holocene-Upper Pleistocene	Low to High	Very Localized
Qca	Colluvium and alluvium, undivided	1	Coarse-grained	Holocene-Mid. Pleistocene	Moderate to Low	Very Localized
Qes	Eolian sand	1	Coarse-grained	Holocene	High	

Artificial Deposits

Name	Description	No. of Bore-holes	Granu-larity	Age	Lique-faction Suscepti-bility	Areal Extent in mapped area
Qf	Artificial fill	0	Mixed	Historical	Low to Very High	Localized

6.3   Data Quality Assessment

The subsurface information originated from 963 boreholes with the majority those obtained from transportation projects sponsored by the Utah Department of Transportation. The most important borehole factors for prediction of liquefaction-induced ground deformation are: SPT N value, fines content and mean grain size of granular sediments of found within the subsurface profile (Youd et al., 2002). The accuracy of the SPT N value is highly influenced by the energy delivered to the drill rod and sampler by the SPT hammer. Fortunately, the hammer energy was known for the majority of the borehole logs because drill rigs used for the geotechnical investigations had been employed by the UDOT. UDOT required the measurement of the hammer energy for the drill rigs working on its recent projects, most notably the I-15 Reconstruction Project (Dames and Moore, 1996 a, b, c; Kleinfelder, 1996 a, b, c, d).

For non-UDOT projects, the hammer energy was estimated based on the type of hammer used for the sampling. A hammer energy ratio of 45 percent of the theoretical maximum was used for donut hammers, 60 percent for safety hammers and 78 percent for automatic trip hammers, as recommended by Seed et al., (1985).

In addition, there was a considerable sampling of the percent of fines content measurements in the database (2,261 samples), because UDOT routinely required sieve analyses on granular material for liquefaction evaluations. The number of mean grain size measurements in the database was less (315); hence methods were needed to account for this under sampling, as described further in the lateral spread displacement map development section of this report.

6.4   Groundwater Evaluations

Liquefaction and the resulting ground displacement cannot occur if the granular sediments are not loose and saturated. Generally, lateral spread displacement almost always occurs in saturated sediments located in the upper 15 m (50 ft) of the soil profile (Bartlett and Youd, 1992); hence, depth to groundwater is required for liquefaction, lateral spread and ground settlement calculations.

A comprehensive groundwater map did not exist for the study area, nor was there sufficient historical data to accurately model water table fluctuations throughout the valley. Thus, the recorded groundwater depths from the geotechnical borehole logs were used for the lateral spread and ground settlement calculations. The maximum depth of the boreholes was approximately 30 to 40 m (100 to 130 feet); hence all groundwater measurements used in this study represent the depths measured in the upper, shallow aquifer of the Salt Lake Valley at the time the geotechnical borehole was completed. The bulk of the boreholes were drilled as part of roadway projects covering a period from about the mid-1980s through the 1990s.

To account for a potential, future rise in the water table, the depth to groundwater was conservatively decreased by 5 feet in all boreholes for our calculations. This was done so as to increase the potential for liquefaction in layers located near the water table. In addition, if part of a soil layer was found below the water table, as indicated on the borehole log, the entire layer was assumed to be saturated for our analyses. By doing so, most loose, granular layers found near the water table had the opportunity to be treated as potentially liquefiable in these evaluations.

6.5   Topography Calculations

The slope of the ground surface and the presence of nearby topographical features (e.g., river and stream channels) are important factors in estimating the potential amount of lateral spread (Bartlett and Youd, 1992). To incorporate these effects, a 1 meter digital elevation model (DEM) from the USGS (USGS, National Map) and free face features such as river channels and canals were used in ArcGIS® analysis to approximate the surface slope and distance and height of a nearby free face, if present, for each borehole location (Bartlett et al., 2005, Olsen et al., 2007). Since the analysis performed in this report, additional higher resolution DEM and LiDAR data have become available (Utah AGRC, Elevation and Terrain Data).

20

7 LIQUEFACTION HAZARD MAPPING

Estimates of pga for the **M**7.0 Wasatch fault zone scenario event were obtained from Wong et al. (2002) and used in accordance with the method and criteria proposed by NCEER (1997) to evaluate the potential for triggering liquefaction. This triggering analysis was done to verify that liquefaction would be triggered in the borehole prior to estimating the amount of lateral spread and ground settlement displacement (Bartlett et al., 2005; Olsen et al., 2007). In short, following the methods outlined in Youd et al., (1997), SPT N values (i.e., blow counts) were normalized and corrected to $(N_1)_{60}$ clean sand values. Subsequently liquefaction triggering analyses were completed at each borehole location (Figure 6-1) using the liquefaction triggering curves found in Youd et al. (1997).

Because of the relatively high expected values of pga in many parts of the Salt Lake Valley, liquefaction is expected to be triggered in recent sediments with $(N_1)_{60}$ clean sand values less than about 30. However, triggering of liquefaction does not necessarily generate liquefaction-induced ground failure, so liquefaction triggering maps are not as useful as ground failure maps for planning and damage evaluations. Hence, the next sections focus on the development of ground failure maps.

7.1 Lateral Spread Displacement Map Development

Lateral spread ground displacement is generally restricted to liquefied, saturated, granular deposits having $(N_1)_{60}$ values less than 15 (Bartlett and Youd, 1992). Thus, lateral spread hazard ground failure maps do not directly require estimates of pga for the mapping process, but they do require estimates of earthquake moment magnitude, M_w, and surface distance to the causative fault, R, as the primary seismic inputs (km). The lateral spread ground failure maps presented in this report are a continuation of work completed for the northern part of the Salt Lake Valley by Bartlett et al. (2005) and Olsen et al. (2007) and are based on Bartlett and Youd (1992) and Youd et al., (2002).

Lateral spread displacements were estimated by the Youd et al. (2002) regression model at each borehole location shown in Figure 6-1 as further described in Appendix C. In addition to the seismic inputs discussed in the previous paragraph, the model requires the following topographical and soil inputs: distance to free face and height of free face (if applicable), W, ground slope, S, (if applicable), and cumulative thickness, average fines content and mean grain size of all saturated granular layers with SPT $(N_1)_{60}$ N values less than 15 (T_{15} F_{15} and D50$_{15}$, respectively). The scenario analysis was based on a median **M**7.0 earthquake on the Salt Lake City segment of the Wasatch fault zone (Wong et al., 2002) while the entered values of horizontal distances, R, varied based on the proximity of the fault to the borehole.

The fines and mean grain size measurements for saturated, granular layers were evaluated according to the major soil type listed on the borehole log by layer and geologic unit, where the latter varied with depth in many cases. For example, recent alluvium often was underlain by upper Pleistocene Lake Bonneville lacustrine deposits. For such cases, the fines and mean grain size measurements were assigned to the respective geologic unit using the soil descriptions from the borehole logs and the interpreted layering obtained from adjacent cone penetrometer (CPT) soundings. However, laboratory-determined fines content and mean grain size values were not available for some saturated, granular layers in some borehole logs. Hence, a classification system was developed to assign data quality indicators to each individual datum (i.e., granular layer) contained in the geotechnical database (Bartlett et al., 2005). In this system, a "1" was assigned to data where the supporting measurements were obtained from the geotechnical report. In total there were 2,261 fines content and 315 mean grain size measurements in the database that had a data quality ranking of "1." A data quality indicator of "2" was given to layers where the fines content and mean grain size could be reasonably estimated from nearby borehole logs at the same project site, and an indicator of "3" denoted data that were averaged from other nearby boreholes based on their soil type and geologic unit. Missing soil unit weight, fines content and mean grain size data that could not be estimated from nearby boreholes were averaged

22

by soil type using data quality "1" measurements from the entire database. For these averages, a data quality indicator of "4" was assigned to data that represented averaged properties for the same soil type and geologic unit; and a data quality indicator of "5" was assigned to data that represented averaged properties for the same soil type irrespective of the geologic unit. These data quality indicators are tabulated in the Microsoft Access [TM] database (ULAG, 2016) for all saturated granular layers. Fine-grained, plastic layers and layers above the water table or that had $N1_{60}$ values above 15 were excluded from the lateral spread displacement evaluations. In addition, no SPT values were averaged for this study; if such data were missing from the borehole logs, the information was not used.

Lateral spread displacement values were calculated using the Youd et al. (2002) regression model for each borehole having a factor of safety against liquefaction triggering less than or equal to 1.1, as calculated by the method found in NCEER (1997). Measurements of T_{15} were accumulated throughout the borehole to a depth of 15 m (50 ft) and F_{15} and $D50_{15}$ were averaged in the T_{15} layer, as recommended by Youd et al., 2002. This accumulation and averaging of these factors for each borehole was done irrespective of the origin and age of the sediments.

All boreholes with factors of safety against liquefaction triggering greater than 1.1 were assigned a lateral spread displacement of zero m (0 ft). The estimated horizontal displacements (D_H) were further categorized as "minimal" (zero m) (i.e., zero in); "low" (0.0 to 0.1 m) (i.e., 0 to 4 in); "moderate" (0.1 to 0.3 m) (i.e., 4 to 12 in); "high" (0.3 to 1.0 m) (i.e., 12 to 39 in); and "very high" (greater than 1.0 m) (i.e., greater than 39 in). The above ranges were assigned according to ground displacement that produces damage to structures based on observations from previous earthquakes (Youd, 1980; Black et al., 1999). Horizontal ground displacement less than 0.1 m (4 in) is expected to produce little damage and the damage is repairable. Horizontal ground displacement from 0.1 to 0.3 m (4 in to 12 in) is expected to produce severe damage, but the damage is repairable. Horizontal displacement greater than 0.3 m (12 inches) is expected to produce severe damage that is not repairable. Beyond this 0.3-m (12 inch) threshold,

severe damage or collapse is expected, depending on the nature and fragility of the structure.

Subsequently, lateral spread displacement hazard categories were assigned to the mapped major surficial geologic units by statistical analyses of the estimated displacements from all boreholes located within each respective geologic unit or group of units representing having similar characteristics (e.g., near-surface soil type, origin, deposition and age).

Using the method discussed by Bartlett et al. (2005) and Olsen et al. (2007), cumulative histograms of increasing hazard severity were developed to determine an 85 percent non-exceedance threshold for the **M**7.0 scenario event (Appendix C, Figures C-2 to C-7). The 85 percent non-exceedance criterion means that less than 15 percent of the estimated displacements exceeded the upper bound of the hazard category that was assigned to the respective geologic unit or group of units. Thus, the mapped estimate approximately represents a mean plus one standard deviation estimate for each mapped unit with a 15 percent, or less, probability of exceedance. This 15 percent exceedance criterion represents a consensus of the Utah Liquefaction Advisory Group made in its 2009 annual meetings (UGS Liquefaction Advisory Group Website).

In a few areas, several clearly defined homogenous or nearly homogenous clusters of similar displacement values were found that differed from the remaining estimates represented within the same geologic unit. In these cases, the geologic units were subdivided prior to conducting statistical analysis, so that the displacement estimates were more locally homogenous. This subdivision was done using the superposition of the surficial geology (Figure 2-1) and estimates of the ground displacement calculated at the borehole locations (Figure C-1).

7.2   Ground Settlement Displacement Map Development

Liquefaction-induced ground settlement estimates were calculated by averaging the results of Tokimatsu and Seed (1987) and the Yoshimine et al. (2006) methods, where the latter method is based on work proposed by Ishihara and Yoshimine (1992). These methods are commonly used in engineering practice to estimate liquefaction-induced ground settlement for the free field condition (i.e., without the influence of overlying or adjacent foundations). Both methods estimate ground settlement based on SPT N values, which are contained in geotechnical database.

The Tokimatsu and Seed (1987) method was used to estimate volumetric strain in saturated clean sands based on cyclic stress ratio and SPT values, $(N_1)_{60}$ (Figure 7-1). The method is based on correlations of field measurements and supplementary laboratory experimental data used to develop predictive curves of post-liquefaction settlement (i.e., volumetric strain) as a function of SPT N values based on settlements recorded during the 1964 Niigata, 1968 Tokachioki and 1968 Miyagiken Oki, Japan earthquakes. For the purposes of our study, the curves presented in Figure 7-1 were digitized into over 1,400 interpolated data points (Appendix B, Figure B-1) and included in an analysis to estimate volumetric strain for each liquefiable layer.

The Yoshimine et al. (2006) method is based on a series of equations to describe the liquefaction-induced volumetric strain prediction curves presented in Ishihara and Yoshimine (1992) that were derived from strains observed in cyclic laboratory testing performed by Nagase and Ishihara (1988). These curves correlate factor of safety against liquefaction triggering to the maximum single amplitude of shear strain (γ_{max}) based on relative density estimated from SPT N_1 values (Figure 7-2). The maximum single amplitude of shear strain is then used to estimate post-liquefaction volumetric strain due to reconsolidation (Figure 7-3). The Yoshimine et al. (2006) equations were used in the ArcGIS® routines to facilitate rapid calculations (Appendix B).

To estimate liquefaction-induced settlement using the Tokimatsu and Seed (1987) method, the field measured blow count data contained in the geotechnical

database were normalized and corrected to $(N_1)_{60}$ clean sand values and liquefaction triggering analyses were completed at each borehole location following the methods outlined in Youd et al. (2002). A reference table was created from the data points interpolated from Figure B-1 and to estimate liquefaction-induced volumetric strains where the factor of safety against liquefaction triggering was less than or equal to 1.1. The required input variables consisted of $(N_1)_{60}$ values normalized and corrected to clean sands using the method of Youd et al. (2002) and cyclic stress ratios calculated in accordance with the guidelines presented in Tokimatsu and Seed (1987). The scenario analysis was based on the median ground motion associated with a **M**7.0 earthquake on the Salt Lake City segment. Settlement at each borehole location was calculated by multiplying the volumetric strains and the corresponding thickness of each respective liquefiable soil layer. A ground settlement value of zero m (0 ft) was assigned to all borehole locations having factors of safety for liquefaction triggering greater than 1.1.

To estimate liquefaction-induced settlement by Yoshimine et al. (2006), the raw blow count data contained in the geotechnical database were normalized and corrected to $(N_1)_{60}$ clean sand values following the methods outlined in Youd et al. (2002). To account for the hammers energy ratio used in Japanese practice, the $(N_1)_{60}$ clean sand values were converted to N_1 values using the guidelines given in Seed et al. (1985). Following the method of Yoshimine et al. (2006), the N_1 values were converted to relative densities using the relation of Meyerhof (1957), and the likelihood of liquefaction triggering was calculated based on the Japan Highway Association (2000). Using the relative densities and the factors of safety against liquefaction triggering, the maximum single amplitude of shear strain was calculated for all sites with a factor of safety against liquefaction triggering less than or equal to 1.1. From this, liquefaction-induced volumetric strains were estimated by the relative densities and the maximum single amplitude of shear strain. Settlements were calculated by multiplying the volumetric strain by the thickness of each respective liquefiable soil layer. A ground settlement value of 0 m (0 ft) was assigned to all borehole locations with factors of safety for liquefaction triggering greater than 1.1.

The results from each method were compared at each borehole to determine if there were significant differences in the settlement estimates obtained from the two analysis methods. The evaluation of the **M**7.0 earthquake settlement estimates produced an average difference of 0.004 m between the two methods, with a maximum difference of 0.083 m. Of the 963 boreholes, the Tokimatsu and Seed (1987) method predicted higher settlements than that of Yoshimine et al. (2006) for 232 boreholes, and the opposite was true for 444 boreholes. Both methods predicted no settlement in 287 boreholes. A method-to-method comparison of the predicted differences showed that 74 percent of the boreholes had predicted values within 0.01 m, 92 percent were within 0.025 m and 99 percent were within 0.05 m. Hence, it was concluded that the two methods produced relatively similar results when considering the variability of the input data. Subsequently, the average of the two methods was considered appropriate to estimate the ground settlement at each liquefiable borehole location.

Lastly, the ground settlement estimates were categorized as "low" (0 to 0.05 m) (0 to 2 in); "moderate" (0.05 to 0.1 m) (2 to 4 in); "high" (0.1 to 0.3 m) (4 to 12 in); and "very high" (greater than 0.3 m) (12 in) based on recommendations of the ULAG members (UGS Liquefaction Advisory Group website). Similar to the lateral spread displacement map, hazard categories were assigned to the major geologic units by statistical analysis of the estimated displacements from all boreholes located within each respective geologic unit or group of units with similar subsurface characteristics (e.g., near-surface soil type, origin, deposition and age). In brief, the hazard category assignments for the **M**7.0 ground settlement scenario map were based on an 85 percent, or greater, probability of non-exceedance (Appendix B).

7.3   Combined Liquefaction-Induced Ground Displacement Hazard Map

A combined liquefaction-induced ground displacement hazard map for a **M**7.0 rupture of the Salt Lake City segment of the Wasatch fault zone is presented in Figure 7-4. This map combines the lateral spread (horizontal displacement) and ground settlement (vertical displacement) hazard. It shows the range of estimated values of

horizontal displacement resulting from liquefaction-induced lateral spread and of vertical displacement resulting from liquefaction-induced ground settlement for the **M**7.0 scenario event. The mapped horizontal and vertical displacement estimates have an 85 percent, or greater, probability of non-exceedance for the scenario event.
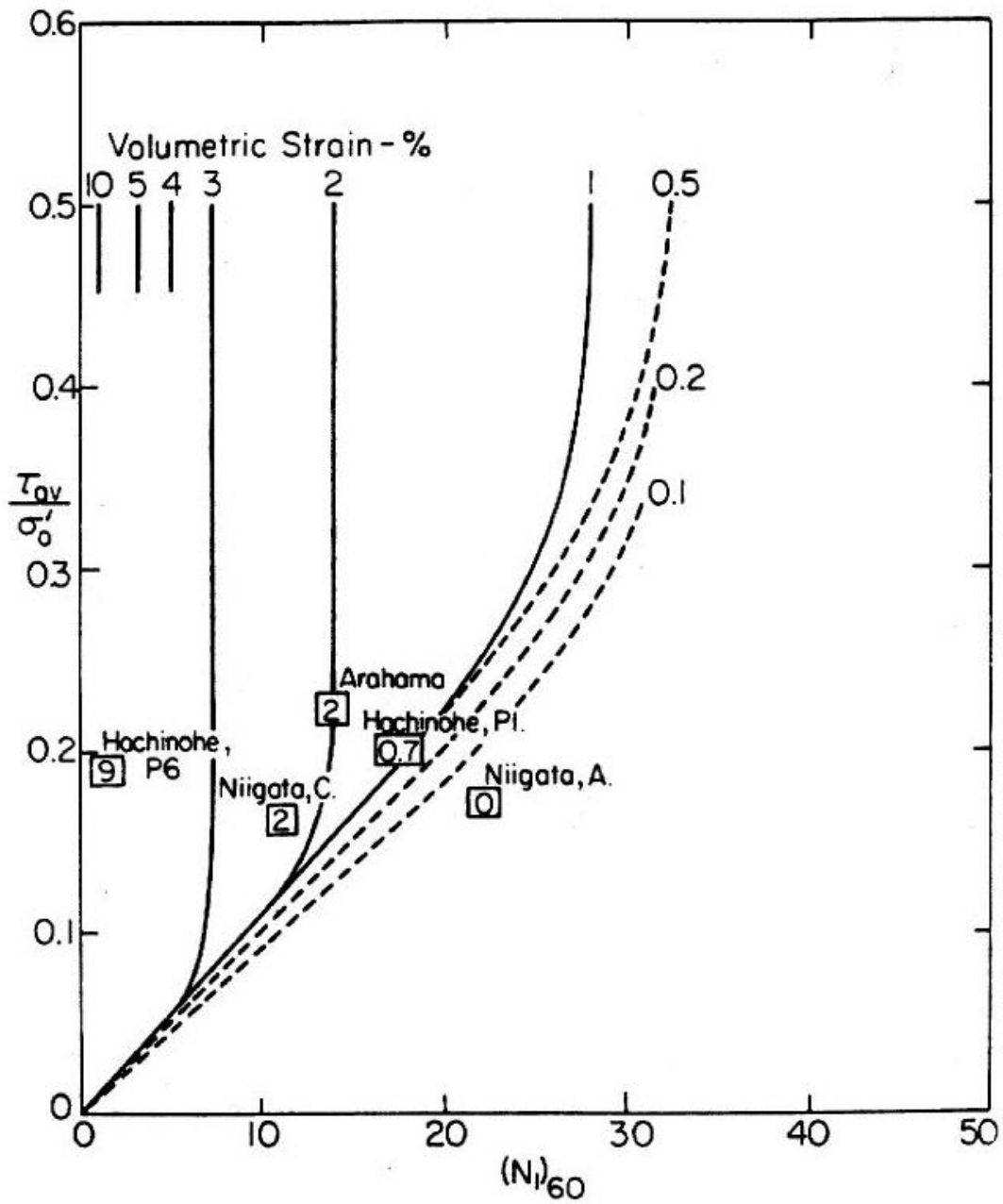
Figure 7-1. Relationships between $(N_1)_{60}$, Cyclic Stress Ratio and Volumetric Strain for Saturated Clean Sands (Tokimatsu and Seed, 1987).
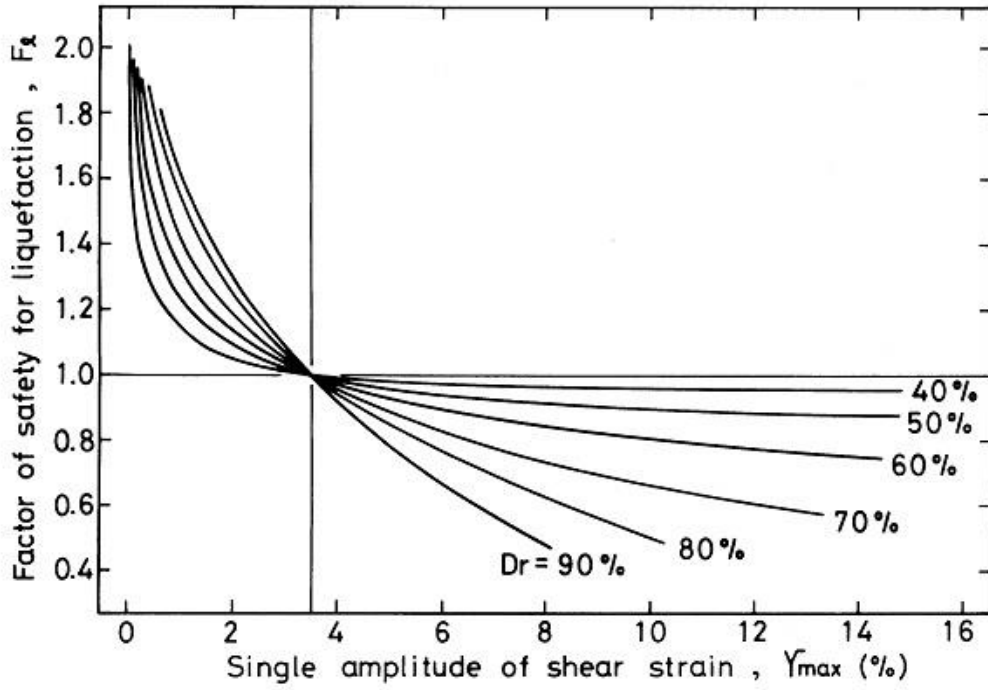
Figure 7-2. Relationships between liquefaction factor of safety and maximum shear strain (Ishihara and Yoshimine, 1992).
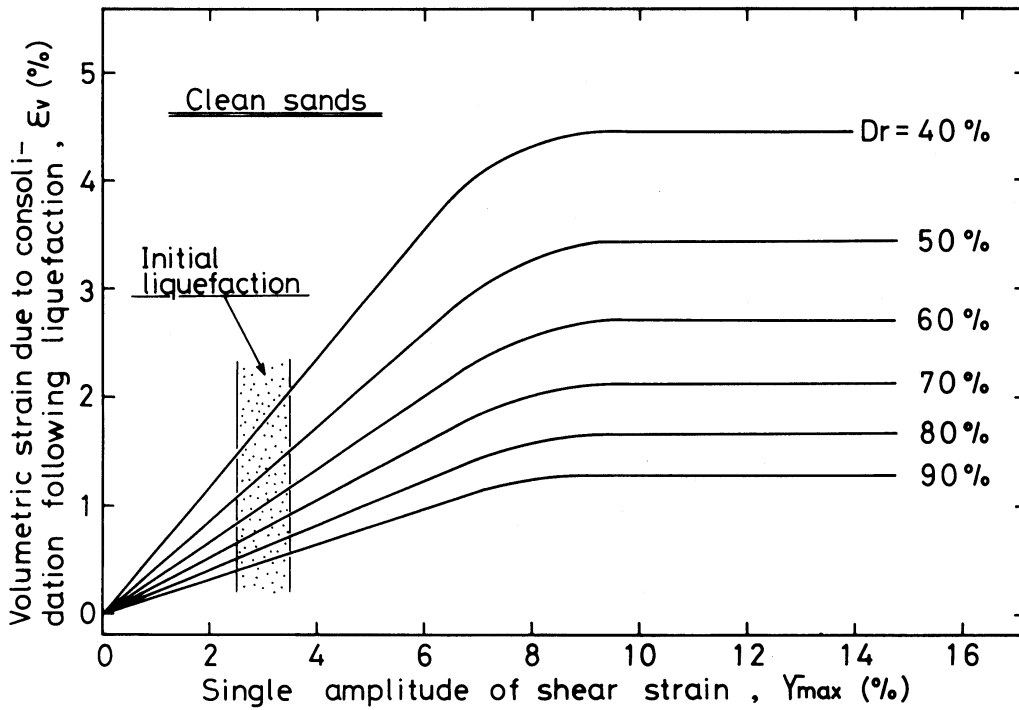
Figure 7-3. Relationships between re-consolidated volume change and shear strain (Ishihara and Yoshimine 1992).

30
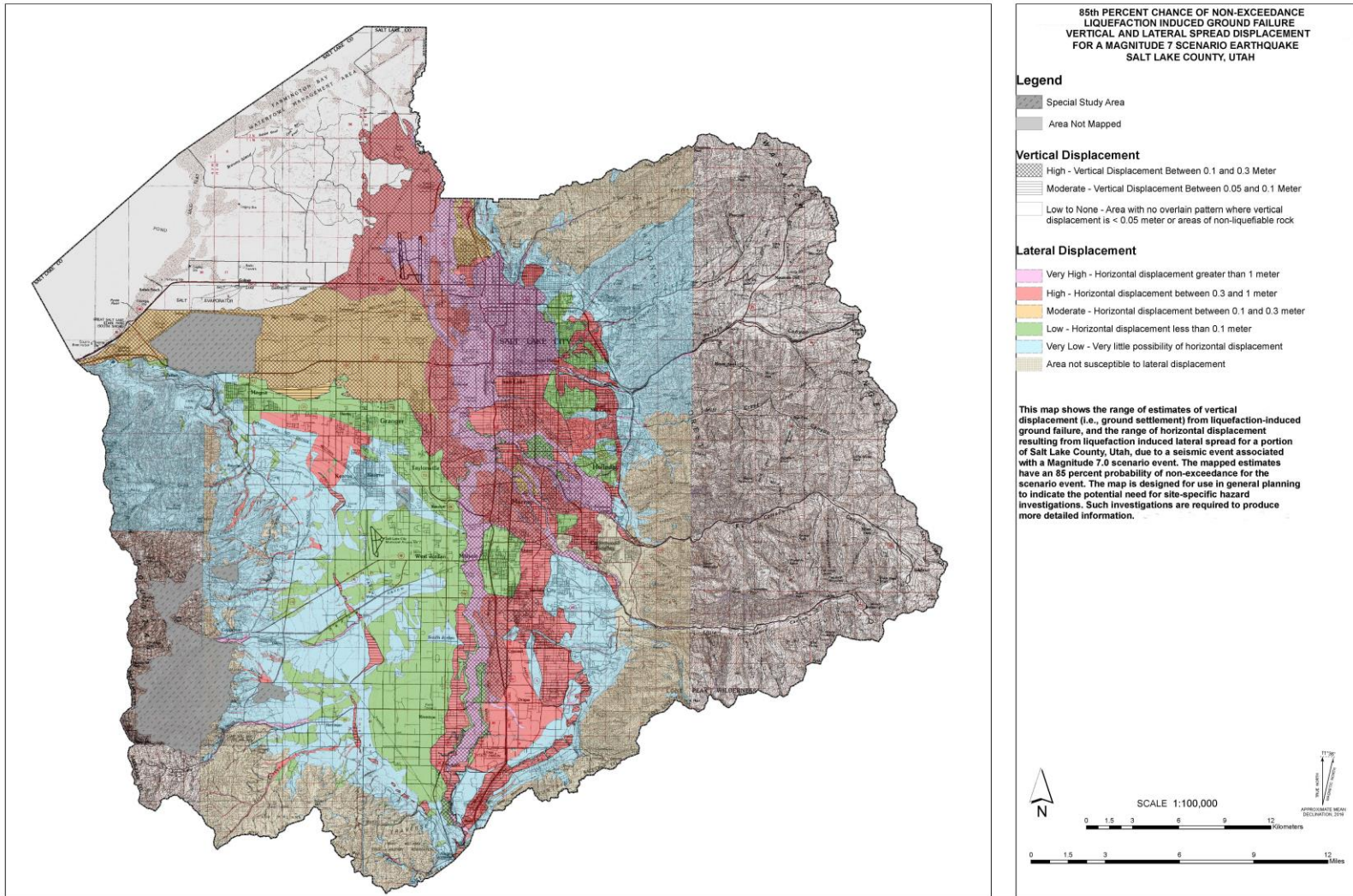
Figure 7-4. Liquefaction-induced ground displacement hazard with an 85 percent, or greater, non-exceedance probability threshold for the Salt Lake Valley, Utah for a M7.0 scenario earthquake on the Salt Lake segment of the Wasatch fault zone.

8 CONCLUSIONS

A liquefaction-induced displacement hazard map presented herein was developed for Salt Lake County, Utah using an extensive geotechnical database that complemented surficial geological mapping efforts. Because the map is displacement based, it is believed to better represent the damage potential to the built-environment than previously published liquefaction potential maps, such as that of Anderson et al., (1987), which only indicates the potential for liquefaction effects.

The map shown in Figure 7-4 was developed for the median estimate of strong motion associated with a **M**7.0 event on the Salt Lake City segment of the Wasatch fault zone. The results of the hazard calculations suggest that increased lateral spread and ground settlement hazard exist in the central part of the valley along and near the Jordan River and its tributaries, and in the northeastern part of the valley. The increased ground displacement hazard in these areas is due to the presence of young, relatively loose granular deposits and the potential for the presence of relatively shallow groundwater. The mapped surficial geology in these areas generally consists of saturated, recent alluvial, river, stream and lake deposits.

The map shown in Figure 7-4 is recommended for preliminary planning and zoning purposes because it has been developed for the characteristic **M**7.0 earthquake on the Salt Lake City segment of the Wasatch fault zone; hence it represents a likely earthquake scenario for planning purposes. For areas where the mapped ground displacement hazard rating is moderate, or higher, site-specific geotechnical investigations and calculations are recommended to support requisite engineering evaluations, as required and detailed in the appropriate jurisdictional codes and ordinances. The additional site-specific subsurface information should be planned so as to reduce the inherent uncertainties associated with regional mapping efforts, such as this one, and allow for improved decision making regarding the potential of liquefaction damage to infrastructure at proposed site(s).

The Qly unit in the northwestern part of the study area (Figure 2-1) contained only 5 boreholes and was assigned a moderate lateral spread hazard and a high ground settlement hazard (Figure 7-4) based on susceptibility mapping by Castleton et al., (2011). In addition, alluvial and lacustrine units found in the southeast quadrant of the mapped area are under-sampled (Figure 6-1). However, these units (QTaf, Qafy, Qafo, Qlbg, Qlbs) were classified as having very low to low liquefaction susceptibility using the Youd and Perkins (1978) classification (Figure 7-4). It would be beneficial to obtain more subsurface data in this under-sampled area to confirm this preliminary assessment and to evaluate the depth of groundwater in this area.

9 REFERENCES

Anderson, L. R., Keaton, J. R., Bay, J. A., 1987, *Liquefaction potential map for the Northern Wasatch Front, Utah*, Final Report to the U.S. Geological Survey.

Anderson, L. R., Keaton, J. R., Spitzley, J. E., and Allen A. C., 1994, Liquefaction potential map for Salt Lake County, Utah: Utah State University Department of Civil and Environmental Engineering and Dames and Moore, unpublished final technical report prepared for the U.S. Geological Survey, National Earthquake Hazards Reduction Program Award No. 14-08-0001-19910, 48 p; published as Utah Geological Survey Contract Report 94-9, 1994.

Arnow, T., van Horn, R., and LaPray, R., 1970, The pre-Quaternary surface in the Jordan Valley, Utah, U.S. Geological Survey Professional Paper 700, p. D257-D261.

American Society of Civil Engineers (ASCE/SEI) 7-10, *Minimum Design Loads for Buildings and Other Structures*, Chapter 20, Site Classification Procedure for Seismic Design.

Ashland, F. X., and McDonald, G. N., 2003, Interim map showing shear wave velocity characteristics of engineering geological units in the Salt Lake Valley, Utah metropolitan area, Utah Geological Survey Open File Report 424, 43 p. pamphlet, scale 1:75,000, CD-ROM.

Bartlett, S. F. and Youd, T. L., 1992, *Case histories of lateral spreads caused by the 1964 Alaska earthquake*, Tech. Rep. No. NCEER-92-0021, National Center for Earthquake Engineering Research, State University of New York at Buffalo, N. Y.

Bartlett S. F., Olsen, M. J., and Solomon, B. J., 2005, *Lateral spread hazard mapping of northern Salt Lake County for a magnitude 7.0 scenario earthquake*, Technical Report submitted to the United States Geological Survey, USGS Award No. 04HQGR0026, 218 p.

Biek, R. F., Solomon, B. J., Keith, J. D., and Smith, T. W., 2004, *Interim geologic maps of the Copperton, Magna, and Tickville Spring quadrangles, Salt Lake and Utah Counties, Utah*, Utah Geological Survey Open-File Report 434, scale 1:24,000.

Biek, R. F., Solomon, B. J., Smith, Tracy W., Keith, J. D., 2007, *Geologic Map of the Copperton Quadrangle, Salt Lake County, Utah, UGS Map 219.*

Black, B.D., Solomon, B.J., and Harty, K.M., 1999, Geology and geologic hazards of Tooele Valley and the West Desert Hazardous Industry Area, Tooele County, Utah : Utah Geological Survey Special Study 96, 65 p., scale 1:100,000.

Black, B. D., Hecker, S., Hylland, M. D., Christenson, G. E., and McDonald, G. N., 2003, *Quaternary fault and fold database and map of Utah,* Utah Geological Survey, Map 193DM.

Bray, J.D., O'Rourke, T. D., Cubrinovski, M., Zupan, J., Jeon, S, Taylor, M. Toprak, S., Hughes, M., van Ballegooy S., Bouziou, D., 2013, *Liquefaction Impact on Critical Infrastructure in Christchurch*, Final Technical Report, U.S. Geological Survey Award Number G12AP20034, March 22, 2013, 51 p.

Castleton, J.J., Elliott, A.H., and McDonald, G.N., 2011, Geologic hazards of the Magna quadrangle, Salt Lake County, Utah: Utah Geological Survey Special Study 137, 73 p., 10 plates, scale 1:24,000.

Cotton, Shires and Associates, Inc., 1999, Final geologic peer review, Salt Place Convention Center expansion, Salt Lake City, Utah, July 30, 1999.

Dames and Moore, (1996a). "Geotechnical Report for the Reconstruction of Structures and Embankments 600 South Section I-15 Corridor From 600 South to 960 South," UDOT Contract No. SP-15-7(129)310, Station 31+275 to 32+420, Salt Lake City, Utah, Sept. 1996.

Dames and Moore, (1996b). "Geotechnical Report for the Reconstruction of Structures and Embankments 1300 South Section I-15 Corridor," UDOT Contract No. SP-15-7(132)308, Station 29+300 to 31+275, Salt Lake City, Utah, Sept. 1996.

Dames and Moore, (1996c). "Geotechnical Report for the Reconstruction of Structures and Embankments 2400 South Section I-15 Corridor," UDOT Contract No. SP-15-7(1287308, Station 26+800 to 29+300, Salt Lake City, Utah, Sept. 1996.

DuRoss, C.B., Hylland, M.D., McDonald, G.N., Crone, A.J., Personius, S.F., Gold, R.D., and Mahan, S.A., 2014, Holocene and latest Pleistocene paleoseismology of the Salt Lake City segment of the Wasatch fault zone, Utah, at the Penrose Drive trench site, in DuRoss, C.B. and Hylland, Lake Valley, Utah—new paleoseismic data from the Salt Lake City segment of the Wasatch fault zone and the West Valley fault zone — Paleoseismology of Utah, Volume 24: Utah Geological Survey Special Study 149, p. 1–39, 6 appendices, 1 plate, CD.

Erickson, G., 2007, *Probabilistic liquefaction potential mapping of the Salt Lake Valley, Utah*, M.S. Thesis, Department of Civil and Environmental Engineering, University of Utah.

Frankel, A., Petersen, M., Mueller, C., Haller, K., Wheeler, R., Leyendecker E. V., Wesson, R., Harmsen, S., Cramer, C., Perkins, D., and Rukstales, K., 2002, *Documentation for the 2002 update of the National Seismic Hazard Maps*, U.S. Geological Survey Open File Report 02-420.

Hamada, M., Yasuda, S., Isoyama, R. and Emoto, K, 1986, *Study on liquefaction induced permanent ground displacements,* Association for the Development of Earthquake Prediction in Japan, Tokyo, Japan.

Hinckley, D. W., 2010, *Liquefaction-Induced Ground Displacement Mapping for the Salt Lake Valley, Utah,* M.S. Thesis, Department of Civil and Environmental Engineering, University of Utah, 149 p.

International Building Code (IBC), 2015, Published by International Code Council (ICC).

Ishihara, K. and Yoshimine, M., 1992, Evaluation of settlements in sand deposits following liquefaction during earthquakes, Soils and Foundations, Vol. 32(1): 173-188.

Japan Highway Association, 2000, *Seismic design code of highway bridges*, Vol. V (in Japanese), pp. 119-126

Jarva, J. L., 1994, *Liquefaction-potential map for a part of Salt Lake County, Utah*, Utah Geological Survey, Public Information Series, PI-25.

Kachadoorian R., 1968, *Effects of the earthquake of March 27, 1964 on the Alaska highway system*, U.S. Geological Survey Professional Paper 545-C.

Kaneko, M., Sasaki, Y., Nishikawa, J., Nagase, M. and Mamiya, K., 1995, *River dike failure in Japan by earthquakes in 1993*, Proc. 3rd International Conference in Recent Advances in Geotechnical Earthquake Engineering and Soil Dynamics, St. Louis, Paper No. 6.13, pp. 495-598.

Keaton, J. R., and Anderson, L. R., 1995, *Mapping liquefaction hazards in the Wasatch Front region: opportunities and limitations*, Environmental and Engineering Geology of the Wasatch Front Region, Utah Geological Association, Publication 24.

Keaton, J. R., Currey, D. R. and Olig, S. J., 1993, Paleoseismicity and earthquake hazards evaluation of the West Valley fault zone, Salt Lake City urban area, Utah Geological Survey Contract Report 93-8, 55 p.

Kleinfelder Inc., 1999, Geological investigation, proposed Salt Palace Expansion II, Salt Lake City, Utah, prepared by Kleinfelder Associates, Feb. 26, 1999.

Kleinfelder, Inc. (1996a). "Preliminary Geotechnical Exploration Report," I-15 Corridor Reconstruction Section 4, 600 South, Project No. SP-15-7(129)310, Station 32+080 to 35+044, Salt Lake City, Utah, Sept. 1996.

Kleinfelder Inc. (1996b). "Geotechnical Exploration Report," I-15 Corridor Reconstruction Section 9, State Street, Project No. SP-80-3(41)125, Station 1+220 to 1+687, Salt Lake City, Utah, Sept. 1996.

Kleinfelder Inc. (1996c). "Geotechnical Exploration Report," I-15 Corridor Reconstruction Section 8, 3300 South, Project No. SP-15-7(144)305, Station 28+600 to 24+500, Salt Lake City, Utah, Sept. 1996.

Kleinfelder Inc. (1996d). "Geotechnical Exploration Report," I-15 Corridor Reconstruction Section 10, 900 W., Project No. SP-020(1)17, Station 1+000 to 10+640, Salt Lake City, Utah, Sept. 1996.

Korbay S. R. and McCormick W. V., 1999, *Faults, lateral spreading, and liquefaction features, Salt Palace Convention Center, Salt Lake City*, Association of Engineering Geologists Program with Abstracts, 42nd Annual Meeting, Little America Hotel, September 26-29, 1999.

Lawson A. C., 1908, *The California Earthquake of April 18, 1906*, Report of the State Earthquake Investigation Commission, Carnegie Institution of Washington, Publication 87, 2 vols.

Leeflang, B, T., 2008, *Ground Displacement Investigations in Downtown Salt Lake City, Utah Using the Cone Penetrometer*, Thesis, Department of Civil and Environmental Engineering, University of Utah, 165 p.

Lund, W. R., 2005, Consensus preferred recurrence-interval and vertical slip-rate estimates, Utah Geological Survey Bulletin 134, CD-ROM.

Lund, W. R., 1990, Engineering geology of the Salt Lake City Metropolitan Area, Utah, Association of Engineering Geologists, Bulletin 126, Salt Lake City, Utah, pp. 1-66.

Machette, M. N., Personius, S. F., and Nelson, A. R., 1992, Paleoseismology of the Wasatch fault zone – A summary of recent investigations, conclusions, and interpretations, in Gori, P.L., and Hays, W.W., editors, Assessment of regional earthquake hazard and risk along the Wasatch Front, Utah, U.S. Geological Survey Professional Paper 1500, pp. A1-A71.

McKean, A. P. and Hylland, M. D., 2013, *Interim Geologic Map of the Baileys Lake Quadrangle, Salt Lake and Davis County, Utah, UGS OFR-624, 2013.*

McCulloch, D. S. and Bonilla, M. G., 1970, *Effects of the earthquake of March 27, 1964, on the Alaska railroad,* U.S. Geological Survey Profession Paper 545-D, 161 pp.

McSaveney, E., 2013, *Historic earthquakes – The 2010 Canterbury (Darfield) earthquake*, Te Ara – the Encyclopedia of New Zealand, http://www.TeAra.govt.nz/en/historic-earthquakes/page-12 (accessed 3 November 2016).

Meyerhof, G. G., 1957, *Discussion for Session I*, Proceedings: Fourth International Conference on Soil Mechanics and Foundation Engineering, Vol. 3, 10 p.

Miller, R. D., 1980, *Surficial geologic map along part of the Wasatch Front, Salt Lake Valley, Utah,* U.S. Geological Survey Miscellaneous Field Studies Map MF-1198, scale 1:100,000.

Nagase, H. and Ishihara, K., 1988, *Liquefaction-induced compaction and settlement of sand during earthquakes*. Soils and Foundations, Vol. 28(1): pp. 66–76.

National Center for Earthquake and Engineering Research (NCEER), 1997, "Proceedings of the NCEER Workshop on Evaluation of Liquefaction Resistance of Soils," edited by Youd, T. L., and Idriss, I. M., Technical Report NCEER-97-0022, National Center for Earthquake Engineering Research.

Olsen, M. J., Bartlett, S. F. and Solomon, B. J., 2007, *Lateral spread hazard mapping of the northern Salt Lake Valley, Utah, for M7.0 scenario earthquake*, Earthquake Spectra, Vol. 23, Number 1, pp. 95-113*.*

Osmond, J. C., Hewitt, W. P., and Van Horn, R. V., 1965, *Engineering implications and geology, Hall of Justice excavation, Salt Lake City, Utah,* Utah Geological and Mineral Survey Special Studies No. 11, 35 p.

Paleoseismology of Utah Series, from http://geology.utah.gov/hazards/technical-information/paleoseismology-of-utah-series/, accessed 30 November 2016.

Personius, S. F., and Scott, W. E., 1992, Surficial geologic map of the Salt Lake City segment and parts of adjacent segments of the Wasatch fault zone, Davis, Salt Lake, and Utah Counties, Utah: U.S. Geological Survey Miscellaneous Investigations Map I-2106, scale 1:50,000.

Petersen, M. D., Frankel, A. D., Harmsen, S. C., Mueller, C. S., Haller, K. M., Wheeler, R. L., Wesson, R. L., Zeng, Y., Boyd, O. S., Perkins, D. M., Luco, N., Field, E. H., Wills, C. J., and Rukstales, K. S., 2008, *Documentation for the 2008 update of the United States National Seismic Hazard Maps*, U.S. Geological Survey Open-File Report 2008–1128, 61 p.

Power, M. S. and Holzer, T. L. 1996, *Liquefaction maps*, ATC Technical Brief 1, ATC-35 Research Utilization Project, Applied Technology Council, 12 p.

Scott, W. E., and Shroba R. R., 1985, *Surficial geologic map of an area along the Wasatch fault zone in the Salt Lake Valley, Utah*: U.S. Geological Survey Open-File Report 85-448, scale 1:24,000, 18 p.

Seed, H. B., Idriss, I. M., and Arango, I., 1983, *Evaluation of liquefaction potential using field performance data*, Journal of Geotechnical Engineering, ASCE, 109(3), pp. 458-482*.*

Seed, H. B., Tokimatsu, K., Harder, L. F., and Chung, R. M., 1985, *Influence of SPT procedures in soil liquefaction resistance evaluations*, Journal of Geotechnical Engineering, ASCE, 111(12), pp. 1425-1445.

Seed, R. B., Cetin, K. O., Moss, R. E. S., Kammerer, A. M., Wu, J., Pestana, J. M., Riemer, M. F., 2001, *Recent advances in soil liquefaction engineering and seismic site response evaluation*, Proceedings: Fourth International Conference on Recent Advances in Geotechnical Earthquake Engineering and Soil Dynamics and Symposium in Honor of Professor W. D. Liam Finn, San Diego, California, March 26-31, 2001, 45 p.

Seed, R. B., Cetin, K. O., Moss, R. E. S., Kammerer, A. M., Wu, J., Pestana, J. M., Riemer, M. F., Sancio, R. B., Bray, J. D., Kayen, R. E., and Faris, A., 2003, *Recent advances in soil liquefaction engineering, a unified and consistent framework*, Keynote Address, 26th Annual Geotechnical Spring Seminar, Los Angeles Section of the GeoInstitute, American Society of Civil Engineers, H.M.S. Queen Mary, Long Beach, California, USA, University of California, Berkeley, Earthquake Engineering Research Center, Report No. EERC 2003-06, 71 p.

Simon, D. and Bymaster, W., 1999, Report of geologic investigation, Salt Palace Convention Center Expansion Project, 100 South West Temple Street, Salt Lake City, Utah, prepared by SBI Geotechnical and Environmental Engineering, March 29, 1999.

Solomon, B. J., Biek, R. F., Smith, T.W., 2007, *Geologic Map of the Magna Quadrangle of Salt Lake County, Utah*, UGS Map 216.

Solomon, B. J., Storey, N., Wong, I. G., Silva, W. J., Gregor, N., Wright, D., and McDonald, G. N., 2004, *Earthquake-hazards scenario for a M7 earthquake on the Salt Lake City segment of the Wasatch fault zone*, Utah Geological Survey, Special Study 111DM, 65 p.

Smith, R. B. and Arabasz, W. J., 1991, *Seismicity of the Intermountain seismic belt*, in Slemmons, D. B., Engdahl, E. R., Zoback, M. D. and Blackwell, D. D., eds., *Neotectonics of North America: Boulder Colorado*, Geological Society of America, Decade Map Volume 1.

Tokimatsu, K. and Seed, H. B., 1987, *Evaluation of settlements in sand due to earthquake shaking*, Journal of Geotechnical Engineering, ASCE, Vol. 113(8), pp. 861-878.

UGS Liquefaction Advisory Group Webpage, Nov. 28, 2016, retrieved from: http://geology.utah.gov/hazards/earthquakes-faults/utah-earthquake-working-groups/liquefaction-advisory-group/.

United State Geological Survey, The National Map Webpage, Nov. 28, 2016, retrieved from: https://nationalmap.gov/elevation.html.

Utah AGRC, Elevation and Terrain Data Webpage, Nov. 28, 2016, retrieved from: https://gis.utah.gov/data/elevation-terrain-data/

U of U Utah Liquefaction Advisory Group Webpage, Nov. 28, 2016, retrieved from: http://www.civil.utah.edu/~bartlett/ULAG/

Utah Geological Survey GeoData Archive System Webpage, retrieved from: https://geodata.geology.utah.gov/pages/home.php?login=true, accessed Nov. 28 2016.

Working Group on Utah Earthquake Probabilities (WGUEP), 2016, "Earthquake probabilities for the Wasatch Front region in Utah, Idaho and Wyoming: Salt Lake City, Utah," Utah Geological Survey Miscellaneous Publication 16-3, 164 p.

Wong, I., Silva, W., Wright, D., Olig, S., Ashland, F., Gregor, N., Christenson, G., Pechmann, J., Thomas, P., Dober, M., and Gerth, R., 2002, *Ground-shaking map for a magnitude 7.0 earthquake on the Wasatch fault, Salt Lake City, Utah, metropolitan area,* Utah Geological Survey Miscellaneous Publication MP 02-05, 50 p., Utah Geological Survey Public Information Series 76.

Youngs, R. R., Swan, F. H., Power, M. S., Schwartz, D. P. and Green, R. K., 1987, Probabilistic analysis of earthquake ground shaking hazard along the Wasatch Front, Utah, in Gori, P. L. and Hays, W. W., eds., Assessment of Regional Earthquake Hazards and Risk Along the Wasatch Front, Utah: U. S. Geological Survey Professional Paper 1500 K-R, p. M1-M110.

Yoshida, Y., Tokimatsu, K., Yasuda, S., Kokusho, T. and Okimura, T., 2001, *Geotechnical aspects of damage in Adapazari City during 1999 Kocaeli, Turkey earthquake*, Soils and Foundations, Japanese Geotechnical Society, Vol. 41, No. 4, pp. 25-45.

Yoshimine, M., Nishizaki, H., Amano, K., and Hosono, Y., 2006, *Flow deformation of liquefied sand under constant shear load and its application to analysis of flow slide of infinite slope*, Soil Dynamics and Earthquake Engineering, 26(2-4), pp. 253-264

Youd, T.L., 1980, Ground failure displacement and earthquake damage to buildings: American Society of Civil Engineers, 2nd Conference on Civil Engineering and Nuclear Power, Knoxville, Tenn., v. 2, p. 7-6-2 to 7-6-26.

Youd, T. L. and Hoose, S. N., 1978, *Historic ground failures in Northern California triggered by earthquakes,* U.S. Geological Survey Professional Paper 993.

Youd, T. L. and Perkins, D. M., 1978, *Mapping liquefaction-induced ground failure potential*, Journal of the Geotechnical Engineering Division, ASCE, Vol. 104, pp. 443-446.

Youd, T. L. and Perkins, D. M., 1987, *Mapping of liquefaction severity index*, Journal of Geotechnical Engineering, ASCE, Vol. 113(11), pp. 1374-1392.

Youd, T. L., Idriss, I. M., Andrus, R. D., Arango, I., Castro, G., Christian, J. T., Dobry, R., Finn, W. D. L., Harder, L. F., Jr., Hynes, M. E., Ishihara, K., Koester, J. P., Liao, S. S. C., Marcuson, W. F., III, Martin, G. R., Mitchell, J. K., Moriwaki, Y., Power, M. S., Robertson, P. K., Seed, R. B., and Stokoe, K. H., II, 2001, *Liquefaction resistance of soils: summary report from the 1996 NCEER and 1998 NCEER/NSF workshops on evaluation of liquefaction resistance of soils*, Journal of Geotechnical and Geoenvironmental Engineering, ASCE, Vol. 127, No. 10, October, 2001, pp. 817-833.

Youd, T. L., Hansen, C. M., and Bartlett S. F., 2002*, Revised multilinear regression equations for prediction of lateral spread displacement*, Journal of Geotechnical and Geoenvironmental Engineering, Vol. 128, No. 12, p. 1007-1017.

# A   GEOLOGIC AND GEOTECHNICAL DESCPTION OF MAPPED UNITS

A.1   Introduction

Bartlett et al., (2005) have compiled a statistical description of the geologic units found in the northern part of the mapped area (mapped units located north of 3500 South Street, Figure 6-1). The descriptions of the geologic units given in this appendix are modified from Personious and Scott (1992) and Biek et al. (2004). In addition, histograms from the dataset have been included to show the Soil-type, $N1_{60}$ blow-count distribution for granular soils, and Plastic Index distribution for fine soils within the major geologic units with adequate sampling. To accomplish these evaluations, the layers in each borehole were assigned to their respective geologic unit using the borehole soil descriptions and the adjacent CPT logs, when available.
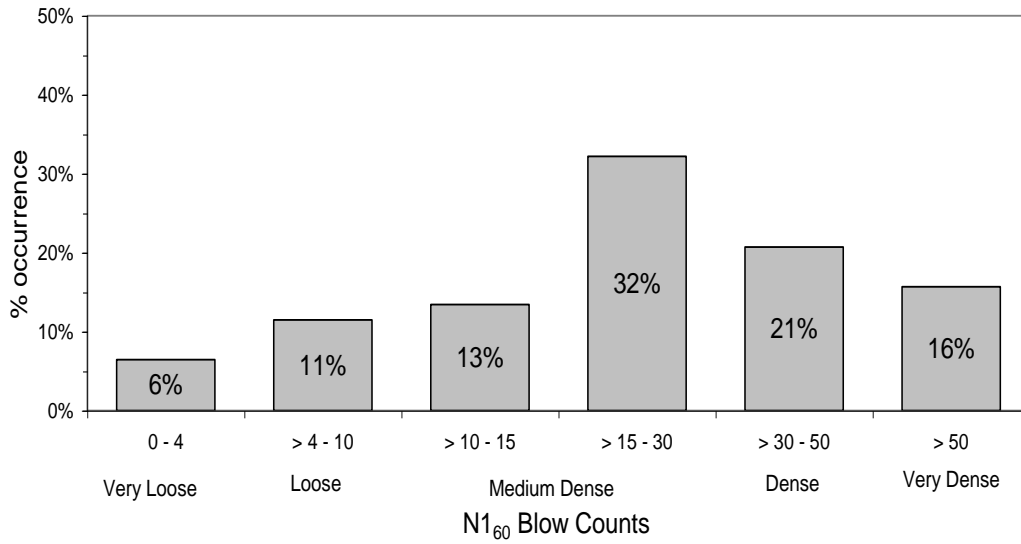
A.2   Stream Alluvium Deposits

Qal_1 – Modern stream alluvium 1 (upper Holocene). Poorly to moderately sorted sand, silt, and minor clay and gravel along the Jordan River and lower reaches of its tributaries; deposits along upper reaches of tributaries consist of pebble and cobble gravel, and minor sand and silt; parallel bedding and cross-bedding; forms modern flood plain and terraces less than 5 m above modern stream level; subject to flooding and high water table; exposed thickness 1 - 3 m.

The Qal_1 unit it is composed of well–graded sand and silty sand (67%) with some silt (11%) and clay (15%), as shown in Figure A-1. These deposits are medium dense, with a substantial amount of very loose and loose soils, as shown in Figure A-2. Thus, these deposits are very susceptible to liquefaction and lateral spread. As shown in Figure A-3, the fine soils found within this unit are generally medium plastic in nature.
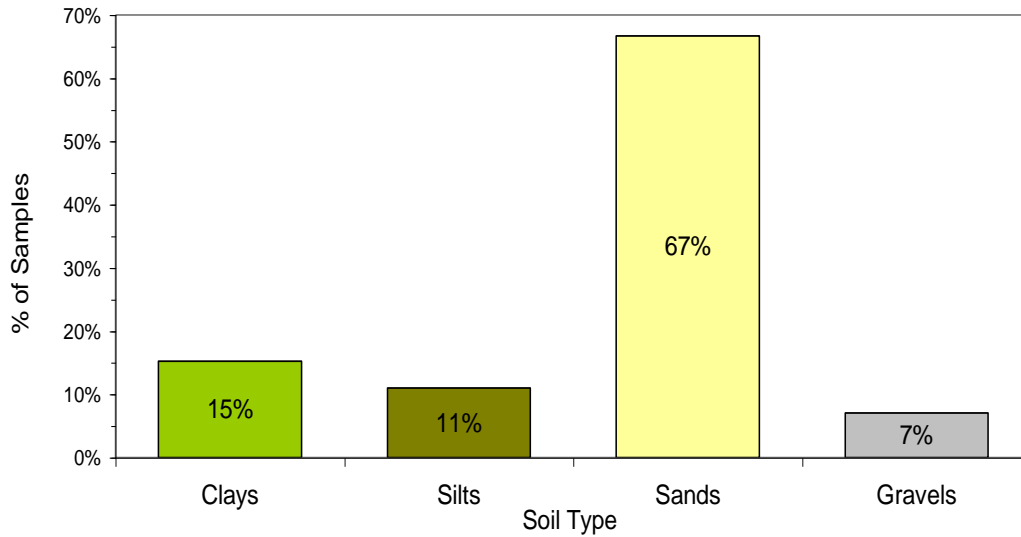
Figure A-1. Soil type distribution for the Qal$_1$ unit based on 137 samples in the northern part of the mapped area.
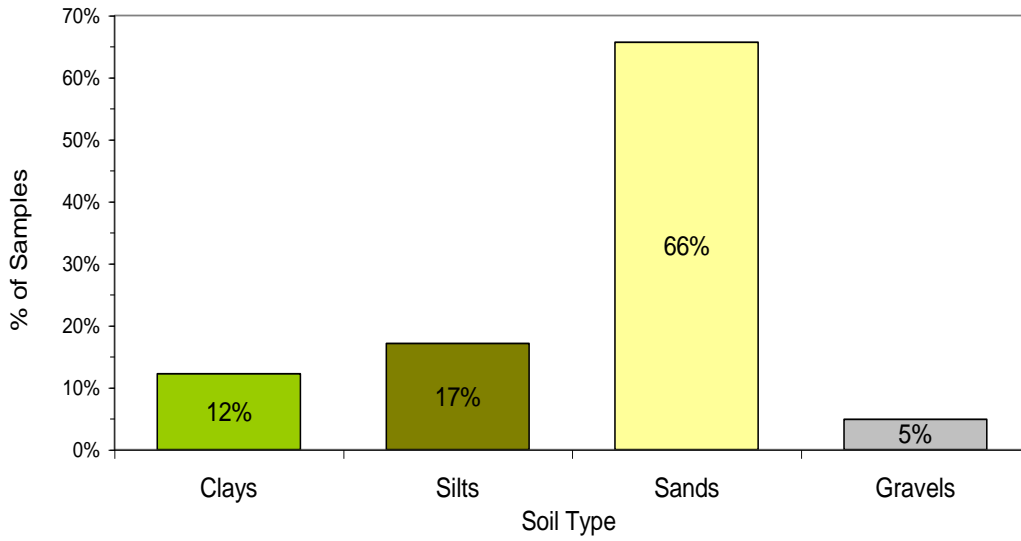

Figure A-2. N1$_{60}$ value distribution for the Qal$_1$ unit based on 89 granular samples the northern part of the mapped area.
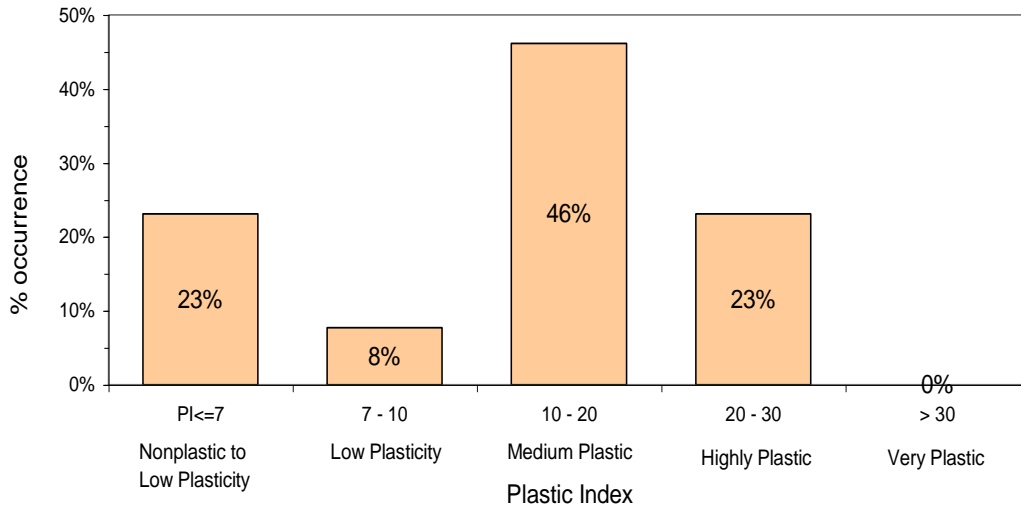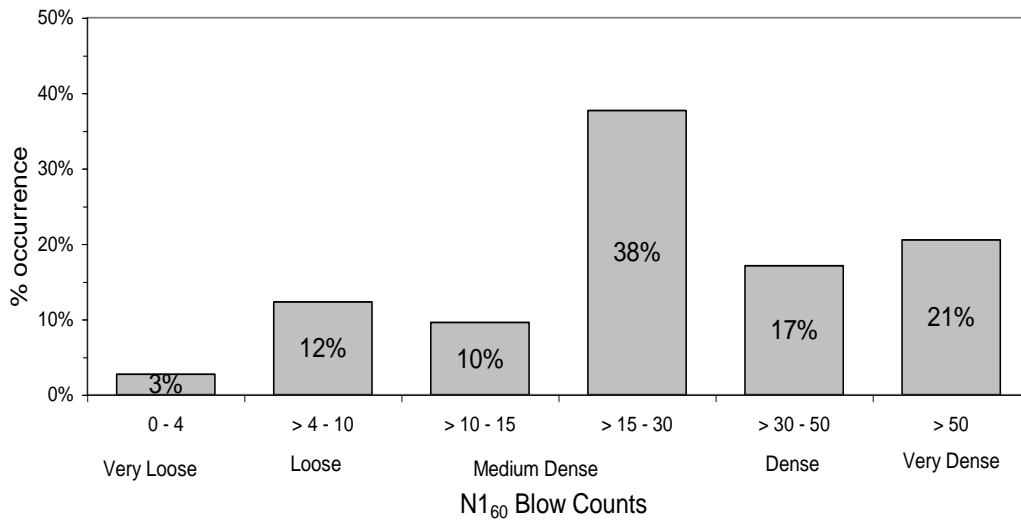
Figure A-3. Plastic index distribution for the Qal_1 unit based on 13 samples from fine-grained soils in the northern part of the mapped area.

Qal_2 - Stream alluvium 2 (middle Holocene to upper Pleistocene). Poorly to moderately sorted sand, silt, clay, and local gravel along Jordan River and lower reaches of its tributaries; deposits along upper reaches of tributaries consist of pebble and cobble gravel, and minor sand and silt; parallel bedding and cross-bedding; deposited by streams graded to recessional stands of Lake Bonneville and to lakes of early Holocene age; forms terraces more than 5 m above modern stream level, usually inset into deposits of the Bonneville lake cycle; exposed thickness 1 - 5 m.

The Qal_2 is composed of well–graded sand and silty sand (66%) with some silt (12%) and clay (17%), as shown in Figure A-4. These deposits are medium dense, with a substantial amount of very loose and loose deposits, as shown in Figure A-5. The loose deposits, however, are less than that found in the Qal_1 unit. As shown in Figure A-6, the fine-grained soils are generally low to medium plastic in nature.

Figure A-4. Soil-type distribution for the Qal2 geologic unit based on 245 samples.

Figure A-5. N160 blow-count distribution for the Qal2 geologic unit based on 146 granular samples in the northern part of the mapped area.
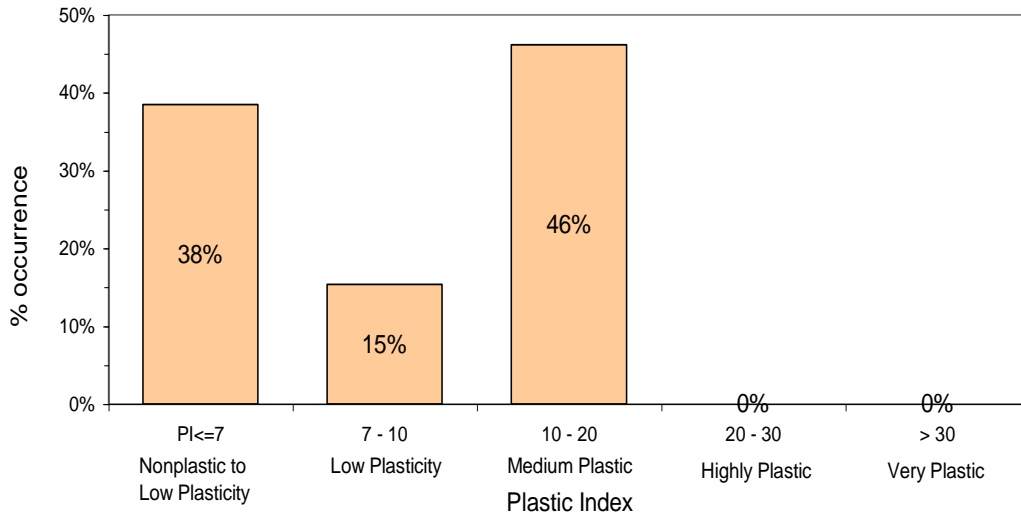
Figure A-6. – Plastic-index distribution in the Qal2 geologic unit based on 13 fine-grained soil samples in the northern part of the mapped area.

**Qaly - Younger stream alluvial deposits (Holocene to Upper Pleistocene).**
Consists of moderately sorted sand, silt, clay, and pebble to boulder gravel deposited in stream channels and flood plains; includes abandoned flood plains that postdate the Bonneville shoreline of latest Pleistocene Lake Bonneville; the alluvial deposits are incised by active stream channels, and locally include small alluvial-fan and colluvial deposits; includes modern and older, post-Lake Bonneville stream deposits (Qal$_1$ and Qal$_2$) that are undifferentiated because units are complexly overlapping; mapped along streams emanating from the Oquirrh Mountains; forms terraces along Jordan River from Taylorsville north to Salt Lake City International Airport; probably less than 6 m thick.

The Qaly unit contains well–graded sand and silty sand (60%) with some silt (18%) and clay (19%), as shown in Figure A-7. These deposits are medium dense, with a substantial amount of loose and medium dense deposits, as shown in Figure A-8. Thus, these deposits are susceptible to liquefaction and lateral spread. There was insufficient data to analyze the plasticity of the fine soils within this unit.
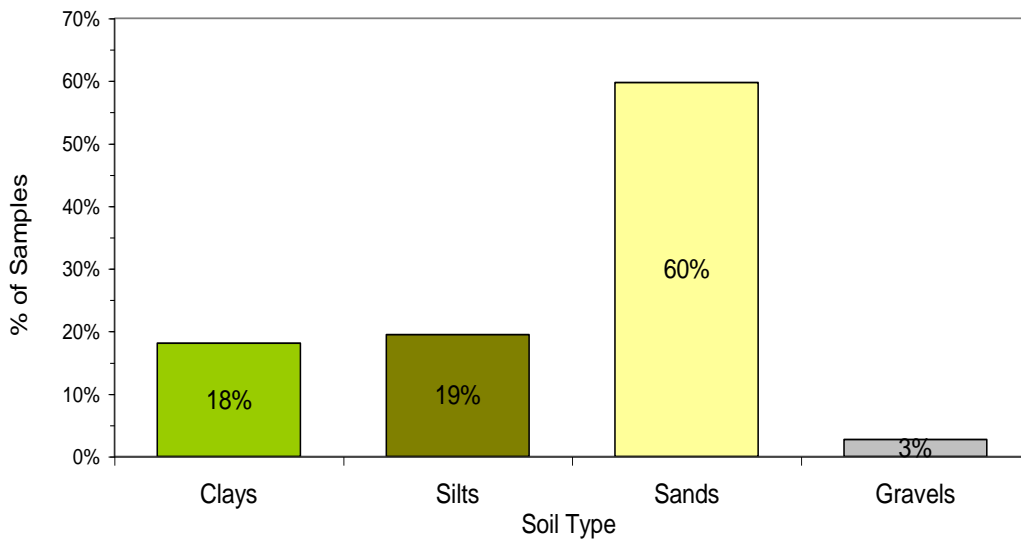
Figure A-7. Soil-type distribution for the Qaly geologic unit based on 149 samples in the northern part of the mapped area.

.
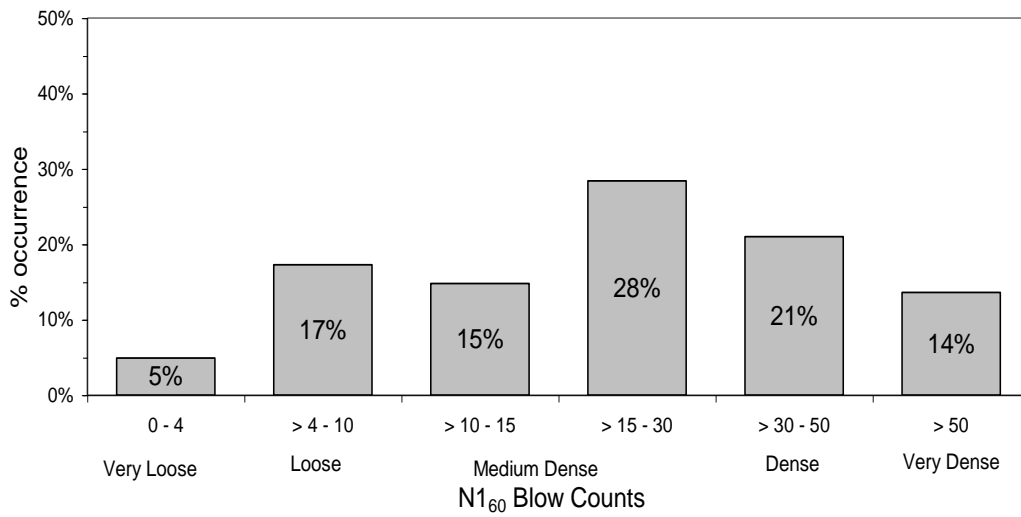
Figure A-8. N1$_{60}$ blow-count distribution for the Qaly geologic unit based on 81 granular samples in the northern part of the mapped area.

.

Qalp - Stream alluvium related to the Provo (regressive) phase of the Bonneville lake cycle (upper Pleistocene). Clast-supported pebble and cobble gravel, locally bouldery, in a matrix of sand and silt; poorly sorted, clasts subangular to round; parallel bedding and cross-bedding locally massive; deposited by streams graded to the Provo shoreline and other shorelines of the regressive phase of the Bonneville lake cycle; also deposited as topset beds on deltaic deposits related to the Provo shoreline; fluvial scarps are preserved on the surfaces of some deposits; thickness 1 - 10 m.

The Qalp unit is composed of sand (49%) and gravel (34%) with some silt, as shown in Figure A-9. These deposits are very dense, as shown in Figure A-10. Thus, these deposits are not very susceptible to liquefaction and lateral spread. Since these deposits are older in age than the other alluvial deposits, this is expected (Youd-Perkins 1978). There was insufficient data to analyze the plasticity of the fine soils within this unit.
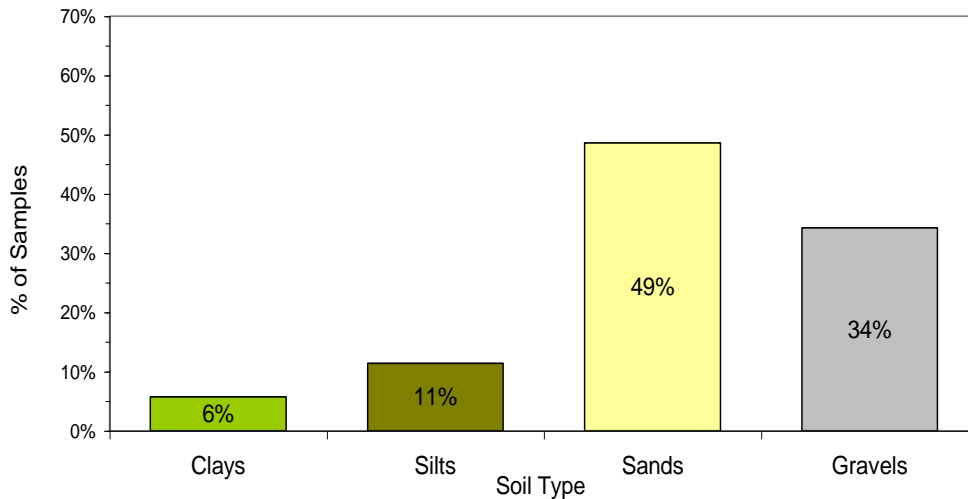

Figure A-9. Soil-type distribution for the Qalp geologic unit based on 70 samples in the northern part of the mapped area.
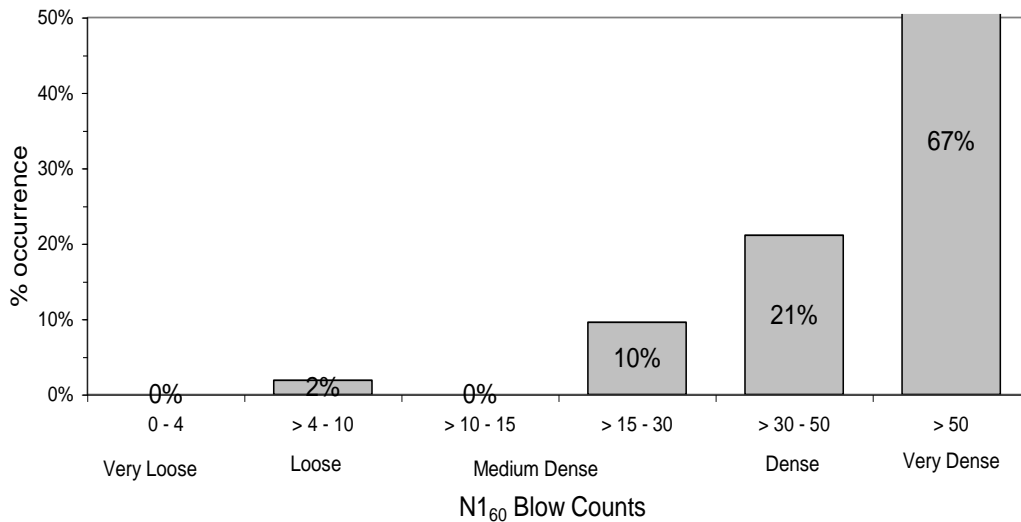
Figure A-10. N160 blow-count distribution for the Qalp geologic unit based on 52 granular samples in the northern part of the mapped area.
.

Qalb - Stream alluvium related to the Bonneville (transgressive) phase of the Bonneville lake cycle (Upper Pleistocene). Moderately sorted sand, silt, and pebble to boulder gravel deposited by streams graded to shorelines of the transgressive phase of Lake Bonneville; incised by active streams; mapped south of Harker's Canyon; about 6 m thick.

A.3   Alluvial-fan Deposits

Qaf$_1$ - **Modern alluvial-fan deposits 1 (Upper Holocene).** Poorly to moderately sorted, weakly to non-stratified, clay- to boulder-size sediment in a matrix of sand and silty sand deposited principally by debris flows at the mouths of small, active drainages; upper parts characterized by abundant boulders and debris-flow levies that radiate away from the fan apex; equivalent to the younger part of Qafy, but differentiated where deposits can be mapped separately; may contain small deposits of Qaf$_2$; many deposits of unit Qaf$_1$ too small to be shown at the map scale are included in unit Qaf$_2$; no shorelines present on surfaces; typical soil profiles range from A-Cn to A-Bw-Cox-Cn; generally less than 9 m thick.

A8

Qaf₂ - Alluvial-fan deposits 2 (Middle Holocene to Upper Pleistocene). Clast-supported pebble and cobble gravel, locally bouldery, in a matrix of sand and silty sand; poorly sorted; clasts sub-angular to round; thin to thick, parallel bedding and cross-bedding; locally massive; deposited by perennial and intermittent streams, debris flows, and debris floods (hyper-concentrated floods) graded approximately to modern stream level; may contain small deposits of units Qaf_1, especially near fan heads and along active stream channels; no shorelines present on surfaces; typical soil profiles range from A-Bw-Cox-Cn to A-Bt(weak)-Cox-Cn; typically 1 to >10 m thick.

The Qaf_2 unit contains a substantial amount of sand (36%) and gravel (34%) with some silt (18%) and clay (12%), as shown in Figure A-11. These deposits are dense, as shown in Figure A-12. Thus, these deposits are not very susceptible to liquefaction and lateral spread. As shown in Figure A-13, the fines are generally of low plasticity.
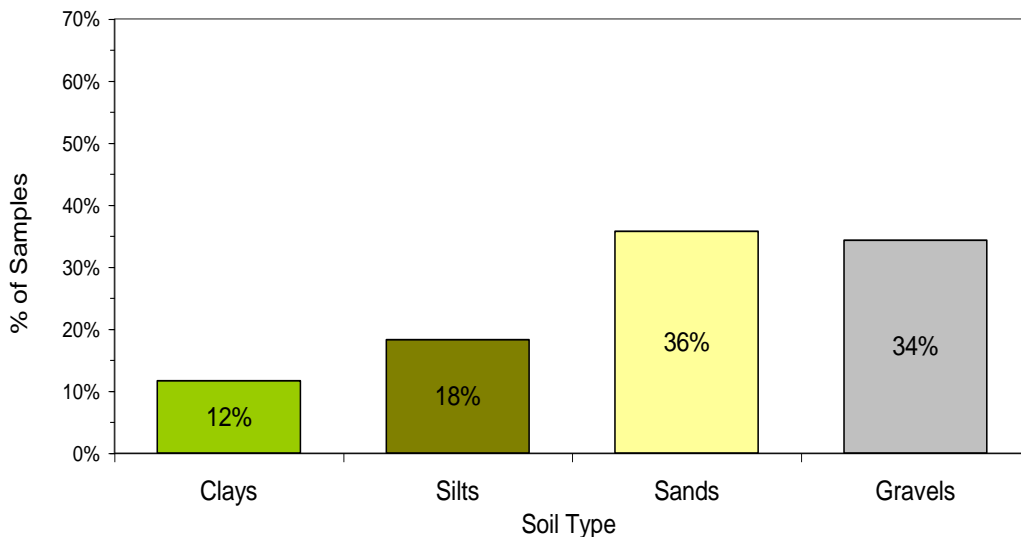
Figure A-11. Soil-type distribution for the Qaf2 geologic unit based on 137 samples in the northern part of the mapped area.
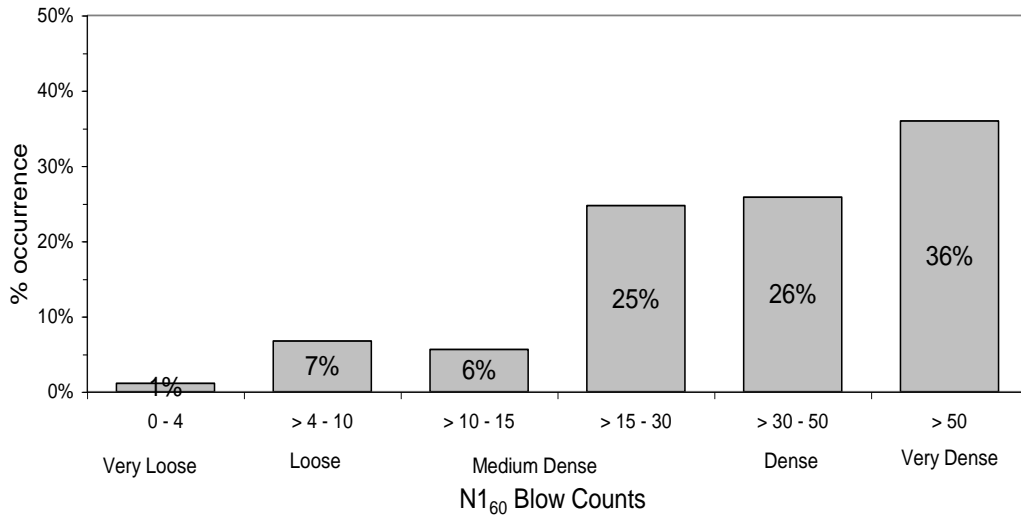
Figure A-12. $N1_{60}$ blow-count distribution for the Qaf_2 geologic unit based on 89 granular samples in the northern part of the mapped area.
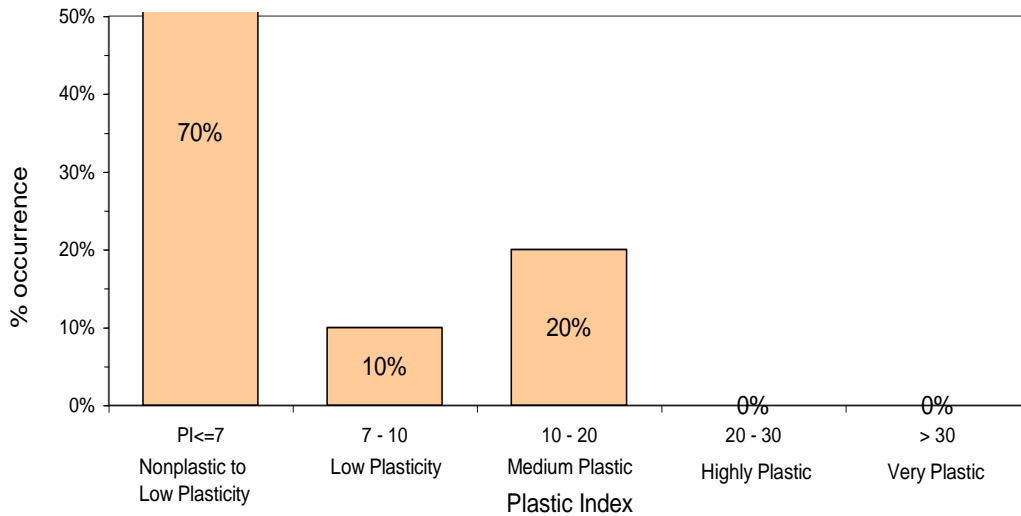
Figure A-13. Plastic-index distribution in the Qaf_2 geologic unit based on 10 fine soil samples in the northern part of the mapped area.

Qafy - Younger alluvial-fan deposits, undivided (Holocene to Upper Pleistocene). Postdates the regressive phase of the Bonneville lake cycle. Poorly to moderately sorted, weakly to nonstratified, clay- to boulder-size sediment deposited principally by debris flows, debris floods, and streams; commonly obscures Lake

Bonneville shorelines; equivalent to modern alluvial-fan deposits (Qaf$_1$) and older, post-Lake Bonneville alluvial-fan deposits (Qaf$_2$) that are undifferentiated because units are complexly overlapping or too small to show separately; upper parts of fans are locally deeply incised; mapped near the Salt Lake Salient near the margins of the Oquirrh Mountains extending as much as 5 km (3 miles) from the range front where drainages incise Lake Bonneville deposits; probably less than 12 m thick.

Qafp - Alluvial-fan deposits related to the Provo (regressive) phase of the Bonneville lake cycle (Upper Pleistocene). Poorly to moderately sorted, clay- to cobble-size sediment deposited principally by debris flows graded to the Provo shoreline; incised by active streams; underlies the broad, gently sloping floor of Little Valley above the Provo shoreline in the northwest part of the Magna quadrangle; probably less than about 12 m thick.

Qafb - Alluvial-fan deposits related to the Bonneville (transgressive) phase of the Bonneville lake cycle (Upper Pleistocene). Poorly to moderately sorted, clay to cobble-size sediment deposited principally by debris flows graded to the Bonneville shoreline; incised by active streams; may be covered by thin deposits of posttransgressive phase alluvium and colluvium; typical soil profile, A-Bt-Cox-C; probably less than about 12 m thick.

Qaf$_4$ - Alluvial-fan deposits 4 (Upper to Middle Pleistocene). Clast-supported pebble and cobble gravel, locally bouldery, in a matrix of sand and silty sand; poorly sorted; clasts sub-angular to round; thin to thick, parallel bedding and cross-bedding; locally massive; forms small fans and fan remnants topographically above or cut by the Bonneville shoreline; correlative deposits probably underlie much of the map area and are buried by younger deposits downslope from the Bonneville shoreline; typical soil profile, A-Bt(moderate-strong)-Cox-Cn; usually 1 to > 10 m thick.

Qaf$_5$ - Fan alluvium 5 (Middle Pleistocene). Clast-supported pebble and cobble gravel, locally bouldery, in a matrix of sand and silty sand; poorly sorted; clasts subangular to round; thin to thick, parallel bedding and cross-bedding; locally massively bedded; forms high fan remnants on ridge tops near front of Wasatch Range; some

remnants may be deposits of old till that lack morainal morphology; typical soil profile, A-Bt(strong)-Cox-Cn; usually 1 to >10 m thick.

**Qafo** - **Older alluvial-fan deposits, undivided (Upper to Middle Pleistocene).** Poorly to moderately sorted, weakly to nonstratified, clay- to boulder-size sediment deposited principally by debris flows, at the base of the Oquirrh Mountains, mapped as part of the Harkers fanglomerate by Slentz (1955); mapped near the Salt Lake salient, where old fan deposits have not been differentiated; forms deeply dissected alluvial apron near Coon Canyon; exposed deposits are truncated by, and thus predate, the Bonneville shoreline; upper to middle Pleistocene age is suggested by development of stage II or III calcic paleosols on fan surfaces, characterized by calcium-carbonate coatings on clasts in a loose matrix with dispersed calcium carbonate; underlies piedmont slopes below the Bonneville shoreline beneath a thin veneer of lacustrine deposits; may be undifferentiated from underlying middle Pleistocene to late Miocene[?] alluvial-fan deposits where mapped in deeply incised stream channels; exposed thickness as much as 45 m.

A.4   Lacustrine Deposits

Consist of gravel, sand, silt, and clay deposited in Lake Bonneville (Bonneville lake cycle), Great Salt Lake, and other smaller lakes. These deposits are divided into four groups: (1) deposits that postdate the Bonneville lake cycle; (2) deposits associated with the Provo shoreline and the regressive phase of the Bonneville lake cycle; (3) deposits associated with the Bonneville shoreline and the transgressive phase of the Bonneville lake cycle; and (4) undivided sediments of the Bonneville lake cycle deposited at altitudes below the Provo shoreline that cannot be assigned to either phase of the Bonneville lake cycle. Sediments deposited near the mountain front are mostly gravel and sand; silt and clay were deposited in quieter, deeper water on the valley (lake) bottom, in sheltered bays between headlands, and less commonly in lagoons behind barrier beaches.
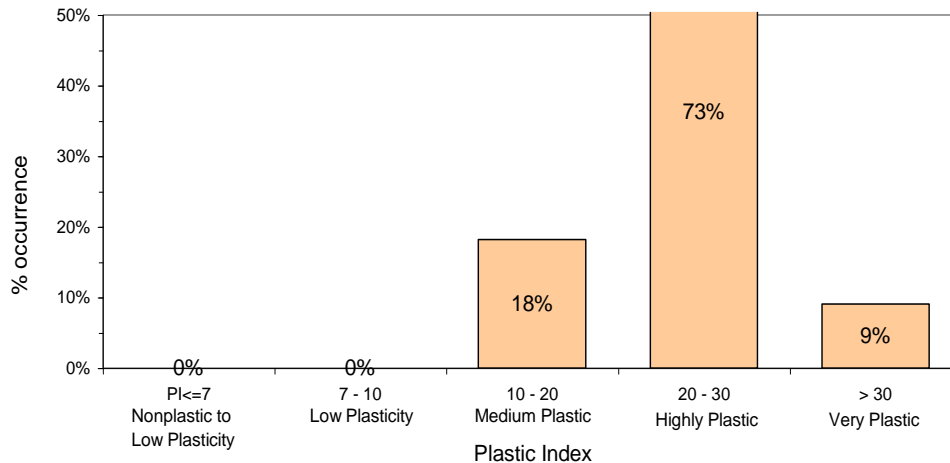
Qly - Young lacustrine and marsh deposits (Holocene). Silt, clay, and minor sand deposited in shallow lakes and marshes after the regressive phase; commonly organic rich; locally may contain peat deposits; occur in areas of standing water or where the water table is or has recently been at the ground surface; includes sediments in mud flats or playas exposed by fluctuations of the Great Salt Lake; commonly grade into and may contain small deposits of unit Qlbpm; subject to lacustrine flooding and high water table; thickness < 5 m.

The Qly unit contains mostly clay (77%) with some silt (15%) and sand (8%), as shown in Figure A-14. There was insufficient data to create a histogram for the blow-counts within granular soils in this unit. However, they are generally loose deposits. This combined with a high water table make the granular soils within these deposits very susceptible to liquefaction and lateral spread. As shown in Figure A-15, the fines are highly plastic fines.
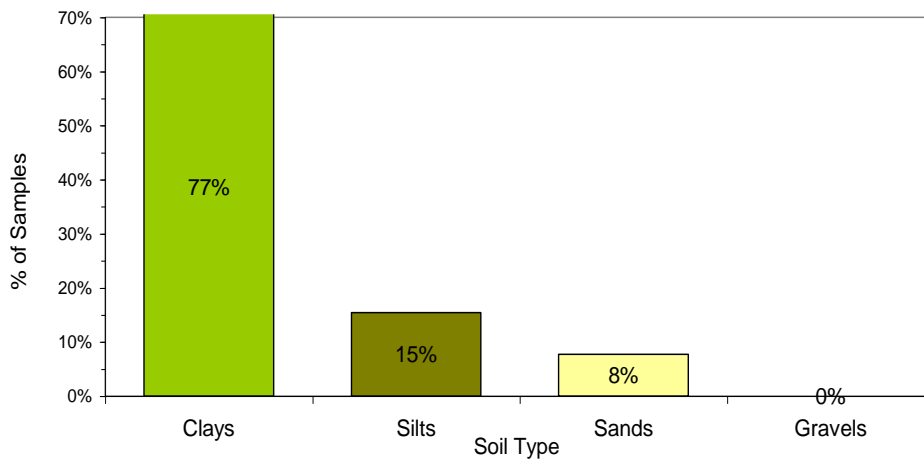
Figure A-14. Soil-type distribution for the Qly geologic unit based on 26 soil samples in the northern part of the mapped area.
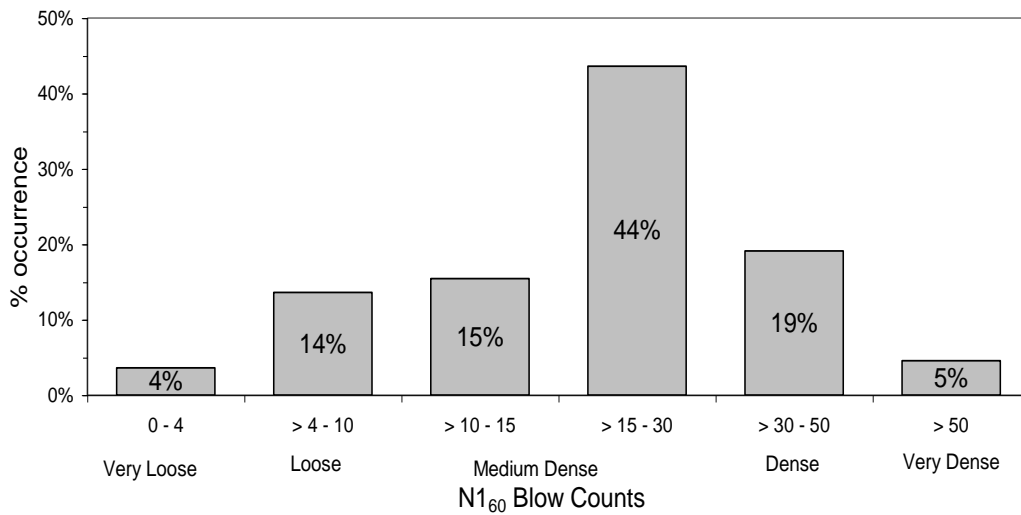
Figure A-15. Plastic-index distribution in the Qly geologic unit based on 11 fine soil samples in the northern part of the mapped area.

Qlaly- Young lacustrine, marsh, and alluvial deposits (Holocene to upper Pleistocene). Undivided clay, silt, sand, peat, and very minor pebble gravel; deposited after the regressive phase of the Bonneville lake cycle in shallow lakes and marshes, in deltas along the lower reaches of the Jordan River, and on distal parts of alluvial fans; deposited in mud flats or playas exposed by fluctuations of Great Salt Lake; local accumulations of gypsum, halite, and other salts commonly form a thin crust on the ground surface; unit probably contains small deposits of unit Qmls in urbanized areas; thickness 1 to > 3 m.

The Qlaly unit is composed of mostly clay (51%) and sand (29%) with a substantial amount of silts (18%) as shown in Figure A-16. These deposits are medium dense, with a substantial amount of very loose and loose deposits, as shown in Figure A-17. This, combined with a high water table make the granular soils within these deposits very susceptible to liquefaction and lateral spread. As shown in Figure A-18, the fines are generally medium-highly plastic.
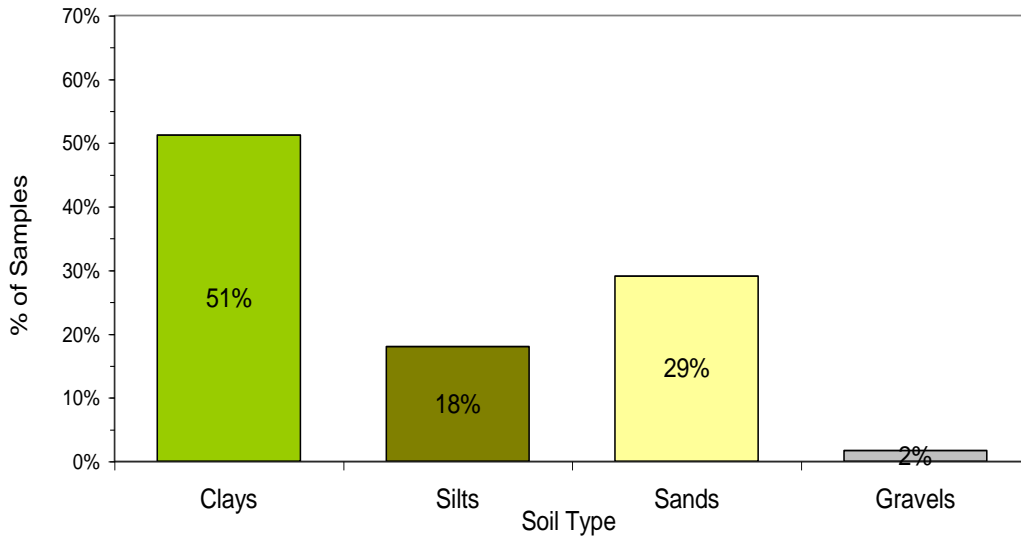
Figure A-16. Soil-type distribution for the Qlaly geologic unit based on 533 samples in the northern part of the mapped area.
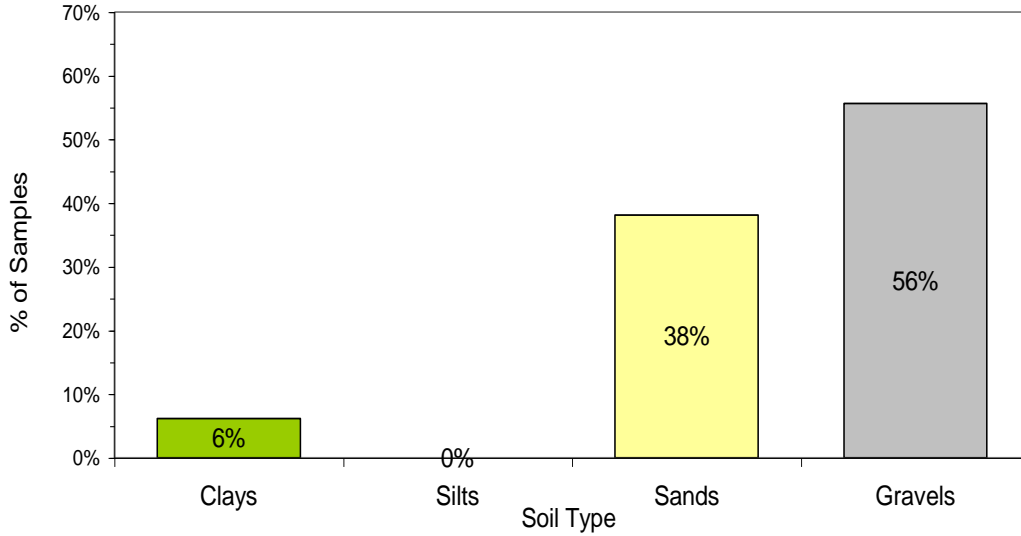

Figure A-17. $N1_{60}$ blow-count distribution for the Qlaly geologic unit based on 110 granular samples in the northern part of the mapped area.
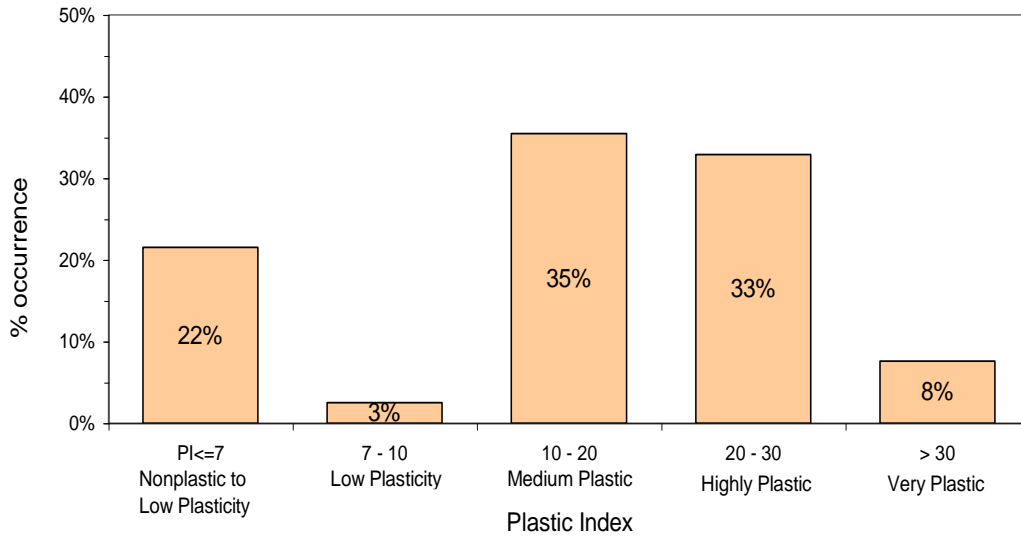
Figure A-18. Plastic-index distribution for the Qlaly geologic unit based on 79 fine-grained soil samples in the northern part of the mapped area.

Qlpg - Lacustrine gravel and sand related to the Provo (regressive) phase of the Bonneville lake cycle (Upper Pleistocene). Moderately to well-sorted, moderately to well-rounded, clast-supported, pebble to cobble gravel and pebbly sand deposited at and below the Provo shoreline; thin to thick bedded; typically interbedded with, or laterally gradational to, lacustrine sand and silt; gastropods locally common in sandy lenses; locally partly cemented with calcium carbonate; the most extensive deposits form beaches along the Provo shoreline and beaches and spits along the Gilbert shoreline; deposited in parallel and cross-bedded, thin to thick beds dipping from horizontal to as much as 15°; deposited in beaches, and spits, as well as small deltas that no longer retain distinctive morphology; forms a cuspate barrier beach in the southeast corner of the Magna quadrangle, called a V-bar by Gilbert (1890), created by converging currents of Lake Bonneville along the Provo shoreline; Currey (1982) measured the altitude of the Provo shoreline on the V-bar at about 1,471 m (4,826 feet) and measured the altitude of the Gilbert shoreline at about 1,296 m (4,252 feet) on a spit in the northern Magna quadrangle; contact with unit Qlbpg is mapped where Qlpg deposits

A16

can no longer be correlated with other regressive-phase deposits or shore-lines;
thickness 1 - 25 m.

Figure A-19. Soil-type distribution for the Qlpg geologic unit based on 97 samples in the northern part of the mapped area.
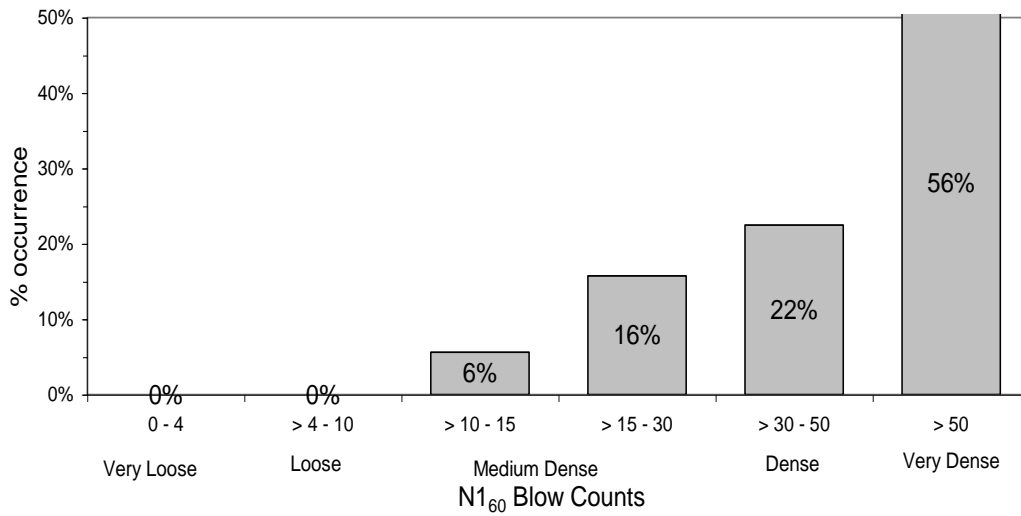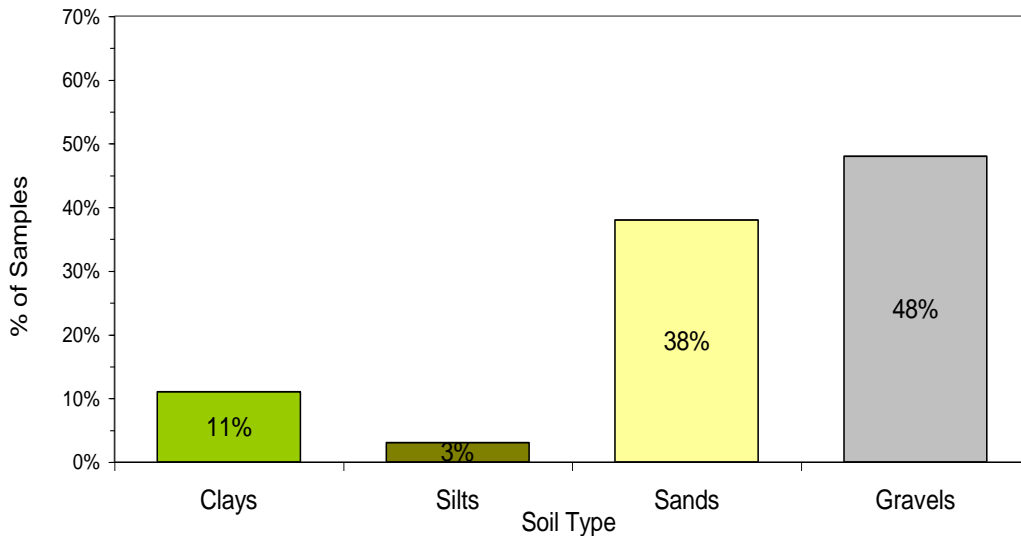

Figure A-20. $N1_{60}$ blow-count distribution for the Qlpg geologic unit based on 89 granular samples in the northern part of the mapped area.
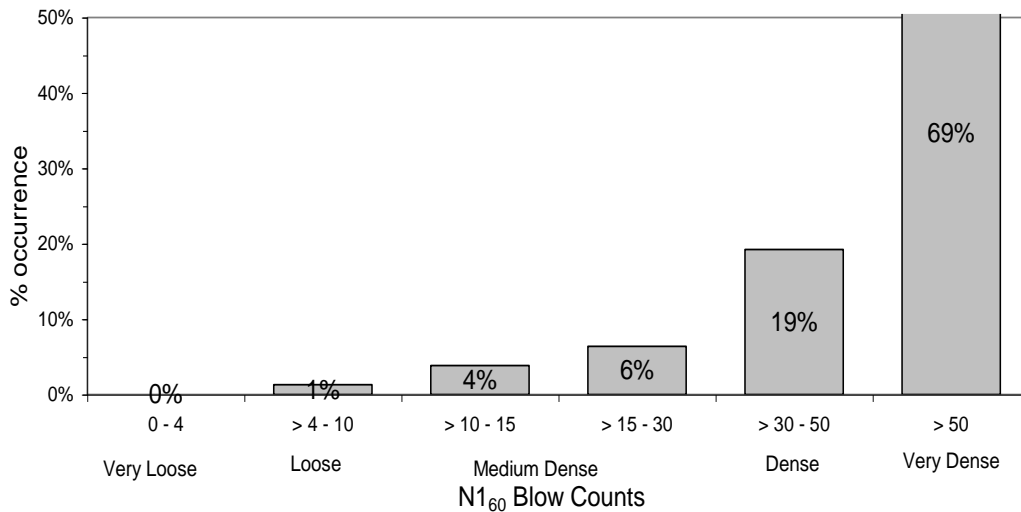
The Qlpg unit is composed of gravels (56%) and sands (38%) as shown in Figure A-19. These deposits are very dense, as shown in Figure A-20. This combined with a relatively deep water table in these regions make these deposits not very susceptible to liquefaction and lateral spread.

Qlpm - Lacustrine clay and silt related to Provo (regressive) phase of the Bonneville lake cycle (Upper Pleistocene). Clay, silt, and minor fine sand deposited in quiet-water areas along the Provo shoreline; more than 1 m thick.

Qlbg- Lacustrine gravel and sand related to the Bonneville (transgressive) phase of the Bonneville lake cycle (Upper Pleistocene). Moderately to well-sorted, moderately to well-rounded, clast-supported, pebble to cobble and rare boulder gravel and pebbly sand deposited between the Bonneville and Provo shorelines; thin to thick bedded; good sorting within beds; clasts subround to round; typically interbedded with, or laterally gradational to, lacustrine sand and silt; gastropods locally common in sandy lenses; locally includes interbedded silt and clay ranging from thin beds and lenses to lagoonal deposits as much as 10 m thick; locally partly cemented with calcium carbonate; typically less than 20 m thick.

Figure A-21. Soil-type distribution for the Qlbg geologic unit based on 100 samples in the northern part of the mapped area.
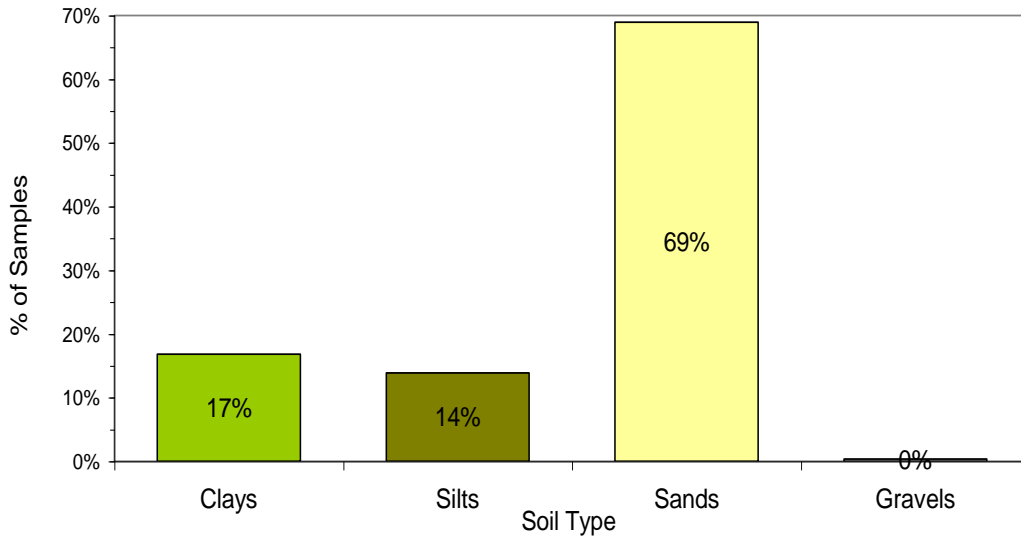
Figure A-22. N1$_{60}$ blow-count distribution for the Qlbg geologic unit based on 78 granular samples in the northern part of the mapped area.

The Qlbg unit contains mostly gravels (48%) and sands (38%), as shown in Figure A-21. These deposits are very dense, as shown in Figure A-22. This combined with a relatively deep water table in these regions make these deposits not very susceptible to liquefaction and lateral spread.

Qlbs- Lacustrine sand and silt related to the Bonneville (transgressive) phase of the Bonneville lake cycle (Upper Pleistocene). Fine- to coarse-grained lacustrine sand and silt with minor gravel deposited between the Bonneville and Provo shorelines; grades downslope to finer grained Lake Bonneville deposits; typically thick bedded and well sorted; gastropods locally common; poorly exposed but probably less than 10 m.

The Qlbs unit contains high amounts of sands (69%) with some clays (17%) and silts (14%) as shown in Figure A-23. These deposits are medium dense to dense, as shown in Figure A-24. Thus, these deposits are not usually susceptible to liquefaction and lateral spread. The fine-grained soils within this geologic unit are generally of low plasticity, but some medium to high plastic soils are present (Figure A-25).

Figure A-23. Soil-type distribution for the Qlbs geologic unit based on 612 samples in the northern part of the mapped area.
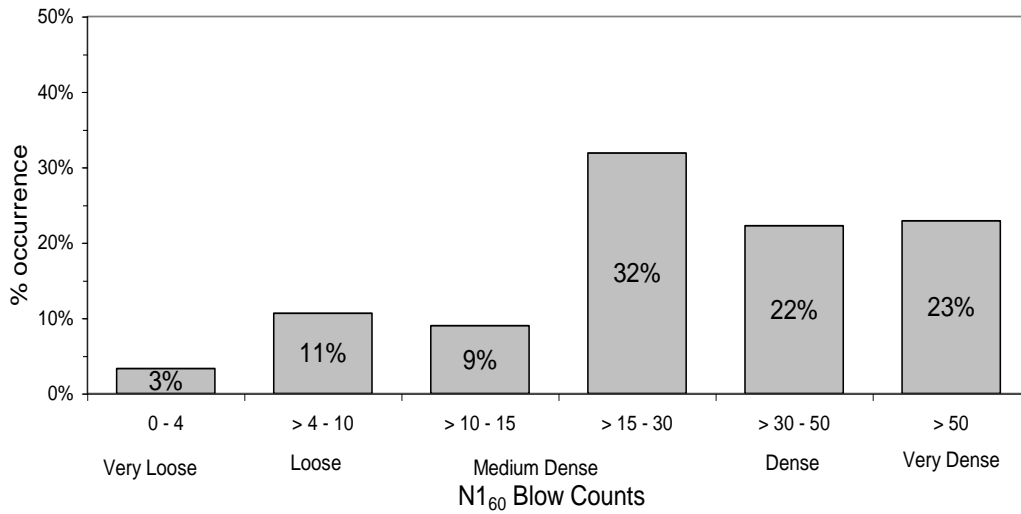
Figure A-24. N1$_{60}$ blow-count distribution for the Qlbs geologic unit based on 301 granular samples in the northern part of the mapped area.
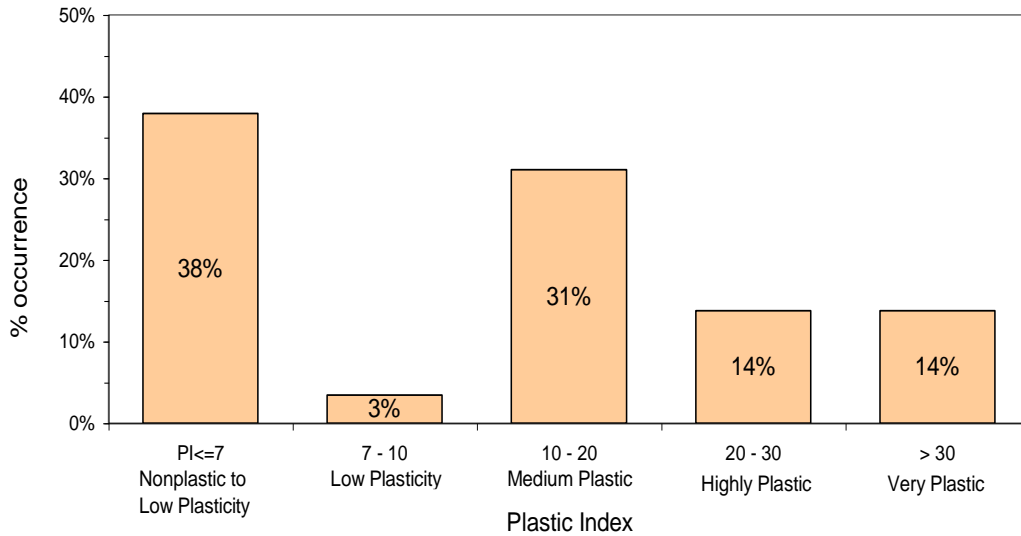
Figure A-25. Plastic-index distribution in the Qlbs geologic unit based on 29 fine-grained soil samples in the northern part of the mapped area.

Qlbm Lacustrine clay and silt related to the Bonneville (transgressive) phase of the Bonneville lake cycle (upper Pleistocene). Clay, silt, and minor fine sand; locally contains medium to coarse sand and pebble gravel; good sorting within beds; deposited in very thin to thick, parallel and crossbedded, horizontal to gently dipping beds; bedding locally disrupted by soft-sediment deformation or liquefaction; deposited in quiet-water environments, in sheltered bays between headlands, in lagoons behind barrier bars, or on the lake floor in deeper water; usually overlie coarse-grained transgressive shoreline deposits, implying deposition in increasingly deeper, quieter water; thickness 1 - 25 m.
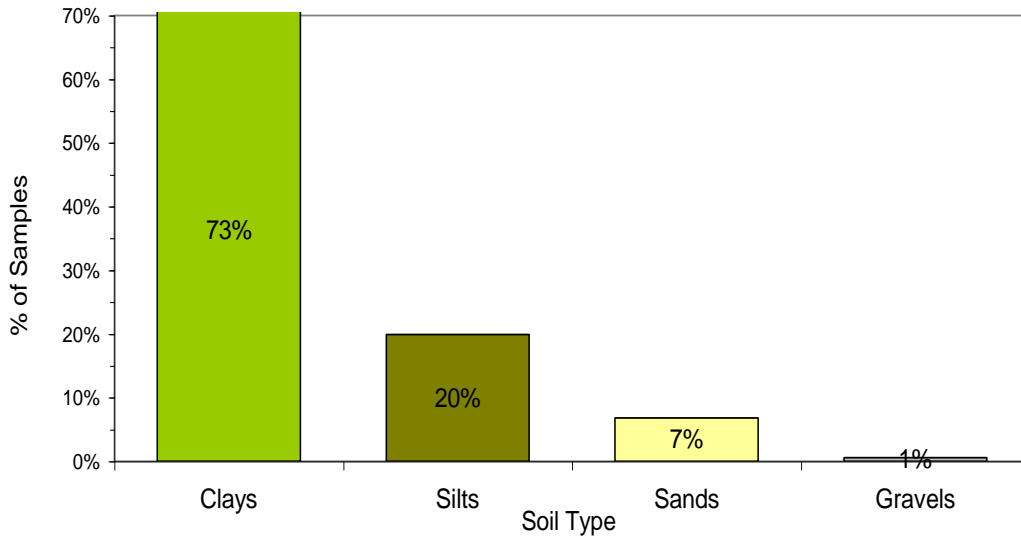
The Qlbm unit is generally composed of clay (73%) deposits with some silt (20%), as shown in Figure A-26. These deposits are medium dense, as shown in Figure A-27. As shown in Figure A-28, the fines are generally low to medium plastic fines.

A21

Figure A-26. Soil-type distribution for the Qlbm geologic unit based on 176 samples in the northern part of the mapped area.

Figure A-27. Blow-count distribution for the Qlbm geologic unit based on 10 granular samples in the northern part of the mapped area.

A22

Figure A-28. Plastic-index distribution in the Qlbm geologic unit based on 33 fine-grained soil samples in the northern part of the mapped area.
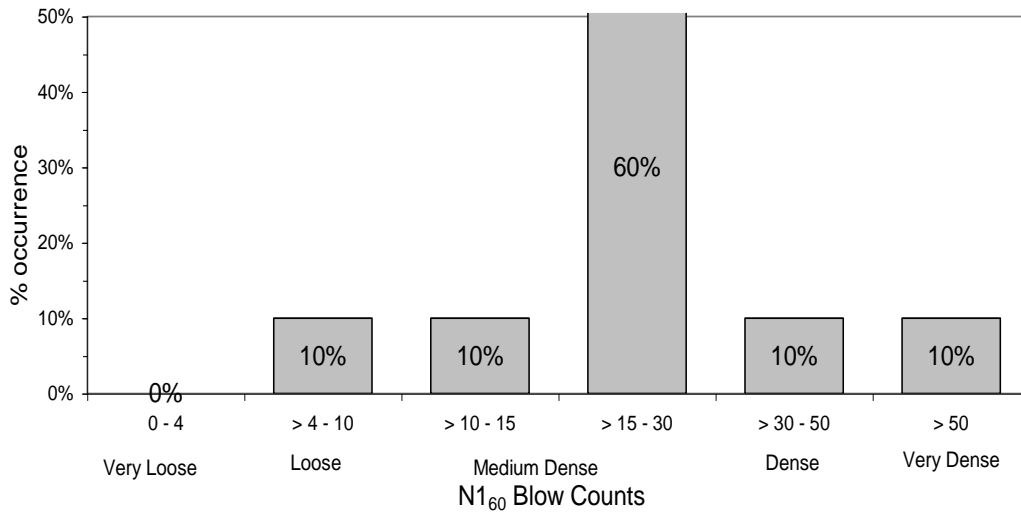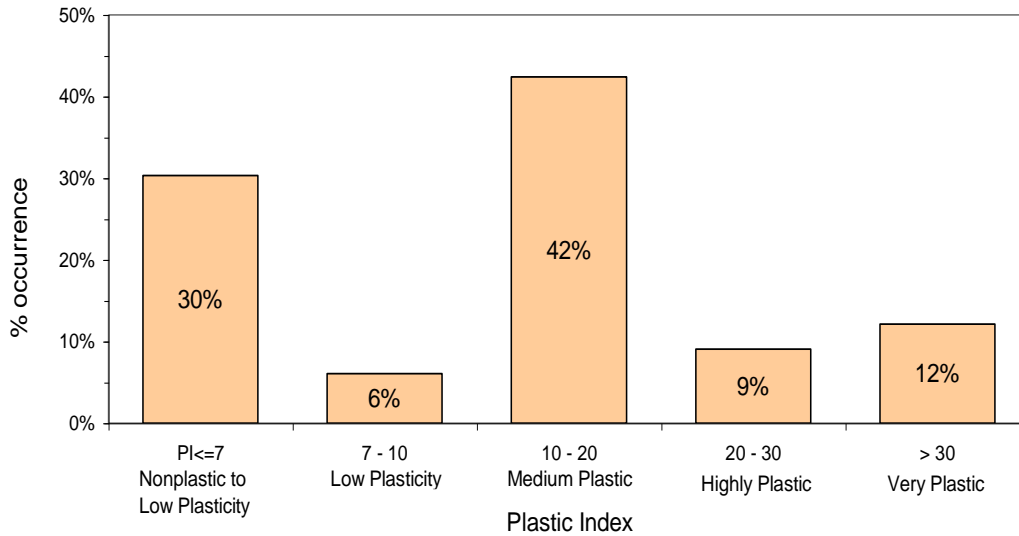
Qlbpg- Lacustrine gravel and sand of the Provo and Bonneville lake cycles, undivided (Upper Pleistocene). Moderately to well-sorted, moderately to well-rounded, clast-supported, pebble to cobble gravel and pebbly sand; deposited at and below the Provo shoreline, where transgressive- and regressive-phase deposits cannot be differentiated and deposits cannot be directly correlated with regressive-phase shorelines; thin to thick bedded; typically interbedded with, or laterally gradational to, lacustrine sand and silt; locally partly cemented with calcium carbonate; may be as much as 25 m thick.

The Qlbpg unit generally contains gravels (68%) with some sands (21%), as shown in Figure A-29. These deposits are very dense, as shown in Figure A-30. This combined with a relatively deep water table in these regions make these deposits not very susceptible to liquefaction and lateral spread.

A23

Figure A-29. Soil-type distribution for the Qlbpg geologic unit based on 91 samples in the northern part of the mapped area.

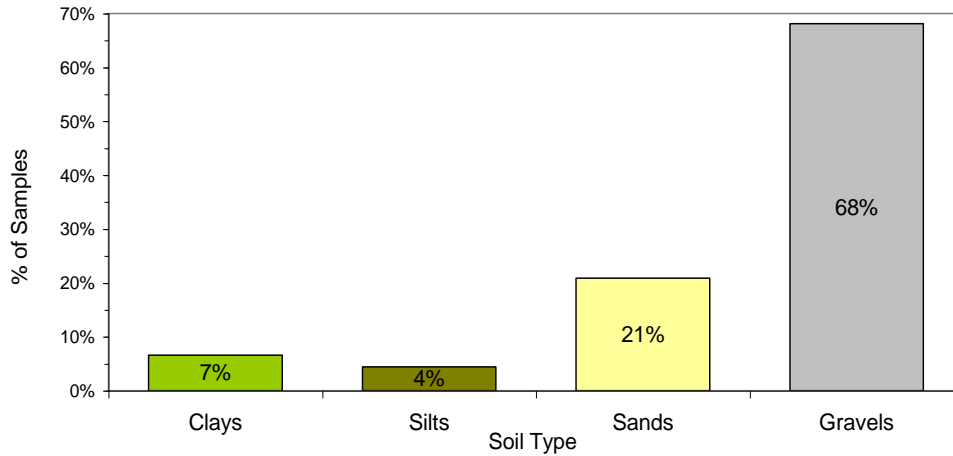**Figure A-30. $N1_{60}$ blow-count distribution for the Qlbpg geologic unit based on 79 granular samples in the northern part of the mapped area.**
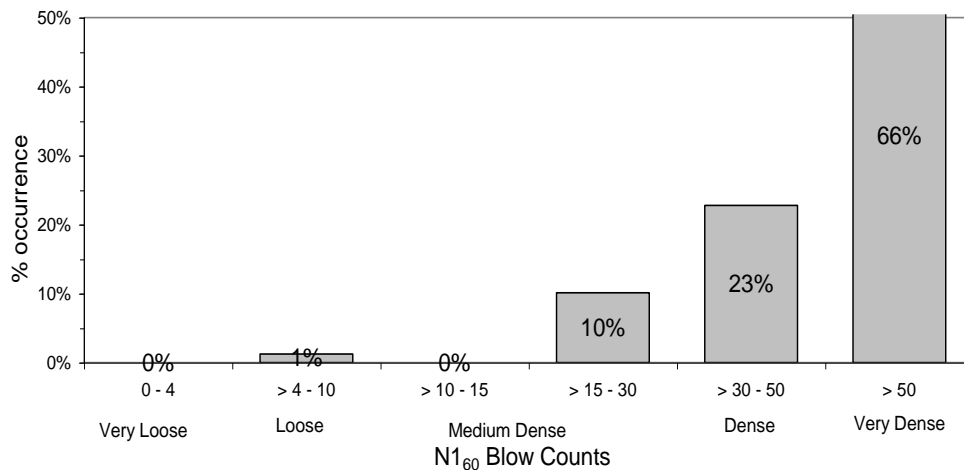
Qlbps- Lacustrine sand and silt of the Provo and Bonneville lake cycles, undivided (Upper Pleistocene). Fine- to coarse-grained lacustrine sand and silt with minor gravel; deposited at and below the Provo shoreline, where transgressive- and regressive-phase deposits cannot be differentiated and cannot be directly correlated with regressive-phase shorelines; grades downslope to finer grained Lake Bonneville deposits; typically thick bedded and well sorted; gastropods locally common; may be as much as 25 m thick.

Commonly, the Qlbps unit is composed of sands (63%), as shown in Figure A-31. These deposits are medium dense to dense, as shown in Figure A-32. Most often, these deposits are very deep. Thus, these deposits are generally not susceptible to liquefaction and lateral spread. The fine-grained soils within this Geologic unit are medium plastic fines, as shown in Figure A-33.
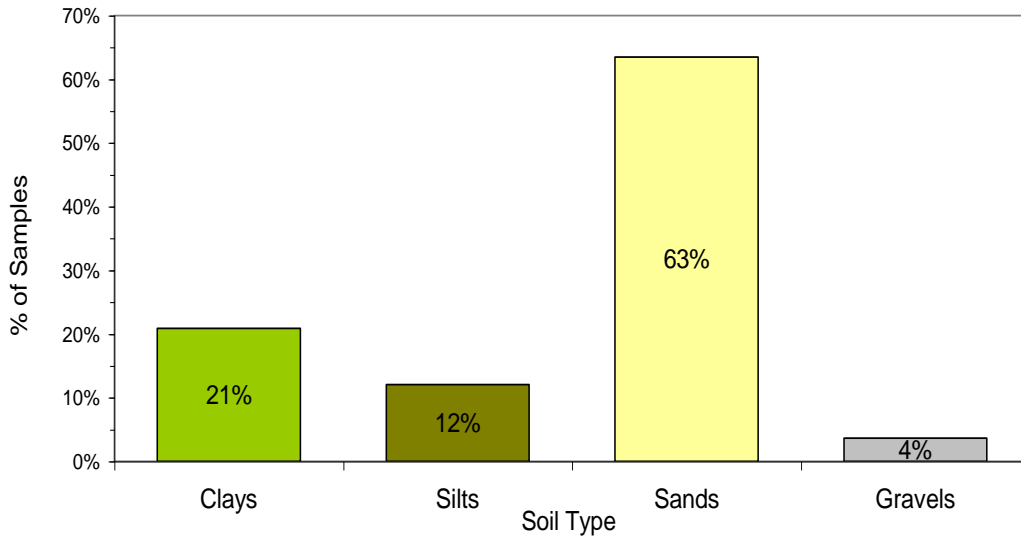

Figure A-31. Soil-type distribution for the Qlbps geologic unit based on 498 samples in the northern part of the mapped area.
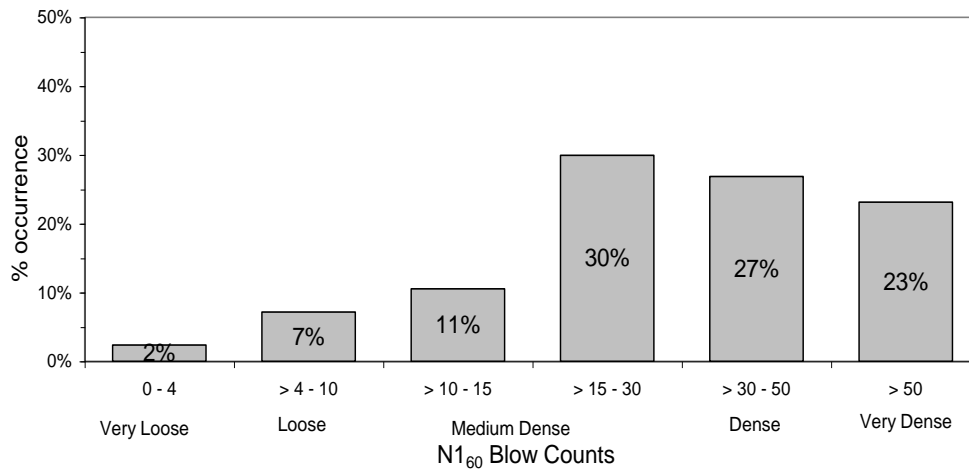

Figure A-32. $N1_{60}$ blow-count distribution for the Qlbps geologic unit based on 294 granular samples in the northern part of the mapped area.
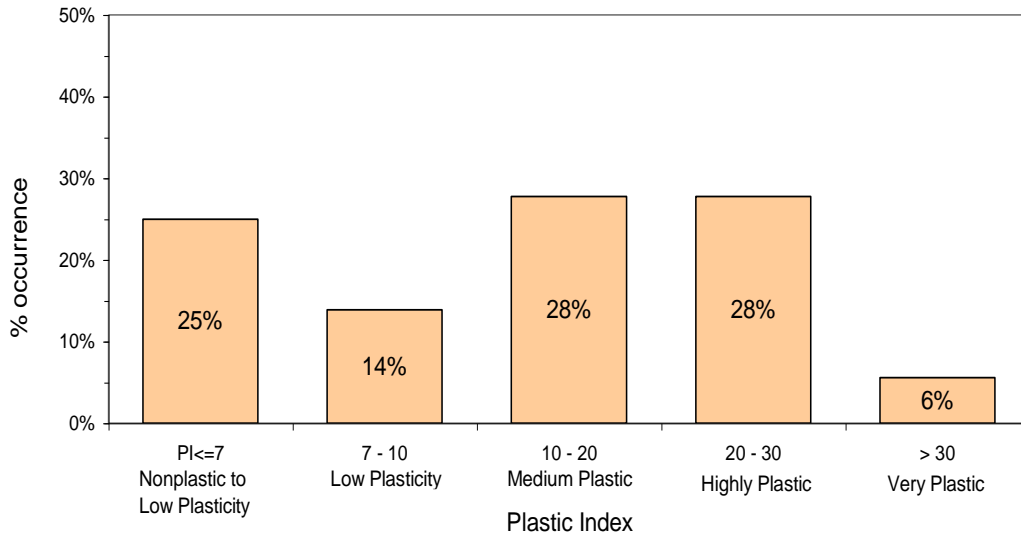
Figure A-33. Plastic-index distribution in the Qlbps geologic unit based on 36 fine-grained soil samples in the northern part of the mapped area.

Qlbpm - **Lacustrine silt and clay of the Provo and Bonneville lake cycles, undivided (Upper Pleistocene).** Calcareous silt, clay, and minor fine-grained sand deposited below the Provo shoreline where transgressive- and regressive-phase deposits cannot be differentiated and deposits cannot be directly correlated with regressive-phase shorelines; deposited in deep and (or) quiet water in the lower part of the basin; typically laminated or thin bedded; ostracodes locally common; grades upslope into lacustrine sand and silt; may be as much as 25 m thick.

Commonly, the Qlbpm unit is composed of clays (75%) with some silt (12%) and sand (12%) interbeds, as shown in Figure A-34. These deposits are medium dense, as shown in Figure A-35. These deposits generally are moderately susceptible to liquefaction and lateral spread, as the silt and sand interbeds within this unit have a high liquefaction potential when close to the Wasatch Fault Zone. The fine-grained soils within this geologic unit are medium to highly plastic, as shown in Figure A-36.

Figure A-34. Soil-type distribution for the Qlbpm geologic unit based on 535 samples in the northern part of the mapped area.
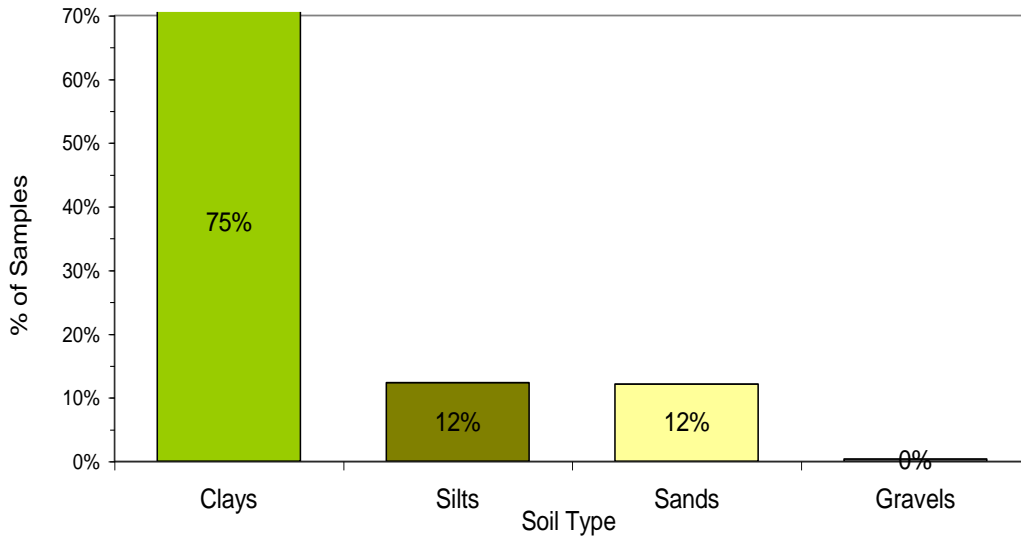

Figure A-35. N1$_{60}$ blow-count distribution for the Qlbpm geologic unit based on 414 granular samples in the northern part of the mapped area.
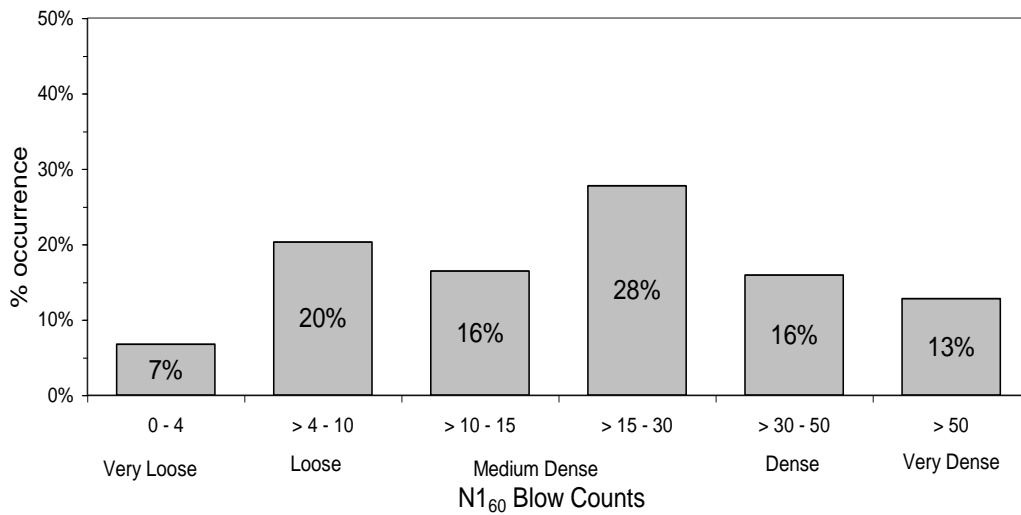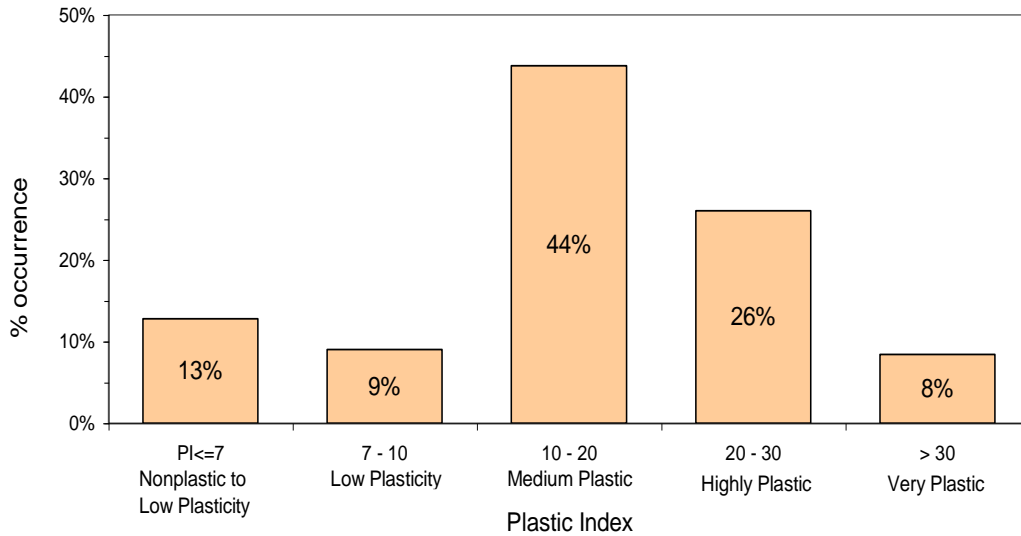
Figure A-36. Plastic-index distribution in the Qlbpm geologic unit based on 665 fine-grained soil samples in the northern part of the mapped area.

A.5   Mass-movement Deposits

Qmsy- Younger landslide deposits (**Historical to upper Pleistocene).** Very poorly sorted, clay- to boulder-size, locally derived material deposited by rotational and translational movement; characterized by moderately subdued landslide features suggesting an early Holocene or late Pleistocene age, but some landslides may have historical movement; variable thicknesses as much as 15 m.

Qmls - Lateral-spread deposits (Holocene to upper Pleistocene). Sand, silt, clay, and minor pebble gravel of the Bonneville lake cycle and younger lacustrine, marsh, and alluvial deposits redeposited by lateral spread as a result of liquefaction, probably during major earthquakes; bedding usually contorted or the deposit is unstratified. Two large deposits at north end of map area were first recognized on aerial photographs by Van Horn (1982). The northern spread appears to truncate the southern spread, the dash-dot contact between the two is based on changes in vegetation and preservation of hummocky topography. Both deposits incompletely truncate the Gilbert shoreline and a topographically lower undesignated shoreline, indicating both lateral spreads

formed less than 10.5 ka. Urbanization probably has destroyed surface evidence of additional deposits in areas mapped as units Qlbpm and Qlaly. Thickness > 1 m.

These areas have been marked on the map as special study zones, since liquefaction and lateral spread have occurred in these locations. Although some of these areas may not currently be liquefiable because of a low ground water table, a special study would still be necessary since they are important to understanding liquefaction and lateral spread and are still susceptible to seismic hazards.

Qmt - Talus deposits (Holocene to upper Pleistocene). Very poorly sorted, angular cobbles and boulders and finer-grained interstitial sediment deposited principally by rock fall on and at the base of steep slopes; mapped on the south side of Little Valley, where quartzitic rock-fall debris from the Permian and Pennsylvanian Kessler Canyon Formation rests on the Bonneville shoreline bench; generally less than 6 m thick.

A.6 Colluvial Deposits

Qchs - Hillslope colluvium (Holocene to upper Pleistocene). Very poorly sorted pebble, cobble, and boulder gravel, usually clast-supported, in a matrix of sand and silt; clasts usually angular to subangular, but unit contains some recycled lacustrine gravel of the Bonneville lake cycle; massive to crude parallel bedding; forms small fans, cones, and debris aprons at the mouths of small canyons and at the bases of bedrock slopes; deposited by mass-wasting processes, sheetwash, and small debris flows; thickness 1 to >10 m

Qca - Colluvium and alluvium undivided (Holocene to middle Pleistocene). Poorly sorted gravel, sand, silt, and clay with parallel bedding and cross-bedding; commonly massive; grain size and texture reflect character of deposits directly upslope; deposited by intermittent streams and mass-wasting processes; forms small fans and debris aprons at base of slopes in unconsolidated deposits; mapped in some grabens along Wasatch Fault zone 1 to >10 m thick.

A.7 Eolian Deposits

Qes- Eolian sand (Holocene and upper Pleistocene). Fine to coarse sand and minor silty sand; moderately to well sorted; thin to medium bedding; usually cross-bedded, locally massive; forms sheets of sand and low parabolic and longitudinal dunes; deposit derived from reworked sandy deposits of the Bonneville lake cycle; can contain, thin (<1 m), discontinuous deposits of loess (windblown silt), which cover most early Holocene and older surficial deposits (Shroba 1984); Loess is weathered and mixed with upper parts of underlying sediments and soils and is not mapped as a separate unit, thickness 1-3 m.

A.8 Artificial Deposits

Qf - **Artificial fill (Historical).** Engineered fill used in road construction and railroad embankments, in crossing drainages, in tailings-pond embankments and levees, and in the construction of State Route 201, Interstates 15, 215 and 80; unmapped fill may be present in any developed area; variable thickness.

Generally, the fill deposits are shallow and well above the ground water table, so the fill itself would not be significant to the liquefaction evaluation. However, the underlying Geologic unit could be potentially liquefiable and would control the hazard in that particular region. For this reason, much of the fill was removed from the map for this study, and the map was created based on the underlying geologic units.

A large active tailings pond containing the waste from washed or milled ore from Kennecott operations occupies the northwest corner of the Magna quadrangle. The tailings-pond embankment in the northwest corner of the Magna quadrangle is as thick as about 50 m, but artificial fill is thinner elsewhere.

B DEVELOPMENT OF GIS GROUND SETTLEMENT ROUTINES

B.1 Introduction

Liquefaction-induced ground settlements were estimated by averaging the calculated results of Tokimatsu and Seed (1987) and Yoshimine et al. (2006) for all liquefiable layers in the top 30 m of each borehole ($FS_{liq} \leq 1.1$). Both methods estimate ground settlement based on SPT N values, which conveniently suits the data available in the geotechnical database. Additional parameters from the geotechnical database such as fines content, soil unit weight and depth to groundwater were also used in the settlement calculations.

The pga estimates for the **M**7.0 scenario event were obtained from Wong et al. (2002) and the pga estimates for the probabilistic events were obtained from the U.S. Geological Survey National Strong Motion Hazard Mapping Project (Petersen et al., 2008). In accordance with the method and criteria proposed by Seed et al. (2001), the Petersen et al. (2008) rock-based pga estimates were adjusted for surface soil effects based on the averaged shear wave velocities assigned to the several site-response units described in Appendix A. The groundwater location and soil unit weight profiles contained in the geotechnical database were used to calculate the total and effective vertical stresses.

B.2 Tokimatsu and Seed Method

Tokimatsu and Seed (1987) estimate volumetric strain in saturated clean sands based on cyclic stress ratio (CSR) and normalized SPT blow counts, $(N_1)_{60}$. In accordance with the guidelines presented in Tokimatsu and Seed (1987), CSR values were calculated by:

$$CSR = 0.65 \left(\frac{a_{max}}{g} \right) \left(\frac{\sigma_o}{\sigma'_o} \right) r_d \qquad \text{(Equation B1)}$$

where a_{max} is the maximum horizontal acceleration at the ground surface (i.e., pga); g is the acceleration of gravity (9.81 m/s^2); σ_o is the total overburden pressure at the depth considered; σ'_o is the effective overburden pressure at the depth considered; and r_d is a stress reduction factor that varies from 1 at the ground surface to about 0.9 at a depth of approximately 9 m.

Following procedures recommended by Youd et al. (1997), the raw blow count data contained in the geotechnical database were normalized and corrected to $(N_1)_{60}$ values by:

$$\left(N_1\right)_{60} = N_m C_N C_E C_B C_R C_S \qquad \text{(Equation B2)}$$

where N_m is the measured standard penetration resistance (blow count); C_N is used to normalize N_m to a common reference effective overburden stress (σ'_o) of approximately 100 kPa (1 atm); C_E varies from 0.5 to 1.3 depending on the type and efficiency of the hammer used in the SPT testing; C_B ranges from 1.0 for a 65-mm diameter hole to 1.15 for a 200-mm diameter hole; C_R ranges from 0.75 for less than 3 m of rod to 1.0 for 10 to 30 m of rod; and C_S varies from 1.0 for samplers with liners to a value of 1.1 to 1.3 for samplers without liners. The data required to determine these factors was typically included on the borehole logs used to create the geotechnical database. In the event that borehole diameter, hammer energy or sampler liner data was missing from a particular borehole log, estimates were obtained from a table of typical values for each drilling rig and the type of hammer used (i.e., safety vs. automatic trip hammer).

As previously mentioned, the geotechnical database contains the amount of material finer than the standard No. 200 sieve (FC). This data was used to correct the $(N_1)_{60}$ values to clean sand values based on Youd et al. (2002):

$$\left(N_1\right)_{60-CS} = \alpha + \beta\left(N_1\right)_{60} \qquad \text{(Equation B3)}$$

where the α and β coefficients are determined by:

$$\alpha = 0 \qquad \text{for FC} \leq 5\% \qquad \text{(Equation B4a)}$$

$$\alpha = \exp[1.76 - (190/FC^2)] \qquad \text{for } 5\% < FC < 35\% \qquad \text{(Equation B4b)}$$

$$\alpha = 5.0 \qquad \text{for FC} \geq 35\% \qquad \text{(Equation B4c)}$$

$$\beta = 1.0 \qquad \text{for FC} \leq 5\% \qquad \text{(Equation B5a)}$$

$$\beta = [0.99 + (FC^{1.5}/1,000)] \qquad \text{for } 5\% < FC < 35\% \qquad \text{(Equation B5b)}$$

$$\beta = 1.2 \qquad \text{for FC} \geq 35\% \qquad \text{(Equation B5c)}$$

The soil profiles for each borehole location were screened for liquefaction triggering using Youd et al. (2002). A ground settlement value of zero was assigned to all soil layers with factors of safety against liquefaction triggering greater than 1.1. Triggering analysis was completed as follows:

$$FS_{liq} = \frac{CRR_{7.5}}{CSR} MSF \qquad \text{(Equation B6)}$$

where CSR is determined by Equation 1 above; $CRR_{7.5}$ is the minimum cyclic resistance ratio for liquefaction as defined by the SPT clean-sand base curve which is approximated by (Youd et al., 2002):

$$CRR_{7.5} = \frac{1}{34 - (N_1)_{60}} + \frac{(N_1)_{60}}{135} + \frac{50}{[10 \bullet (N_1)_{60} + 45]^2} - \frac{1}{200} \qquad \text{(Equation B7)}$$

and MSF is a magnitude scaling factor used to adjust for magnitudes other than **M**7.5 (Seed et al., 1983). The scenario analysis was based on a **M**7.0 earthquake on the Salt Lake City segment of the Wasatch fault zone while input magnitudes for the probabilistic analyses varied based on deaggregations of the data presented by Petersen et al. (2008). The MSF's used in the Tokimatsu and Seed analysis were interpolated from the gridded data points presented in Figure B-1 (Seed et al., 1983). A reference table with approximately 1,400 data points was created from the volumetric strain curves presented in this figure. The table allowed volumetric strains to be rapidly determined based on the $(N_1)_{60}$ clean sand blow counts and CSR values. To account for the **M**7.5 calibration of the curves in Figure B-1, the magnitude scaling factors (MSF's) given in Table B-1 were used to adjust the CSR values to $CSR_{7.5}$ as using Tokimatsu and Seed (1987):

$$CSR_{7.5} = \frac{CSR}{MSF}$$ (Equation B8)

The estimated settlement, Δ_{TS}, at each borehole was the summation of the thickness of each liquefiable soil layer, t, times the respective estimated volumetric strain, ε_{vo}:

$$\Delta_{TS} = \sum_{i=1}^{n} t_i \times \varepsilon_{vo,i}$$ (Equation B9)

An estimate of zero settlement was assigned to soils with clean sand $(N_1)_{60}$ values greater than 30 ($CSR_{7.5} \leq 0.3$) or 32 ($CSR_{7.5} > 0.3$). These soils are not susceptible to liquefaction base on the liquefaction triggering curves presented in Youd et al. (2001).

Table B-1. Magnitude Scaling Factors presented by Seed et al. (1983).

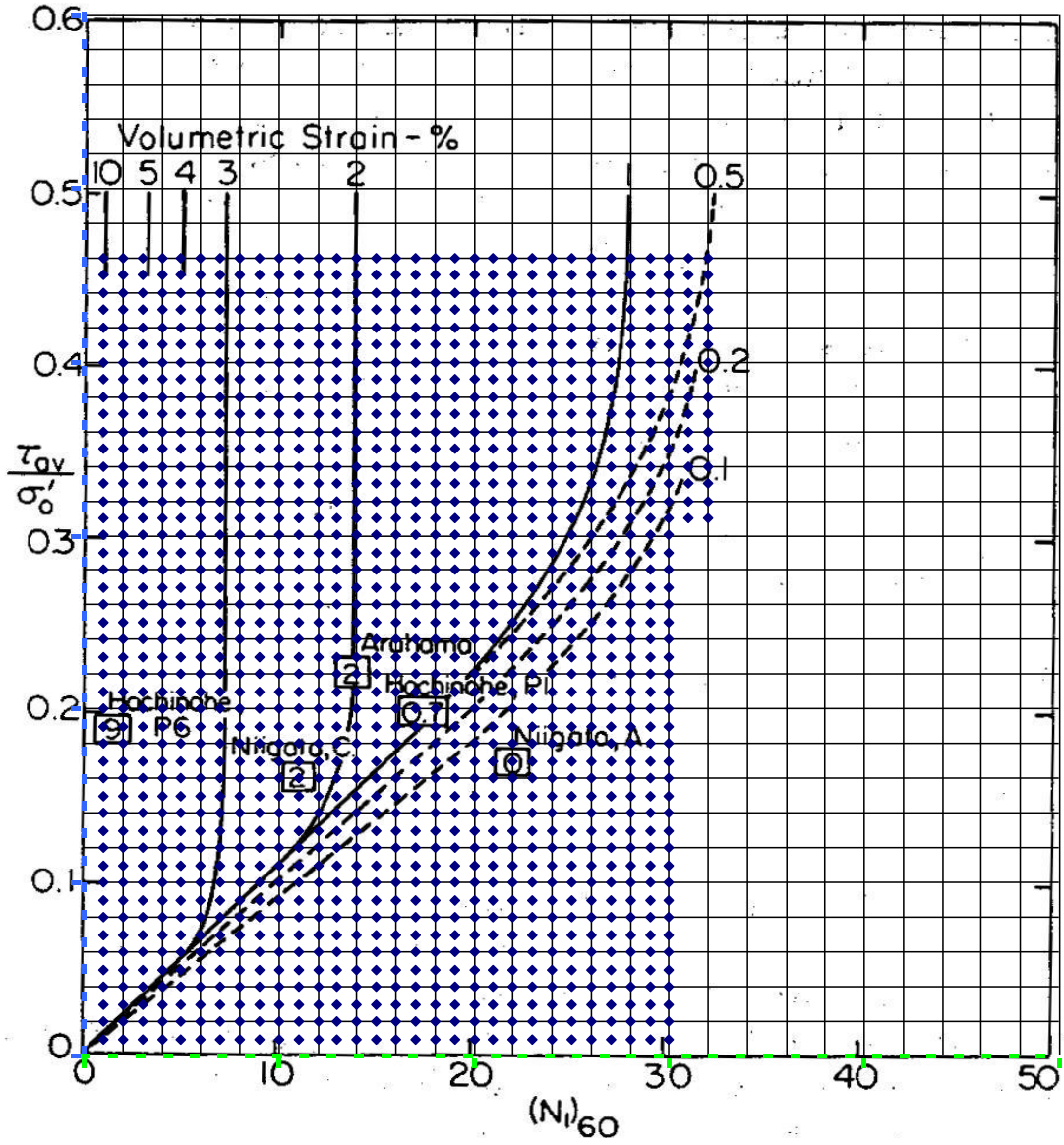| Earthquake Magnitude, M	Magnitude Scaling Factor, MSF
8.25	0.91
7.5	1.0
6.75	1.13
6.0	1.33
5.25	1.5

Figure B-1. Points used to define volumetric strain modified from Tokimatsu and Seed (1987).

B.3   Yoshimine et al. (2006) Method

Yoshimine et al. (2006) published a series of functions that describe the settlement curves presented by Ishihara and Yoshimine (1992). The Ishihara and Yoshimine (1992) curves (Figures B-2 and B-3) relate volumetric strain in clean sands to relative density (via normalized SPT blow counts, N_1) and factor of safety against liquefaction triggering (FS).

The raw blow count data contained in the geotechnical database were normalized and corrected to $(N_1)_{60}$ clean sand values by Equations 2 and 3 (Youd et al., 2002). The soil profiles for each borehole location were then screened for liquefaction triggering using Equations 1, 6 and 7 as previously described. A ground settlement value of zero was assigned to all soils layers with factors of safety against liquefaction triggering greater than 1.1.

To implement Yoshimine et al. (2006), the $(N_1)_{60}$ clean sand blow count values were converted to N_1 values using Seed et al. (1985) to account for traditional Japanese sampling practices and techniques used for the development of their method:

$$N_1 = \frac{(N_1)_{60}}{0.9} \quad \text{for } (N_1)_{60} < 20 \qquad \text{(Equation 10a)}$$

$$N_1 = (N_1)_{60} \quad \text{for } (N_1)_{60} \geq 20 \qquad \text{(Equation 10b)}$$

Following the method outlined by Yoshimine et al. (2006), the N_1 values were converted to relative densities, D_r, using Meyerhof (1957):

$$D_r = 21\sqrt{\frac{N_1}{1.7}} \qquad \text{(Equation 11)}$$

and the likelihood of liquefaction triggering, FS, was calculated according to the Japanese Design Code for Highway Bridges (2000):

$$FS = \frac{R}{L} \qquad \text{(Equation 12)}$$

$$R = 0.0882\sqrt{\frac{N_1}{1.7}} \qquad \text{for } N_1 < 14 \qquad \text{(Equation 13a)}$$

$$R = 0.0882\sqrt{\frac{N_1}{1.7}} + 1.6E^{-6}\left(\frac{N_1}{1.7}\right)^{4.5} \qquad \text{for } N_1 \geq 14 \qquad \text{(Equation 13b)}$$

$$L = r_d\left(\frac{\sigma_v}{\sigma'_v}\right)\left(\frac{\alpha}{g}\right) \qquad \text{(Equation 14)}$$

$$r_d = 1.0 - 0.015D \qquad \text{(Equation 15)}$$

where N_1 is the normalized and corrected Japanese-modified SPT blow count, σ_v and σ'_v are the total and effective overburden pressures, respectively, α is the pga for the analysis, D is the depth from the ground surface and r_d is a stress reduction factor.
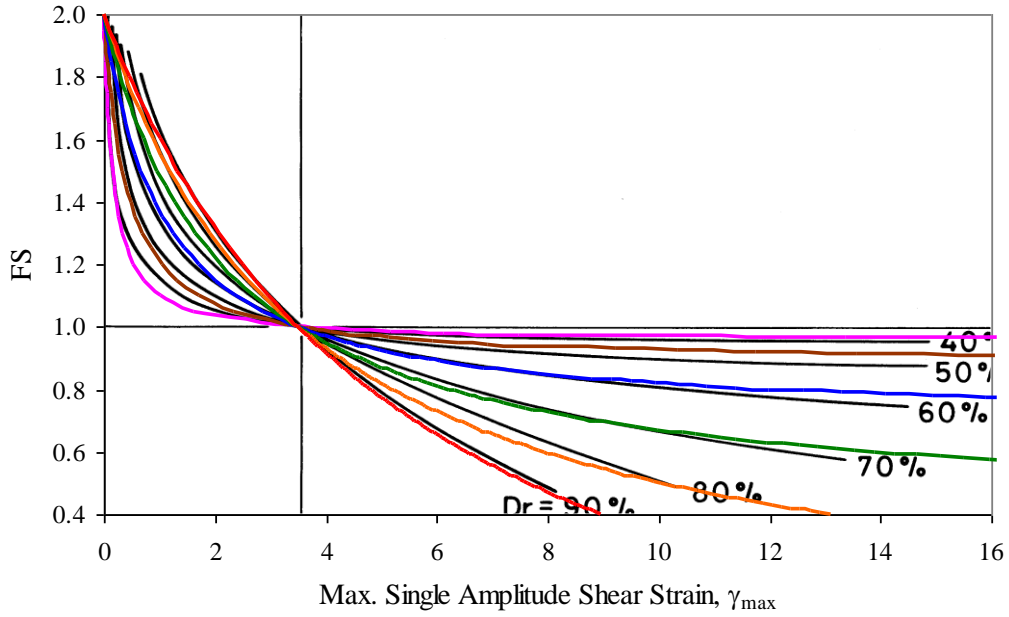
Figure B-2. Curves used to correlate single amplitude shear strain (γ_{max}) to factor of safety against liquefaction (relative density, D_r, calculated from N_1).
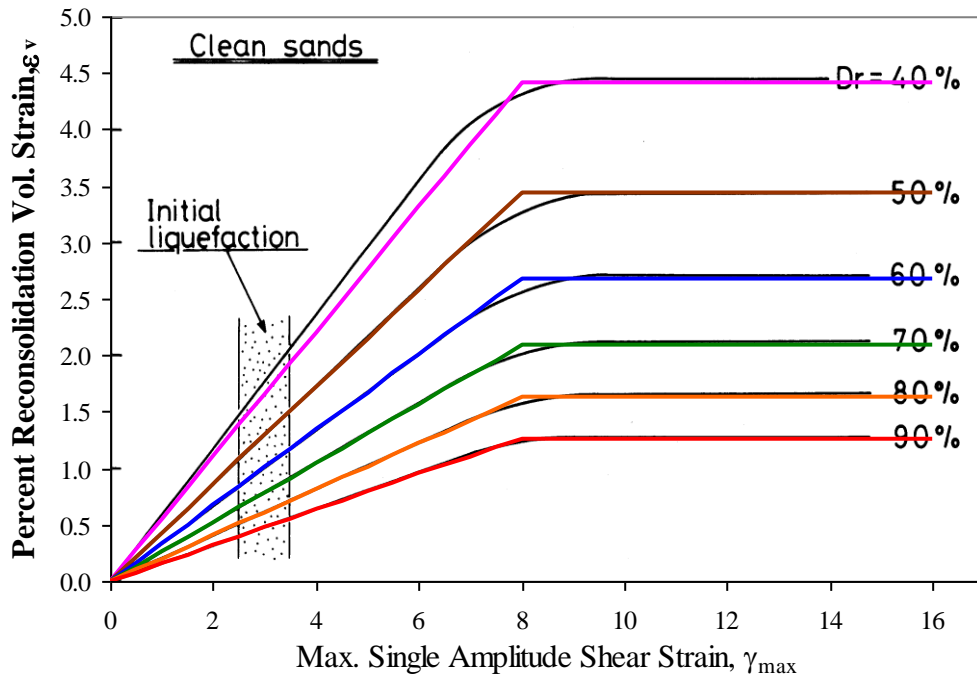

Figure B-3. Curves used to correlate single amplitude of shear strain (γ_{max}) to post-liquefaction settlement.

B9

The maximum single amplitude of shear strain, γ_{max}, for all sites with a factor of safety against liquefaction triggering, FS, less than or equal to 1.1 was calculated using Yoshimine et al. (2006). In the equations below F_{ult} is a nameless intermediate variable and the relative density prior to liquefaction, $D_{r,ini}$, is expressed as an integer (i.e., 65 percent is expressed as 65):

$$\gamma_{max} = 3.5(2 - FS)\frac{1 - F_{ult}}{FS - F_{ult}} \quad \text{if } F_{ult} \le FS \le 2.0 \qquad \textbf{(Equation B16a)}$$

$$\gamma_{max} = 0 \quad \text{if FS} \ge 2.0 \qquad \text{(Equation B16b)}$$

$$\gamma_{max} = \infty \quad \text{if } F_{ult} \le FS \qquad \text{(Equation B16c)}$$

where:

$$F_{ult} = -0.0006 D_{r,ini}^2 + 0.047 D_{r,ini} + 0.032 \quad \text{if } D_{r,ini} \ge 39.2\% \qquad \text{(Equation B17a)}$$

$$F_{ult} = 0.9524 \quad \text{if } D_{r,ini} < 39.2\% \qquad \text{(Equation B17b)}$$

Finally, using the initial relative densities, $D_{r,ini}$, and the maximum single amplitude of shear strains, γ_{max}, percent liquefaction-induced volumetric strains, ε_v, were estimated using Yoshimine et al., (2006):

$$\varepsilon_v = 1.5[\exp(-0.025 D_{r,ini})]\gamma_{max} \quad \text{if } \gamma_{max} \le 8\% \qquad \text{(Equation B18a)}$$

$$\varepsilon_v = 12\exp(-0.025 D_{r,ini}) \quad \text{if } \gamma_{max} > 8\% \qquad \text{(Equation B18b)}$$

The estimated settlement, Δ_Y, at each borehole was the summation of the thickness of each liquefiable soil layer, t, times the respective estimated volumetric strain, ε_v:

$$\Delta_Y = \sum_{i=1}^{n} t_i \times \varepsilon_{v,i}$$
(Equation B19)

As previously mentioned, ground settlement value of zero was assigned to all locations with factors of safety for liquefaction triggering greater than 1.1. Since earthquake magnitude was not a required input variable, no magnitude scaling factors were used with this method.

Comparison of Settlement Estimation Methods

The calculated settlements (Δ_{TS} and Δ_Y) were compared at each borehole to assess the similarities and differences between the two methods. The results for the three analysis events are shown in Table B-2 for the **M**7.0 event. The ground settlement estimates showed an average difference between the two methods of 0.004 m, with a maximum difference of 0.083 m. Of the 963 boreholes, Tokimatsu and Seed (1987) predicted higher settlements than Yoshimine et al. (2006) in 232 boreholes and the opposite for 444 boreholes. Both methods predicted no settlement in 287 boreholes. A method-to-method comparison of the differences showed that 74 percent of the boreholes were within 0.01 m, 92 percent were within 0.025 m and 99 percent were within 0.05 m.

It was concluded that the two methods produced relatively similar results when considering the quality of the input data and the ultimate use of the mapping. Hence, it method was treated as equally likely and the average of the two methods was considered appropriate to estimate the ground settlement, Δ_{liq}, at each liquefiable borehole location:

$$\Delta_{liq} = \frac{\Delta_{TS} + \Delta_Y}{2} \qquad \text{(Equation 20)}$$

able B-2. Comparison of Δ_{TS} and Δ_Y at each Borehole for the Three Analysis Events.

Comparisons	M7.0 Scenario Event
Average Difference, m	0.004
Maximum Difference, m	0.083
Number of Boreholes where $\Delta_{TS} > \Delta_Y$	232
Number of Boreholes where $\Delta_Y > \Delta_{TS}$	444
Number of Boreholes where $\Delta_{TS} = \Delta_Y = 0$	287
Percent of Boreholes where Δ_{TS} and Δ_Y are within 0.010 m	73.9
Percent of Boreholes where Δ_{TS} and Δ_Y are within 0.025 m	92.3
Percent of Boreholes where Δ_{TS} and Δ_Y are within 0.050 m	99.0

C LATERAL SPREAD DISPLACEMENT HAZARD CLASSIFICATION

C.1   Introduction

The lateral spread displacement map is continuation of work completed for the northern part of the Salt Lake Valley by Bartlett et al. (2005) and Olsen et al. (2007). The methods used for this map are consistent with the methods developed in those publications that contain a detailed explanation of the analysis methodology. Lateral spread displacements were estimated by the Youd et al. (2002) regression model for all borehole locations having a factor of safety against liquefaction triggering less than or equal to 1.1. The estimated horizontal displacements (D_H) were further categorized as "none" (0 m); "low" (0 to 0.1 m); "moderate" (0.1 to 0.3 m); "high" (0.3 to 1.0 m); and "very high" (greater than 1.0 m). All boreholes with factors of safety against liquefaction triggering greater than 1.1 were assigned a lateral spread displacement of zero.

C.2   Methods and Classifications

In developing the lateral spread ground displacement map (Figure 7-4), a hazard category was assigned to each geologic unit shown in Figure 2-1 by statistical analysis of the estimated displacements from all boreholes located within the respective geologic unit or group of units with similar subsurface characteristics (e.g., near-surface soil type, origin, deposition and age). A total of 24 geologic units represent soil deposits were assessed and assigned a hazard classification for each map. All 963 boreholes from the geotechnical database are contained within the 24 geologic units.

To assess the localized hazard, the estimated displacement at each borehole location was shown as a colored dot (Figure C-1) that represented the ground displacement hazard categories. In a few areas, homogenous or nearly homogenous dot clusters existed in the same geologic unit that varied from the remaining dots in the unit. In these few cases, the geologic unit was further subdivided prior to conducting statistical analysis. For example, the geologic unit shown highlighted in the middle of

the Figure C-1 is the Qlaly unit (lacustrine, marsh and alluvium deposits). Due to the concentration of increased ground displacement hazard in the northern (upper) part and somewhat lower ground displacement hazard suggested in the southern (lower) part, this geologic unit was subdivided along I-80 (Figure 7-4).
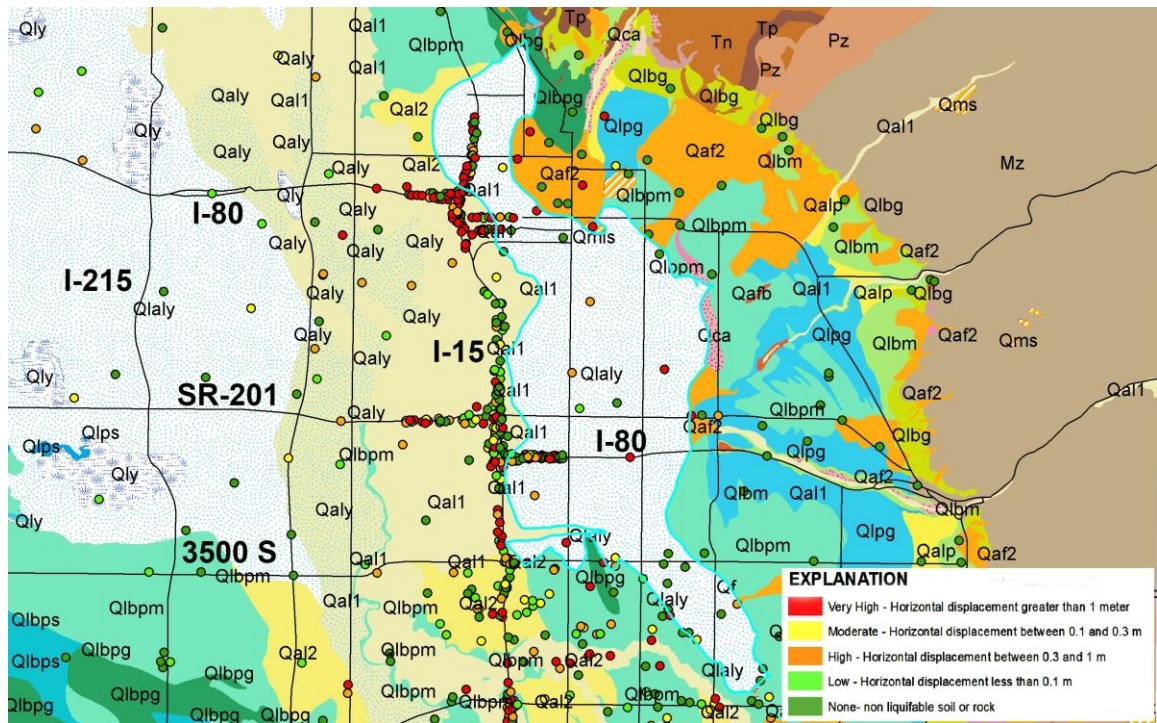

Figure C-1. Ground displacement "Dot map" showing boreholes in the northeast part of the Salt Lake Valley, Utah.

## C.3   **M**7.0 Lateral Spread Scenario Map

Using the methods of Bartlett et al. (2005) and Olsen et al. (2007), cumulative histograms of increasing ground displacement hazard severity were developed to determine an 85 percent non-exceedance ground displacement threshold for the **M**7.0 scenario event. The 85 percent non-exceedance threshold criterion means 15 percent, or less, of the estimated horizontal displacements exceed the upper displacement threshold assigned to the hazard category for the respective geologic unit (Figure C-1). This cumulative histogram corresponds to the lateral spread hazard estimated for the

northern part of the Qlaly geologic unit shown in Figure C-2. Based on the 85 percent

threshold criterion, the lateral spread hazard associated with this geologic unit was

classified as "very high," because approximately 30 percent of the displacement values

exceeded 1 m (39 in.). Several additional histograms included as Figures C-3 through C-7

further illustrate the 85 percent non-exceedance threshold criterion and the subsequent

hazard classification. Similar data and plots are available for all units in the study area

(Hinckley, 2010).
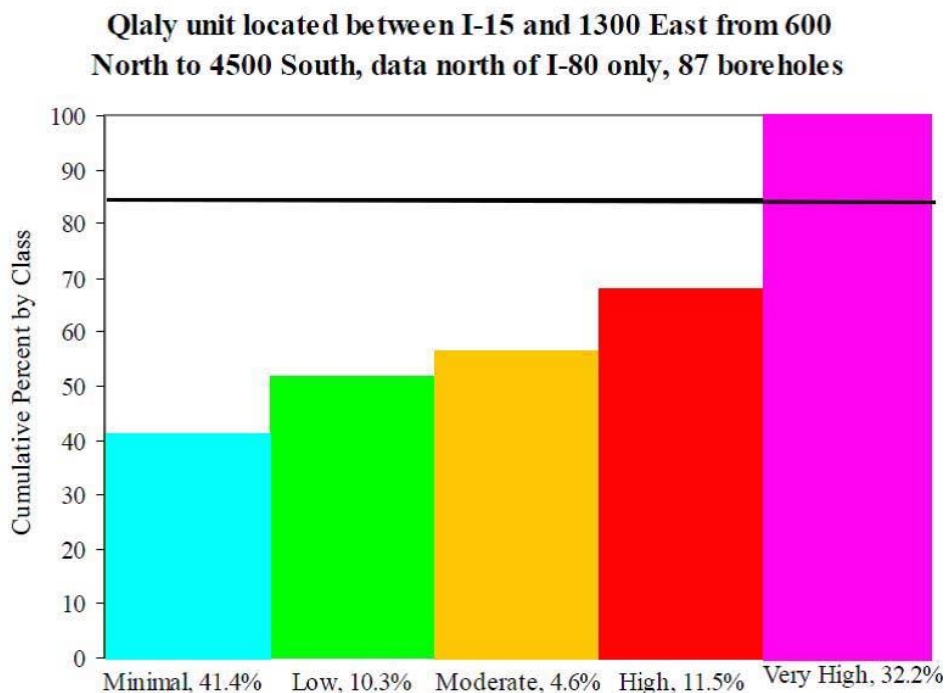
Figure C-2. Histogram showing "very high" hazard classification for lateral spread caused by a M7.0 event on the Wasatch fault for the northern part of Qlaly unit located in northeast part of the Salt Lake Valley.
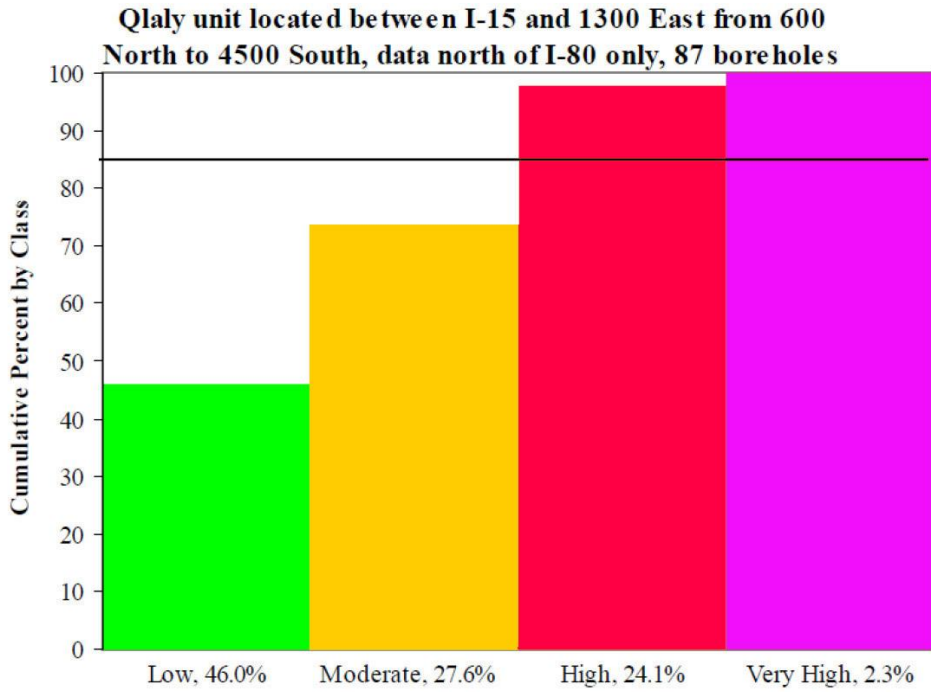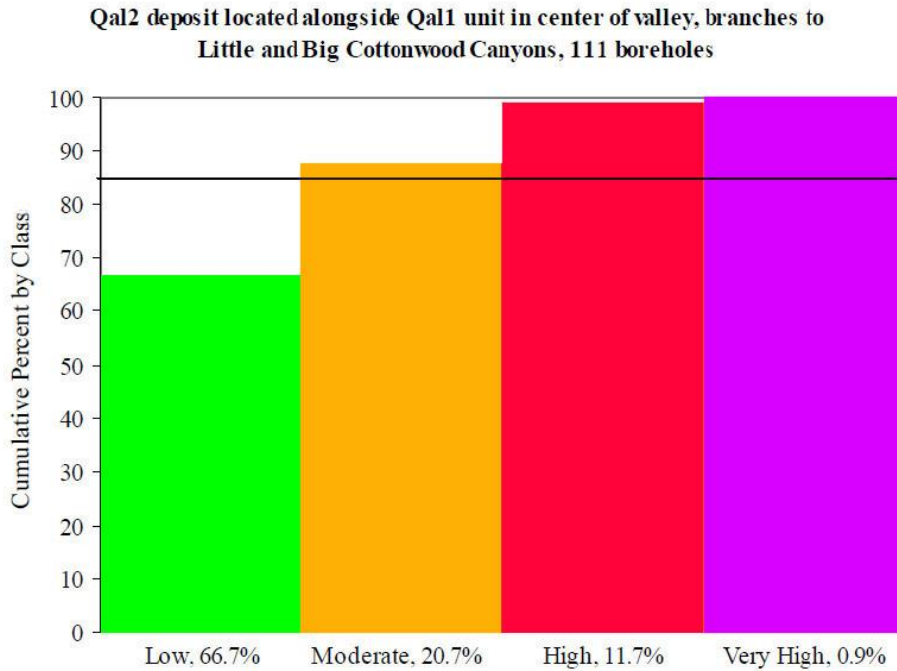
Figure C-3. Histogram showing "high" hazard classification for lateral spread caused by a M7.0 event on the Wasatch fault.
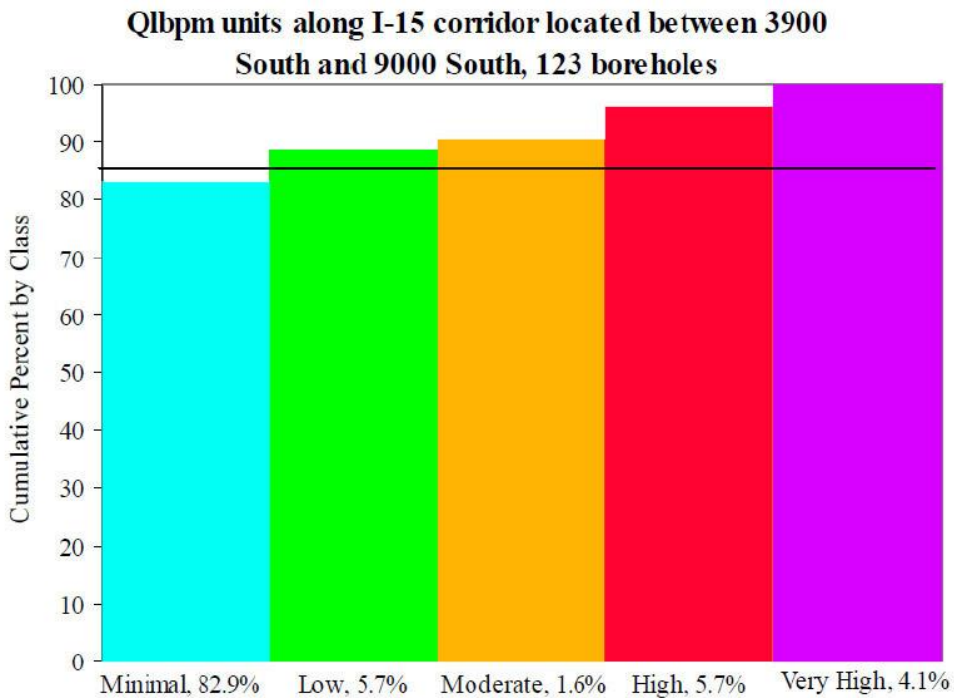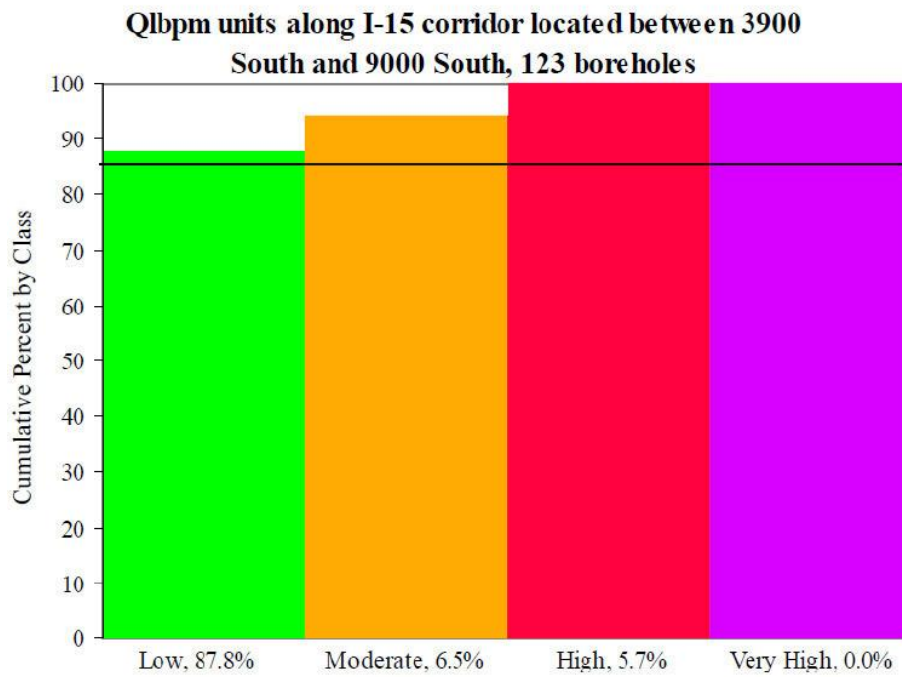

Figure C-4. Histogram showing "low" hazard classification for lateral spread caused by a M7.0 event on the Wasatch fault.
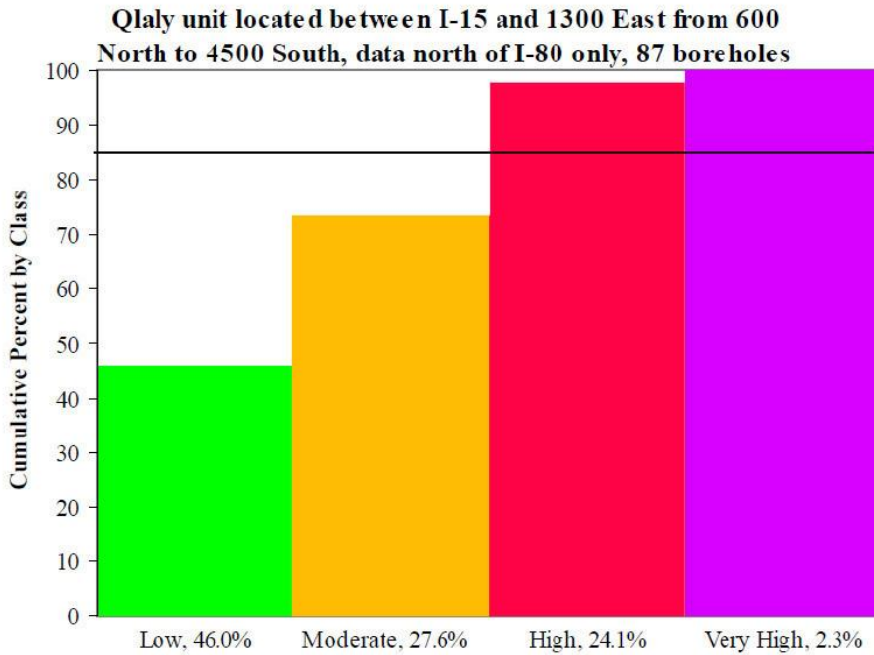
Figure C-5. Histogram showing "high" hazard classification for ground settlement caused by a M7.0 event on the Wasatch fault.

Figure C-6. Histogram showing "moderate" hazard classification for ground settlement corresponding to a M7.0 event on the Wasatch fault.

Figure C-7. Histogram showing "low" hazard classification for ground settlement corresponding to a M7.0 event on the Wasatch fault.